Early North African Acheulean techno-economic systems at Thomas Quarry I - L1 (Casablanca, Morocco)

Rosalia Gallotti[1,2,3], Jean-Paul Raynal[3,4], Abderrahim Mohib[4,5], Paul Fernandes[6], Lionel Magoga[7], Mohssine El Graoui[4], Mathieu Rué[1,6], Giovanni Muttoni[8] & David Lefèvre[1,2]

1) *Université Paul Valéry Montpellier 3, CNRS, UMR 5140 Archéologie des Sociétés Méditerranéennes, Campus Saint Charles, 34199 Montpellier, France*
   e-mail: rosalia.gallotti@univ-montp3.fr

2) *LabEx Archimède, Université Paul Valéry Montpellier 3, Campus Saint Charles, 34199 Montpellier, France*

3) *Université Bordeaux, CNRS, UMR 5199 PACEA-PPP, Bâtiment B18 Allée Geoffroy Saint-Hilaire CS 50023, 33615 Pessac Cedex, France*

4) *Institut National des Sciences de l'Archéologie et du Patrimoine, Angle rues 5 et 7, Avenue Allal El-Fassi, Hay Riad - BP 6828, Rabat-Instituts, Morocco*

5) *Direction Provinciale de la Culture, Centre d'interprétation du Patrimoine du Gharb, Quartier administratif, Bd Mohamed V, Kenitra, Morocco*

6) *Paléotime, 75 avenue Jean Séraphin Achard-Picard, 38250 Villard-de-Lans, France*

7) *5 Rue Alquié, 03200 Vichy, France*

8) *Dipartimento di Scienze della Terra "Ardito Desio", Università degli Studi di Milano, Via L. Mangiagalli 34, 20133 Milan, Italy*

Summary - *North Africa is a key area for understanding cultural processes that led to the Acheulean pan-African emergence and expressions and the related hominin population dynamics. Unfortunately, little is known about the early Acheulean in this vast area of the African continent due to the scarceness of archaeological sites in stratigraphic context with reliable chronometric data, human remains, and technological analyses of the lithic industries. Here, we present the first comprehensive techno-economic analysis of the early Acheulean assemblage from Thomas Quarry I – Unit L1 (ThI-L1, Casablanca, Morocco), which is the earliest Acheulean site of North Africa, unambiguously dated to 1.3 Ma. Fieldwork has unearthed faunal remains and a lithic collection containing over 3800 artefacts, which represents one of the largest series for the early African Acheulean. The assemblage is mainly composed of quartzites and to a lesser extent of silicites, both abundantly available near the site. Previously published results of the silicite study revealed two different productions for the extraction of small flakes and of bladelet-like flakes. In this work, we analyse the techno-economic systems of the quartzite assemblage. Two distinct quartzite productions co-occur, one devoted to the manufacture of Large Cutting Tools (LCTs), the other focused on the extraction of small-medium sized flakes. LCTs were usually produced from large cobbles, less often from large flakes detached mainly using the* entame *core method. The main technical objective was to obtain large pointed tools and, more rarely, large tools with a transversal cutting edge. Results support the existence of a strong synergy between conceptual and operational schemes regulated by the ability to anticipate the final tool morphology and to apply standardized shaping procedures to manufacture recurrent morphotypes. Quartzite small-medium sized flakes were produced by a diversity of flaking methods adapted to the cobble blank morphologies and were not retouched. The results allow to assess that the earliest technical expression of the Acheulean in North Africa is characterised by a high diversification of the stone knapping outcomes, the complexity of the mental templates, and the flexible structure of the operational schemes.*

Keywords - *North Africa, Morocco, Early Acheulean, Techno-economic systems, Small flaking, LCT production.*

Introduction

Over the last two decades, the research on the early Acheulean has multiplied on the African continent. Research overarching aims in East and South Africa included the refinement of the chronostratigraphic framework in which early Acheulean emerged and developed, the opening of new systematic excavations, the investigation about the ecological adaptations of the early Acheulean hominins, their technological behaviors and subsistence strategies (e.g. de la Torre 2016; de la Torre and Mora 2018; Gallotti and Mussi 2018; Kuman and Gibbon 2018; Leader et al. 2018; Lotter and Kuman 2018; Prassack et al. 2018; Stanistreet et al. 2018; Uno et al. 2018; Diez-Martín et al. 2019; Uribelarrea et al. 2019; Yravedra et al. 2019; Sistiaga et al. 2020; Duke et al. 2021; Hovers et al. 2021).

Such as East and South Africa, North Africa is rich in Acheulean sites, well known since the end of the nineteenth century (Bleicher 1875; Collignon 1887; Pallary 1888; Rivière 1896; Boule 1900; Chantre 1908; Breuil 1930; Reygasse 1930). Research expeditions have multiplied over years, but, although several Lower Palaeolithic sites were discovered, most of them lack a stratigraphic context (e.g. Alimen 1955; Balout 1955; Vaufrey 1955; Biberson 1961a; Champault 1966; Clark 1992; Mattingly et al. 2003; Reynolds 2006; Boudad and Guislain 2012; Parenti et al. 2015; Cancellieri 2021). Accordingly, the timing and mode of the early Acheulean emergence and its subsequent development are poorly understood in this part of Africa and many aspects remain open questions.

In Algeria, the site of Tighennif yielded human fossils and animal bones as well as lithic artefacts in the lower deposits probably belong to a normal magnetic polarity interval, either the Brunhes chron or the Jaramillo subchron (Geraads et al. 1986; Geraads 2016). In addition, a few Acheulean tools have been recently found at the top of the Aïn Hanech Formation within the surficial calcrete deposits sealing the stratigraphic sequence. They would have an age of around 1.67 Ma after the estimation of sediment accumulation rate (Parés et al. 2014; Duval et al. 2021). Nevertheless, further work is necessary to confirm such inference.

As regards the Early Pleistocene, the only known North African Acheulean sites in stratigraphic context are in Atlantic Morocco, discovered thanks to the construction works started between the end of ninetieth century and the dawn of twentieth century (Raynal et al. 2017; Mohib et al. 2019; Raynal 2021; Gallotti et al. 2022). The growing city of Casablanca demanded the opening of large quarries allowing the discovery of an exceptional geological, paleontological, and archaeological heritage. The coast of the Moroccan Meseta, between Kenitra in the north and Safi in the south, shows a vast system of longitudinal dune ridges parallel to modern coast that present an exceptional development in the Casablanca region. These morpho-sedimentary units are composed of marine and aeolian calcarenites that have left a record of a succession of palaeo-shorelines since the end of the Miocene. Since 1917, this sequence captured the interest of many geologists and archaeologists and played a central role in the establishment of a Quaternary stratigraphic and cultural framework in North-west Africa (Lecointre 1926, 1952; Breuil 1930; Bourcart 1943; Antoine 1945; Gigout 1951, 1958; Biberson 1956, 1961a,b; Stearns 1978; Lefèvre 2000; Mohib 2001; Raynal et al. 2001, 2002, 2017; Lefèvre and Raynal 2002; Lefèvre et al. 2021).

After the first attempts defining the cultural sequence of the Lower Palaeolithic of the Casablanca region (Neuville and Ruhlmann 1941; Antoine 1952), P. Biberson, who had been entrusted in 1949 to monitor the works in the Casablanca quarries, started systematic excavations, notably at Sidi Abderrahmane where he discovered a fossil *Homo* (Biberson 1956). In 1958, he established the basis of the geological scheme which came into widespread use for the Maghreb, successively refined and finally published in 1961 in a volume devoted to the paleogeographical framework of the Palaeolithic in Atlantic Morocco (Biberson 1961b). Simultaneously, Biberson (1961a) published the results of the excavations carried out since 1950 in several quarries of Casablanca in the monumental volume "*Le Paléolithique inférieur du Maroc Atlantique*". Following a methodology inspired by the technological and typological approaches of F. Bordes (1947, 1950), he established the

fundamental characters of the ancient Palaeolithic industries and proposed an adequate terminology to their definition and the associated descriptive criteria. He defined also the guidelines of the typological evolution of these industries to propose a synthesis that represented the reference for more than 40 years for the ancient prehistory in Atlantic Morocco (Biberson 1961a).

Biberson identified two main civilizations in the Lower Palaeolithic: 1) the Pebble-Culture, which was divided in two stages (ancient and developed), successively defined as "Pre-Acheulean" (Biberson 1967) and 2) the Acheulean, divided into ancient, middle, and developed. He separated further ancient Acheulean into three stages. Biberson (1961a) ascribed the Sidi Abderrahmane *Grande Exploitation* Quarry-Unit M industry to the early Acheulean (stages I and II; Fig. 1A). It contained Acheulean forms (trihedrons, handaxes, cleavers, spheroïds), large flakes (the "Clactonian" component of Neuville and Ruhlmann, 1941) and various forms of cobble tools, associated with a very fragmentary fauna dominated by *Hippopotamus*. Stage III of the early Acheulean was identified by Biberson in layer D of the *Société de Transformation Industrielle* (S.T.I.C.) Quarry (Fig. 1A), located beyond the south extremity of Sidi Abderrahmane *Grande Exploitation* Quarry. This layer yielded a rich quartzite assemblage composed by various types of handaxes, cleavers, trihedrons, bifacial and multifacial cores, and a few bolas.

In 1978, a joint Morocco-France research program began in Casablanca area (Raynal et al. 2017; Mohib et al. 2019; Raynal 2021). New fieldwork, discoveries, absolute dating, and systematic excavations in classical and new sites allowed 1) the revision of the chronostratigraphical framework of the Quaternary littoral deposits of the Casablanca region, establishing a New Casablanca Stratigrafic Scale (Supplementary Material A and Fig. S1; Texier et al. 1994, 2002; Lefèvre 2000; Lefèvre and Raynal 2002; Lefèvre et al. 2021), and 2) the revision of the cultural sequence proposed by Biberson (Raynal et al. 2001, 2002, 2009, 2010, 2017; Raynal and Mohib 2016; Mohib et al. 2019; Gallotti et al. 2020, 2021, 2022).

Thomas Quarry I (Fig. 1A), firstly investigated by Biberson and later on known for its human remains (Ennouchi 1969; Raynal et al. 2010, 2011), was re-examined in 1985 revealing the presence in stratigraphic context (Unit L) of a rich lithic assemblage of quartzites and silicites[1], together with fauna, and approximately dated to ~1.0 Ma based on biochronology and OSL dates (Raynal and Texier 1989; Rhodes et al. 2006). Recently, results of magnetostratigraphy, coupled by geochemical analysis, provided a high-resolution chronology, dating ThI-L to ~1.3 Ma (Gallotti et al. 2021). A first attempt of typological classification ascribed the industry belonging to the first excavation campaigns to a First Regional Acheulean (Raynal et al. 2017; Mohib et al. 2019; Gallotti et al. 2022).

The overarching aim of this paper is to present the first comprehensive techno-economic assessment of the lithic assemblage from ThI-L1, the earliest North African Acheulean site recorded in stratigraphic context. The results of the study of the silicite assemblage, which represent 12.3% of the total artefacts (Gallotti et al. 2020) will be considered in the discussion section. Here, we report the detailed analysis of the quartzite assemblage with specific research aims including the reconstruction of the *chaînes opératoires* and of the conceptual schemes and operational solutions adopted.

Our analysis paid particular attention to the raw material-related knappers' behaviours, i.e. the technical responses to raw material *stimuli*, in order to evaluate the degree of adaptation and/or "emancipation" of the technical process from natural constraints. More precisely, 1) we questioned the human technical responses to the lithological, geometrical (forms and volumes), and topological qualities/limits of the raw materials; 2) we evaluated if technical processes indicate different levels of knowledge and knowhow, linked to specific characteristics of the natural blanks, and 3) we evaluated if technical variability is determined by occasional

---

[1] In scientific literature, the terms flint and chert are controversial depending on whether they are used by geologists, archaeologists, petrographers or sedimentologists. Following Raynal et al. (2022), here we use the general term silicites for hyper-siliceous rocks including chert, flint, silcrete, and hydrothermal silica.
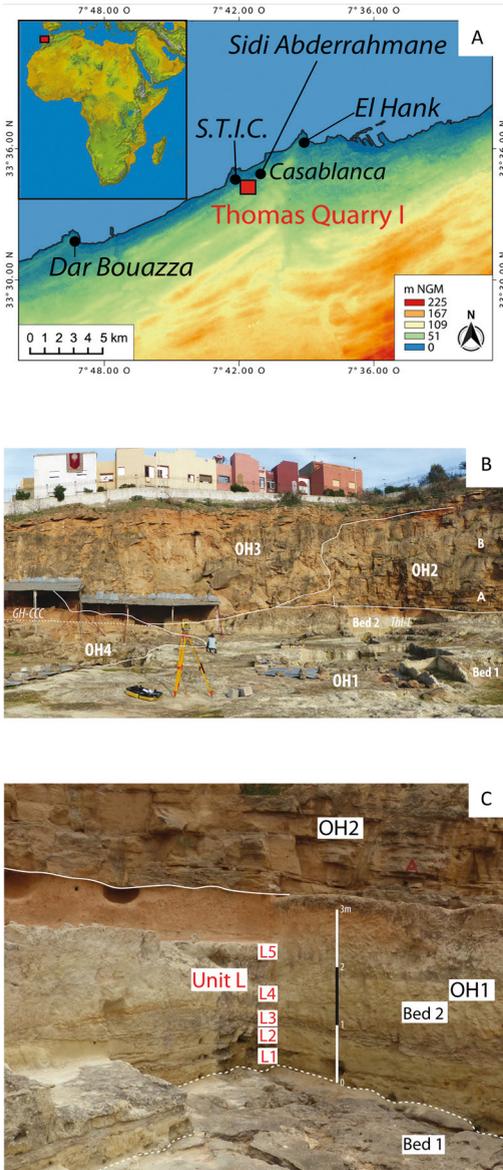
*Fig. 1 - **(A) Map location of the Thomas Quarry I on North-Africa map: modified after NASA/JPL/ NIMA, public domain, via Wikimedia Commons. Casablanca map: modified after NASA/SRTM, 1 arc second global elevation data, created using the free and open source software QGIS v3.18.2 (http:// www. qgis. org). (B) Members 1 to 4 of the OHF at ThI. (C) ThI-L, Zone 1: OH1 Bed 2-Unit L-L1 to L5 deposits.***

choices, i.e. the outcome of the human adaptation, or reveals an invariant knowledge, free from the several constraints imposed by the raw materials.

Results are discussed in the context of the Early Pleistocene North African industries.

Thomas Quarry I-L1 in the Casablanca regional context

The Thomas Quarry I Pleistocene deposits belong to the Oulad Hamida Formation (OHF) which includes four allostratigraphic units - OH1 to OH4 Members from bottom to top (Fig. 1B; Supplementary Material A and Fig. S1).

Thomas Quarry I-Unit L (ThI-L) archaeological site belong to OH1-Bed 2 deposits (Fig. 1B). It consists of over 2-3 m succession of yellow fine to coarse locally trough cross-bedded sands and calcareous mudstone, called L1 to L4 (Fig. 1C). Bioclastic sands more or less bioturbated, partially decarbonated, and cemented form L5 at the upper part of Bed 2. They represent aeolian deposits which accumulated in damp vegetated depressions with evidence of pedogenesis during warm episodes of subaerial exposure (Texier et al. 2002; Gallotti et al. 2021; Lefèvre et al. 2021).

The archaeology of ThI-L is limited to archaeostratigraphic sub-units L1 at the base and L5 at the top (Fig. 1C). ThI-L1 has been surveyed and tested on about 1000 m² and systematically excavated in 1988-1996 and 2006-2008 in two main areas of 68 m² (Zone 1) and 75 m² (Zone 2) and 20 m² of test trenches (Fig. 2A-E). ThI-L5 has been excavated only in Zone 1. Both sub-units yielded faunal remains, lithic artefacts, and unmodified pebbles/cobbles.

OH1-Bed2 limestone was dated to 989 ± 208 ka and 948 ± 599 ka, using the OSL signal of quartz grains with large uncertainties (Rhodes et al. 2006). Paleomagnetism indicates that OH1-Bed 2 is older than MIS 31 (Jaramillo Subchron) and possibly older than MIS 35. Reverse polarity of OH1-Bed 2 and alternation of pedogenesis during warm episodes and Saharan dust inputs allow to correlate L1 to Marine Isotope Stage (MIS) 43 or 39, and subunit L5 to MIS 41 or early MIS 37 (Gallotti et al. 2021; Supplementary Material A and Fig. S1).
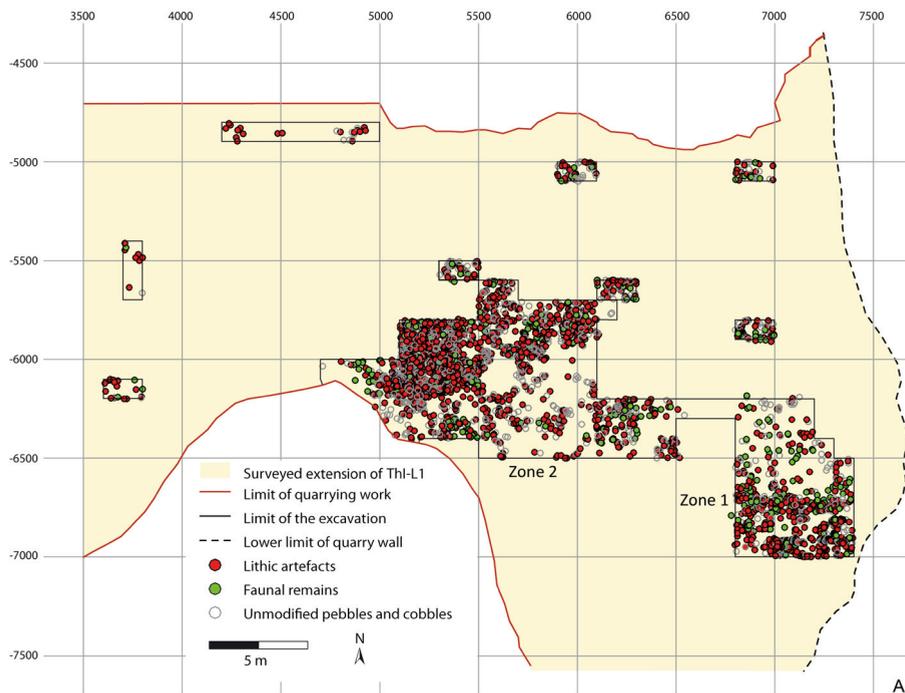
Fig. 2 - (A) Horizontal plan with the distribution of all the mapped remains at ThI-L1. (B) View of the ThI-L1 excavation in 2007. (C) View of the Zone 2 excavation of ThI-L1 in 2007. (D, E) Details of the Zone 2 excavation of ThI-L1 in 2008.

CATEGORIES	MAPPED	SIEVING	TOTAL	%
Cores	442	-	442	*13.1*
Core fragments	52	3	55	*1.6*
Whole flakes	438	437	875	*25.9*
Broken flakes	272	609	881	*25.2*
Retouched flakes	1	2	3	*0.1*
Large flakes	17	-	17	*0.5*
LCTs	219	-	219	*6.5*
LCT tips	10	5	15	*0.4*
Hammerstones	30	-	30	*0.9*
Debris	181	655	836	*24.8*
Total artefacts	**1662**	**1711**	**3373**	***100.0***
Pebbles	864	1928	2792	*89.6*
Broken pebbles	24	21	45	*1.4*
Cobbles	275	-	275	*8.8*
Broken cobbles	3	-	3	*0.1*
Total unmodified objects	**1166**	**1949**	**3115**	***100.0***

Materials and methods

Systematic excavations by the Franco-Moroccan Casablanca program at ThI-L1 yielded 3845 lithic artefacts (3373 of quartzites and 472 of silicites) and 3677 unmodified objects (3115 of quartzites and 562 of silicites). Sediments have been collected from each 1 m², dissociated with diluted acetic acid and sieved by water to recover lithic small items (Tab. 1).

As the study about the silicite assemblage has been recently published (Gallotti et al. 2020; Supplementary Material B, Tab. S1, and Figs. S2 and S3), we report here the study of the quartzite assemblage analysed between 2017-2019 and in 2022, which is stored at the field laboratory of ThI and at *Institut National des Sciences de l'Archéologie et du Patrimoine* (INSAP) in Rabat.

The study of the artefacts is founded on the techno-economic approach following the *chaîne opératoire* concept (Leroi-Gourhan 1964, 1971; Lemonnier 1976, 1986; Pelegrin 1985; Geneste 1989, 1991; Perlès 1991; Inizan et al. 1999). We examined all the technical sequences involved in lithic production in order to decipher the related skills and competencies. The analysis of unmodified items (pebbles and cobbles) recovered at ThI-L1 was conceived as an integral part of the techno-economic analysis (Inizan et al. 1999; Goldman-Neuman and Hovers 2011; Gallotti and Mussi 2017). As first step in *chaîne opératoire* reconstruction, we performed the particle size distribution analysis of the lithic industry, which allows to evaluate the integrity of the collected series (Schick 1986; Lenoble 2005; Bertran et al. 2012; Maurin et al. 2017). In addition, experimental knapping was carried out on quartzite cobbles collected in current or fossil beaches, i.e., 19 productions for a total of 1350 items measured (Fig. S4). The details of the analysis procedures are available in the Supplementary Material C and Figs S4 and S5.

Results

The quartzite assemblage composition and its integrity

Two main quartzite productions coexisted at ThI-L1: one devoted to the production of LCTs, the other focused on the flaking of small to medium-sized flakes. Cobbles and rare pebbles bearing percussion marks were used as active hammerstones for knapping (Tab. 1).

All cores were exploited to produce exclusively small-medium flakes. However, small-medium flakes could belong to both small flaking and LCT shaping but are dimensionally distinct from the large flakes used as blanks for the LCT manufacture (Fig. 3A). This metrical dichotomy corresponds to an intrinsic and not an arbitrary division.

The number of negative scars on the analysed cores and LCTs accounts to 5770, 3401 belonging to LCTs and 3333 to cores, while the number of the analysed small-medium sized
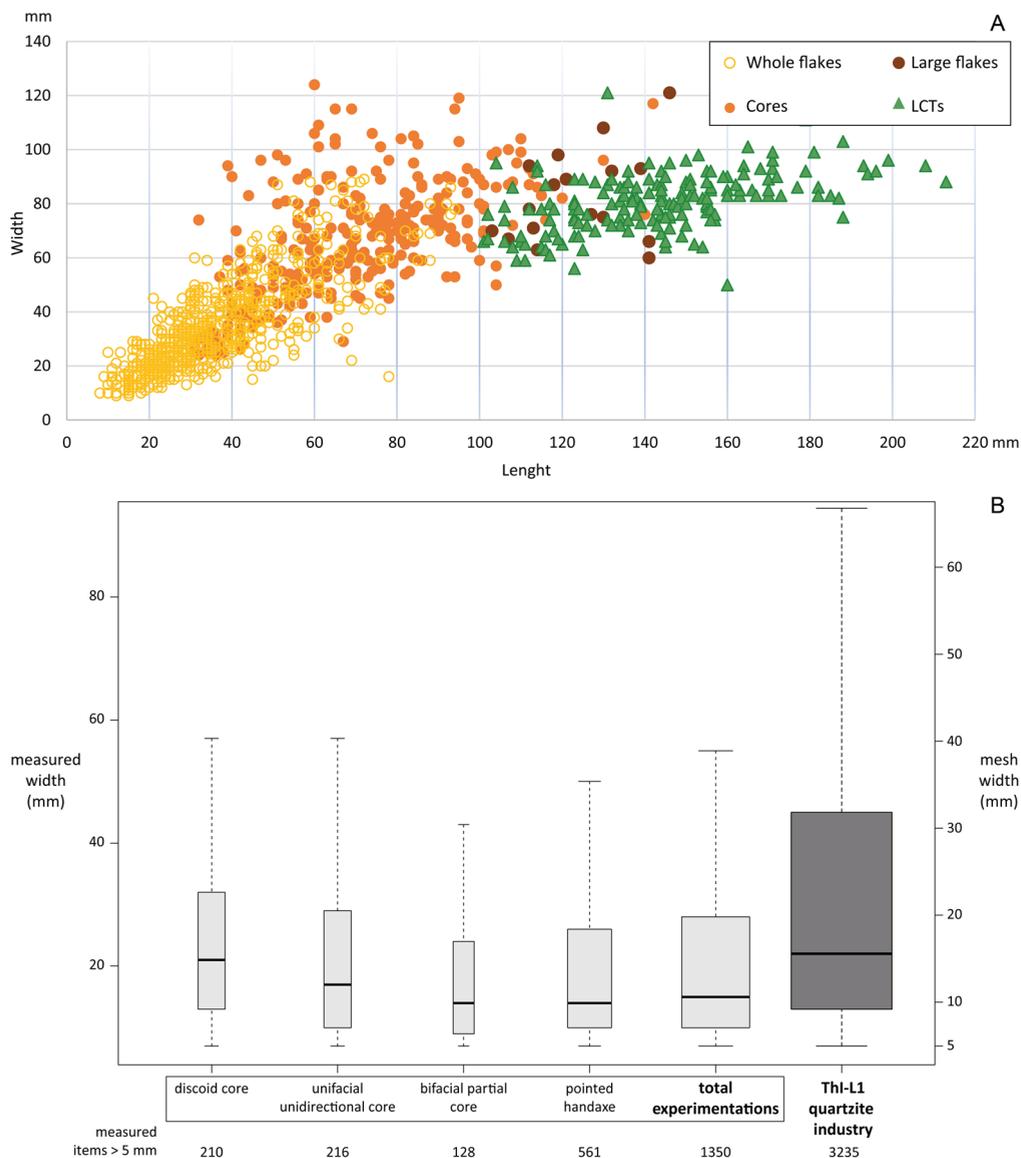
Fig. 3 - (A) Size distribution (mm) of quartzite cores, whole flakes (including retouched flakes), large flakes, and LCTs. (B) Distribution of the experimental flake width >5 mm by type of production and comparison with ThI-L1 industry (outliers not shown).

flakes (whole, broken, and retouched) is 1615. Flake count shows a large deficit, but flakes document all the knapping stages and methods identified in the core and LCT analysis and cannot be automatically interpreted as the result of a spatio/temporal fragmentation of the *chaînes opératoires*.

Experimentation provides clues to understand flakes production. The distribution of the experimental flake width is relatively constant

ThI-L1 quartzite industry (N=3235)

experimental flaking on Casablanca quartzites (N=1350):
- ● n > 50 flakes
- ● n < 50 flakes

experimental flaking from Bertran *et al.* 2012
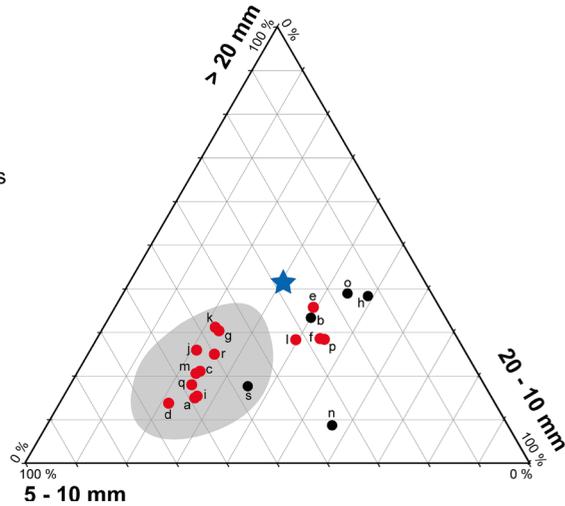
ThI-L1 industry, total > 5 mm without hammerstones

mesh	5-10 mm	10-20 mm	> 20 mm	
width	7,1 - 14,1 mm	14,1 - 28,3 mm	> 28,3 mm	total
N	902	990	1343	3235
%	28 %	31 %	42 %	100 %

ref.	technical objective	5-10 mm	10-20 mm	> 20 mm	total
a	beveled handaxe	110	49	28	**187**
b	bifacial partial core	4	6	5	**15**
c	bifacial partial core	34	15	13	**62**
d	bifacial partial core (broken)	33	11	7	**51**
e	discoid core	21	33	30	**84**
f	discoid core	19	31	20	**70**
g	discoid core (broken)	26	13	17	**56**
h	pick	6	23	18	**47**
i	pointed handaxe	159	72	42	**273**
j	pointed handaxe	43	17	21	**81**
k	pointed handaxe	36	17	24	**77**
l	pointed handaxe (broken point)	31	38	27	**96**
m	pointed handaxe (broken point)	19	8	7	**34**
n	unifacial unidirectional core	8	13	2	**23**
o	unifacial unidirectional core	3	8	7	**18**
p	unifacial unidirectional core	14	24	15	**53**
q	unifacial unidirectional core	29	12	9	**50**
r	unifacial unidirectional core	28	14	14	**56**
s	unifacial unidirectional core (broken)	8	6	3	**17**
	total	631	410	309	1350

***Fig. 4** - Ternary diagram of 5-10 mm, 10-20 and >20 mm fractions, and table of results.*

from one technical objective to another (Fig. 3B). The ternary diagram representing the proportion of 5-10 mm, 10-20 and >20 mm fractions of both archaeological and experimental series allows the following results (Fig. 4):

- The particle size composition of the ThI-L1 series shows a large proportion of coarse fractions. On the ternary diagram (Fig. 4), it is outside the experimental area defined by Bertran et al. (2012), in the area of sites residualized by runoff. Some of the smaller objects have therefore disappeared from the initial assemblage, as also shown by the techno-economic study of the industry. Due to the water assisted deposition environment, runoff partly explains this sorting. Fabric analysis of large elongated quartzite artefacts and bones distributed on the archaeological surfaces attests just a slight re-orientation (Raynal et al. 2002). Several unmodified pebbles are largely located at bottom of ThI-L1 deposit and this sedimentary structure implies that low current transported and deposited sediments. Nevertheless, artefacts preserve fresh cutting edges, though small items may have been displaced.

- Most of the experimental assemblages which provided sufficient fragments ($n > 50$) present a composition in accordance with the results published by Bertran et al. (2012), mainly based on silicite flaking. However, four experiments (referenced e, f, l and p) show different compositions, with a >10 mm fraction more important. On the ternary diagram, they are located in the same sector, near the point representing ThI-L1 industry (Fig. 4). Even if these four experiments provided a small part of the entire experimental corpus (303 items), they suggest that the convex envelope grouping the knapping experiments for Acheulean industries on quartzite should be extended to the coarser fractions, which future experiments will have to confirm. This result also suggests that the sorting of the ThI-L1 assemblage is probably moderate, affecting only the smallest elements. We must consider that ThI-L1 deposits outcrop on a thousand

square meters. This surface only represents a fraction of Bed 2 which extends on several hundred meters to the South-West and is fossiliferous all along. In such an extended open-air site we must expect a fragmentation of tasks and mobility of artefacts within it, as already pointed out by Champault about the site of Tachenghit (Algeria) cited in Biberson (1961a). Moreover, ThI-L1 was on the edge of a fluctuating water body and this implies some disturbance of its internal organization caused by temporary flooding. Thus, counts of the different knapping products from the excavated areas may not be representative of the site composition and this limits the technological discussion about the actual *chaîne opératoire* segmentation (Gallotti et al. 2020).

Raw materials

The lithic assemblage of ThI-L1 is mainly composed of Paleozoic tenaceous rocks (87.7% of the artefacts and 84.7% of the unmodified objects), i.e., quartzites abundantly available in local primary and secondary sources. The remaining objects are of silicites (Gallotti et al. 2020).

The term "quartzites" includes several varieties of Cambrian-Ordovician basement rocks that form the bulk of the Casablanca anticlinorium and are essentially Acadian and Arenig in age (Cailleux 1994). At the base of the Acadian, there are shales, siltstones, micaceous and chlorite sandstones (Bouznika shales), then arkozic feldspathic arenites and feldspathic grauwackes interspersed with fine sandstones that form a bar in the landscape (El Hank "quartzite" formation (Fig. 1A); Delarue et al. 1956; Destombes and Jeannette 1956, 1966); on the roof of the Acadian, more or less coarse green schists, grauwackes and arenites form the Dar Bouazza series (Hamoumi and Izart 1994; André et al. 1987). These Cambrian deposits are interspersed with volcanic facies, flows, tuffs, and conglomerates with volcanic pebbles (Zahraoui 1991). The Ordovician is represented by a thick series of more than 1000 m: conglomerates, chloritothinned pelites, fine sandstones or quartzites form bars (Zahraoui 1991).

Fig. 5 - *(A) Quartzite outcrop and cobble beach at El Hank. (B) Quartzite outcrop at Sidi Abderrahmane. (C) Quartzite outcrop at Dar Bouazza showing a large joint system. (D) Cobble beache at Dar Bouazza. (E) Cobbles from present beaches bearing concussion fractures along the edges (1, 5); broken cores from ThI-L1 showing a joint fracture occurring during flaking (2-4); LCT (6) and core (7) from ThI-L1 showing ancient removals probably due to percussion fractures; core on an ancient flake (8) from ThI-L1.*

The quartzites are low-porous, dense rocks with variable mechanical properties depending upon bedding, cracking, porosity, and alteration. They form the basement of the Mio-Plio-Pleistocene formations of the Casablanca sequence. They were exposed on the foreshores (Fig. 5A) or were locally preserved in points (Fig. 5B). Notched by the wadis and Quaternary paleo-rivers, they largely supplied the alluvial deposits of the wadis and the various ancient beaches with pebbles/cobbles of various shapes and sizes. Even today, the raw material is still available in the form of whole or naturally fractured cobbles (Fig. 5D): from Casablanca to Dar Bouazza (Fig. 1A), there is a diverse range of clasts on today's beaches (whole pebbles/cobbles, broken pebbles/cobbles, blocks, and small fragments).

We have distinguished a light grey facies, very well crystallised, with conchoidal fracture and mechanical properties very close to those of silicites and largely outcropping between El Hank and Sidi Abderrahmane (Fig. 1A; Fig. 5A), and some less silicified and micaceous varieties, less resistant to weathering, greenish to purple and available in the form of cobbles outcropping between Sidi Abderrahmane and Dar Bouazza (Fig. 1A; Fig. 5C). Quartzite unmodified items and artefacts from ThI-L1 mainly belong to the light grey facies.

Present outcrops show large joint systems (Fig. 5C) and internal planar bedding and joints. Beach cobbles retain these "planes", which are often not visible on the external surface. During knapping, they can hinder the propagation of the conchoidal fracture and provoke the breakage of the blanks. In the ThI-L1 assemblage internal joints frequently caused the breakage of the cobbles after detaching few flakes (Fig. 5E: 2-4). Other natural fractures are due to the fortuitous concussion caused by the impact of other stones on cobble beaches. These fractures, usually adjacent and/or overlapping and located on the cobble edge, may mimic intentional knapping removal negatives (Fig. 5E: 1, 5). Unlike joints, the presence of concussion removals could be a possible selection criterion during procurement since they could create suitable angles for knapping and facilitate the initial knapping phases. Indeed, the archaeological assemblage yielded some cores and LCTs displaying previous detachments, well distinguishable from negative scars connected with the flaking/shaping process due to their high degree of abrasion and most probably due to concussion mechanisms (Fig. 5E: 6, 7). However, it cannot be excluded that some of these fractures may represent actual ancient removals, documenting the recycling of rolled artefacts as it would seem to document the core in Fig. 5E: 8, which blank is an ancient flake.

Quartzite unmodified assemblage

The analysed unmodified assemblage is composed by 3115 quartzite items (131.35 kg). Their length varies between 5 and 189 mm and their frequency decreases with increasing length (Fig. S6A). 64.4% are pebbles with a length ≤3 cm, a size never used as blank for knapping. The remaining 35.6% is largely composed by pebbles between 31 and 63 mm (n = 816) followed by medium sized cobbles (n = 160 with a length between 64 and 100 mm), both corresponding to the blank size for small flaking cores, large cobbles (n = 115 with a length between 101 and 189 mm) matching the blank size for both small flaking and LCT manufacture, and broken pebbles and cobbles (n = 48). The three dimensions of these three groups have great variation (Fig. 6A-C). However, the thickness of the large cobbles, regardless of their morphology, varies much less than their length and width (Fig. 6A) and could represent a selection criterion for LCT blanks (see section 4.5).

Among the pebbles and cobbles suitable for knapping, ovoid shape is the most common form (Fig. 7: 2-6; Fig. S6B-D), followed by subcircular (Fig. 7: 1, 7-9, 15; Fig. S6B-D), subquadrangular (Fig. 7: 10-13; Fig. S6B-D) and subtriangular forms (Fig. 7: 14; Fig. S6B-D).

Subquadrangular and subtriangular forms are usually rounded elements preserving the natural angles of the quartzite clast before it was rounded off by the transport. Despite their rounded shape, also ovoid and subcircular pebbles and
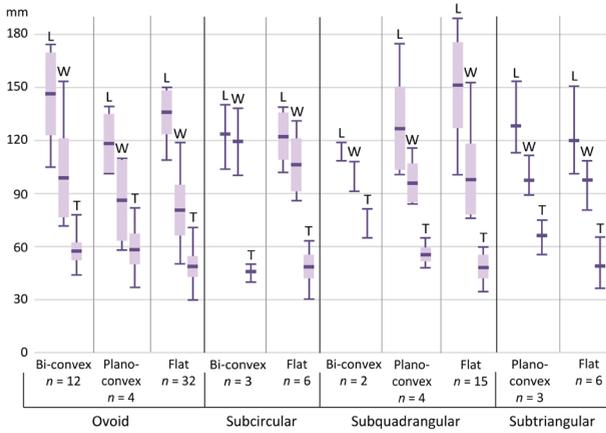
Fig. 6 - Pebble/cobble dimensions. (A) Length (L), width (W), and thickness (T) distribution (mm) of the cobbles with a length >10 cm grouped by shape. (B) Length (L), width (W), and thickness (T) distribution (mm) of the cobbles with a length between 64 and 99 mm grouped by shape. One cobble with a concavo-convex cross-section has not been included. Its dimensions are 99-86-36 mm. (C) Length (L), width (W), and thickness (T) distribution (mm) of the pebbles with a length between 30 and 63 mm grouped by shape.

A
Cobbles with a lenght > 100 mm
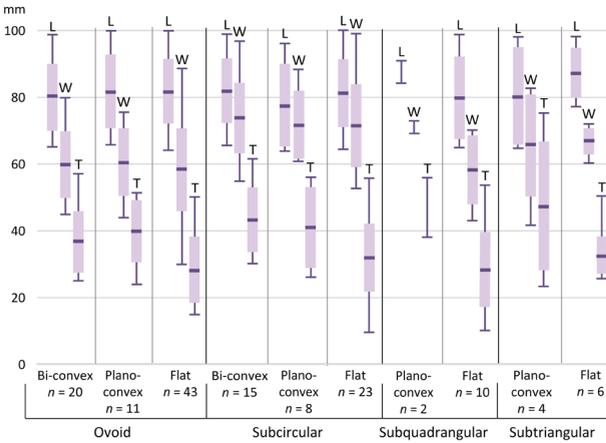
B
Cobbles with a lenght between 64 and 99 mm
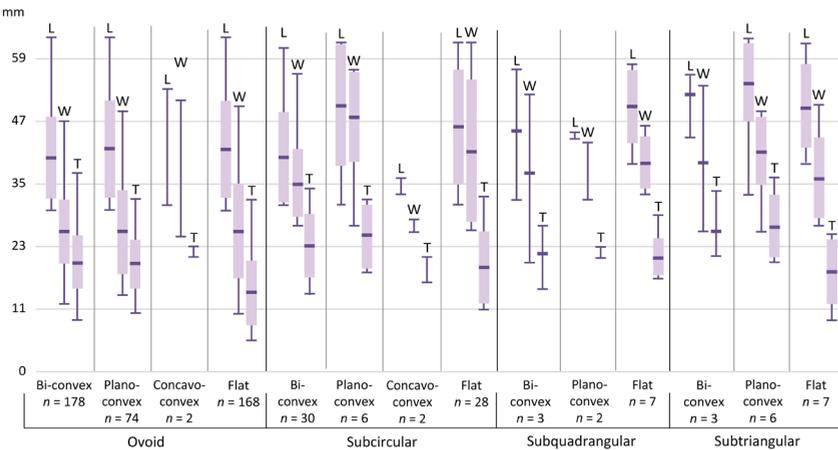
C
Pebbles with a lenght between 30 and 63 mm

Fig. 7 - 1) Large semicircular bi-convex cobble. (2) Large ovoid flat cobble. (3) Large ovoid bi-convex cobble. (4) Ovoid bi-convex cobble. (5) Ovoid bi-convex pebble. (6) Ovoid flat cobble. (7) Subcircular bi-convex cobble with angular planes. (8) Subcircular concavo-convex cobble. (9) Semicircular plano-convex cobble. (10-12) Subquadrangular flat cobbles. (13) Subquadrangular plano-convex cobble. (14) Subtriangular concavo-convex cobble. (15) Subcircular bi-convex cobble.

cobbles can present two or more angular surfaces (Fig. 7: 7). Flat and bi-convex cross-sections are very frequent (Fig. 7: 1-6, 10-12, 15; Fig. S6B-D). Plano-convex elements are less frequent and concavo-convex cross-sections are very few (Fig. 7: 8, 9, 13, 14; Fig. S6B-D).

Large flake production
    Large flakes (*n* = 16; Tab. 1) are *entame* flakes (*n* = 13; Fig. 8: 1, 3, 4) and cortical flakes with plain butts (*n* = 3) or with butt deleted by few small removals (*n* = 1; Fig. 8: 2). *Entame* flakes (see definition in Inizan et al. 1999) were extracted using the cobble-opening flake core method, as described by Sharon (2011, p. 128): "A cobble was struck once at a precise location on the cortex at an obtuse angle… The strike produced a blank that was perfectly suited to handaxe production …with minimal necessity, if at all, of secondary retouch. This method was highly controlled, due to the meticulous attention paid both to raw material block size and shape selection and to the
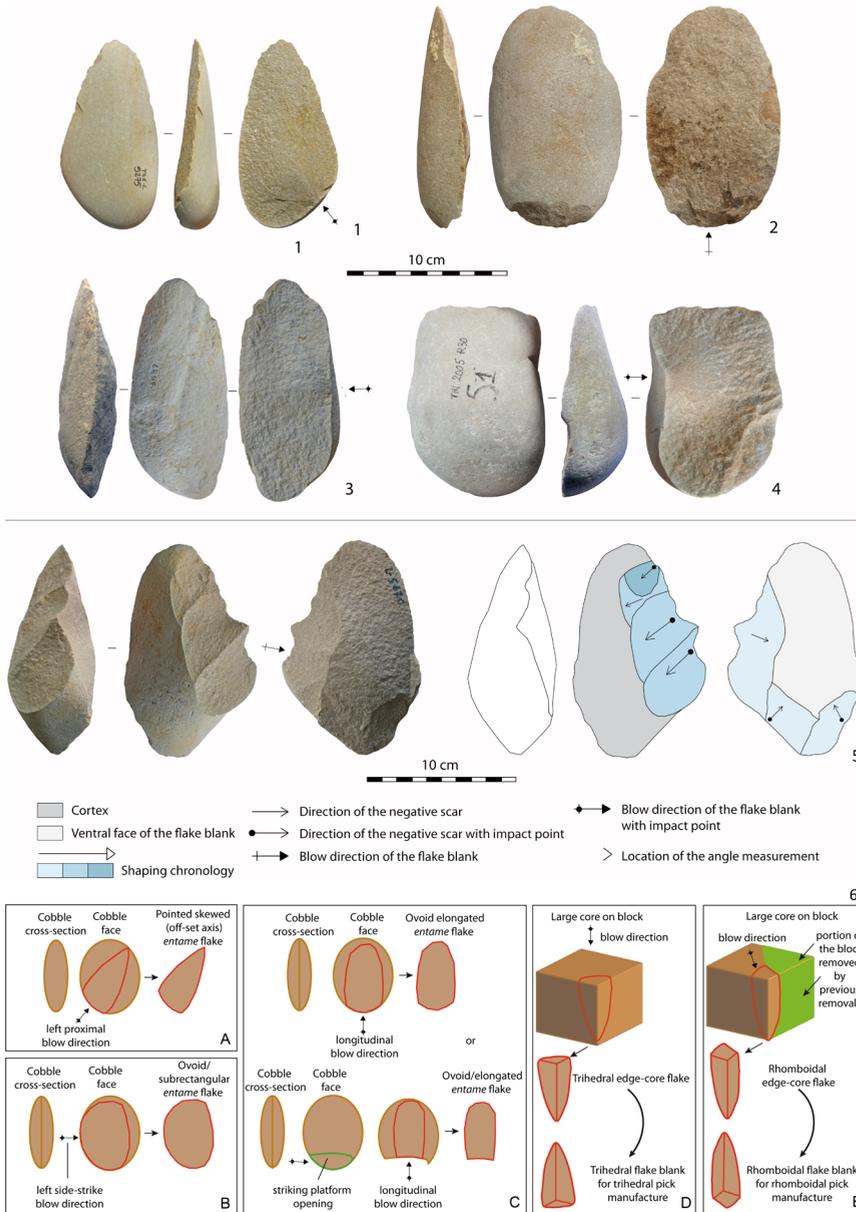
Fig. 8 - (1, 3, 4) Entame *flakes (1: pointed left proximal side-struck flake with an offset axis; 3: ovoid left side-struck flake; 4: subrectangular right side-struck flake). (2) Ovoid longitudinal proximal flake with butt deleted by few small removals; (5) Massive scraper. (6) Schemes of the large flake production: (A)* entame *core method for the production of pointed skewed flakes; (B)* entame *core method for the production of ovoid/subrectangular side-struck flakes; (C)* entame *core method for the production of ovoid longitudinal flakes; (D) production of trihedral edge-core flakes for trihedral pick manufacture; (E) production of rhomboidal edge-core flakes for rhomboidal pick manufacture. Unmodified trihedral and rhomboidal edge-core flakes lack in the ThI-L1 assemblage. They are present only as pick blanks.*

systematic removal of a single, preplanned primary flake". As pointed by Sharon (2010), when extracted from relatively flat cobbles which had the appropriate thickness and surface for striking at the required angle, the flakes produced with this method served as LCT blanks. Most of the large cobbles recorded at ThI-L1 are flat or slightly bi-convex rather thin cobbles (Fig. 6A; Fig. 7: 1-3) and were suitable to play the role of *entame* cores. The average length of these large cobbles (147.3 mm, Fig. 6A) fits well the average length of the large flakes (123.3 mm, Tab. 2).

In addition, *entame* flakes have an average flaking angle of 128° and are pointed (*n* = 7), ovoid (*n* = 1) and subrectangular (*n* = 5). Despite the small size of the sample, their shape does not seem random, but anticipated by the choice of the exact percussion point on the cobble and the consequent blow direction (Fig. 8: 6A-C). Pointed *entame* flakes are all left proximal side-struck flakes with an offset axis (Fig. 8: 1, 6A), except one which is a right proximal side-struck

Tab. 2 - ThI-L1. Dimensions (mm) and weight (g) of the unmodified large flakes according to the shape.

SHAPE		LENGTH	WIDTH	THICKNESS	WEIGHT
Pointed (n =9)	Min.	112.0	60.0	29.0	176.0
	Max.	146.0	121.0	47.0	498.0
	Mean	123.0	85.4	37.3	357.0
	St. dev.	13.1	20.2	6.1	123.4
Sub-rectangular (n = 5)	Min.	103.0	66.0	35.0	268.0
	Max.	141.0	78.0	56.0	421.0
	Mean	118.0	71.4	41.2	330.6
	St. dev.	15.7	5.4	8.6	81.2
Ovoid elongated (n = 3)	Min.	130.0	75.0	32.0	341.0
	Max.	139.0	108.0	38.0	500.0
	Mean	133.0	92.0	35.3	436.7

Tab. 3 - Frequencies of the non-broken LCT blank types.

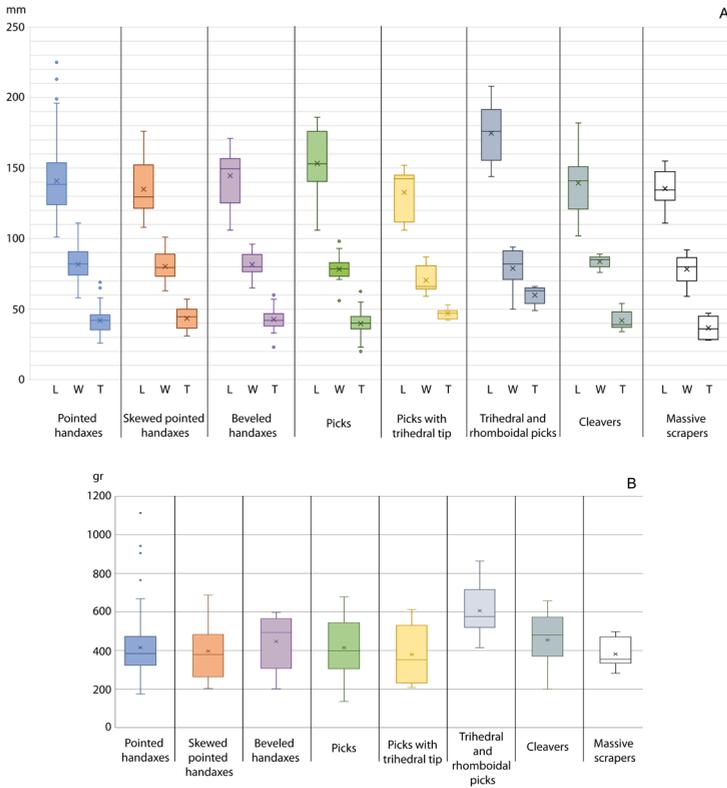| BLANK		SHAPED LCTS							RETOUCHED LCTS
		POINTED HANDAXES (N = 80)	POINTED SKEWED HANDAXES (N = 18)	BEVELED HANDAXES (N = 16)	PICKS (N = 19)	PICKS WITH A TRIHEDRAL TIP (N = 8)	TRIHEDRAL AND RHOMBOIDAL PICKS (N = 8)	CLEAVERS (N = 11)	MASSIVE SCRAPERS (N = 8)
Large cobbles	Bi-convex	22	9	8	-	-	-	-	-
	Plano-convex	15	-	4	1	-	-	-	-
	Flat	38	3	4	8	-	-	-	-
	Angular	6	-	-	2	6	3	-	-
Split cobbles		5	2	-	1	2	-	-	-
Large flakes	Entame flake	5	2	-	2	-	-	9	2
	Cortical flake	9	5	1	3	-	-	2	2
	Flake	-	1	-	2	-	4	-	4
Indeterminable		1	1	-	-	-	3	-	-
Total		**101**	**23**	**17**	**19**	**8**	**10**	**11**	**8**

Fig. 9 - Boxplots of the three dimensions (A) and weight (B) of the LCTs grouped by tool-types. Boxes extend from the 25th to the 75th per-centile of each group's distribution of values. The horizontal line within the box marks the median, the cross within the box marks the mean. Outliers that differ significantly from the rest of the dataset are plotted as individual points beyond the whiskers on the box-plot.

flake (Fig. 8: 3), while the subrectangular and ovoid ones are left (*n* = 3) or right (*n* = 2) side-struck flakes (Fig. 8: 4, Fig. 8: 6A-C). One of the latter resembles type 0 in Tixier's cleaver typology (Tixier 1956) and is also ideal blank for cleaver manufacture (Fig. 8: 4).

Cortical flakes with plain butts were removed after a flake had already been extracted from the cobble core, which negative was used by knap-pers as a striking platform. They are longitudinal flakes, ovoid elongated in shape (Fig. 8: 6C). The average flaking angle is 127°, a value very close to that of the *entame* flakes. This probably means that the striking platform was rectified by a removal to adjust the natural angle of the cobble core.

LCT production

ThI-L1 yielded a rich LCT assemblage, composed of 219 specimens (76.8 kg; Tab. 1) exclusively manufactured in quartzites. Since the

shaping usually does not involve the entire vol-ume of the LCTs, at least on one face, it was pos-sible to recognize the blank type, except for five specimens (Tab. 3).

Twenty-two LCTs have a broken tip. The size of the missing part prevents to reconstruct the shaping process, the morphology, and the dimensions of the LCTs. Fifteen LCT tips have been recorded at ThI-L1 and one of them refits with a broken pick. Among the LCTs that we considered as complete (*n* = 197), 24 specimens show micro-fracture(s) of the tip, but they did not compromise neither the identification of the shaping sequence, nor the morphology and size of the tool.

Only eight LCTs were not shaped but retouched as massive scrapers (Fig. 8: 5). The retouch is limited to portions of the edges, could be unifacial or bifacial as well as invasive or mar-ginal. The blanks are flakes from cobbles with

large portion of the cortex on the dorsal face: five are proximal side-struck skewed flakes and two are side-struck flakes. Only one massive scraper blank is a Kombewa flake and this random product does not indicate the presence of a Kombewa strategy for large flake extraction.

The other LCTs (n = 189) have been manufactured through several shaping processes repeated on several specimens that all tend towards similar morphologies producing different types of LCTs: pointed handaxes (n = 101), skewed pointed handaxes (n = 23), beveled handaxes (n = 17), picks (n = 19), picks with a trihedral tip (n = 8), trihedral and rhomboidal picks (n = 10), and cleavers (n = 11).

Pointed handaxes. Pointed handaxes represent the majority of the LCTs (n = 101). Their length is between 101 and 225 mm (mean 141.3 mm; Fig. 9A; Tab. S2), they are elongated (average L:W ratio = 1.7), and their thickness is the dimension that shows the lowest variation (mean = 42 mm; st. dev. = 8; Fig. 9A; Tab. S2). Their weight is extremely variable, between 175 and 1113 g (mean = 415 g; Fig. 9B; Tab. S2). It must be reminded here that we also found a slight variation in the thickness values of the large unmodified cobbles (Fig. 6A and Fig. 7: 1-3) with a mean at 49 mm, a value very similar to the pointed handaxes thickness (mean = 42 mm). The thickness mean is even closer if we consider only the pointed handaxes in which the central part is spared from shaping and allows to measure the thickness of the cobble blank (mean = 47 mm). Accordingly, the thickness was probably a criterion in the selection of large cobbles for pointed handaxe manufacture.

Blanks are large cobbles (n = 81), flakes (n = 14), and split cobbles (n = 5; Tab. 3). Among large cobble blanks, flat and slightly bi-convex forms (Fig. 10: 2, 3, Fig. 11: 12 and Fig. S7: 1, 2) dominate, followed by plano-convex (Fig. 10: 1 and Fig. 11: 1) and angular ones (Fig. 10: 4; Tab. 3). Six of these cobbles have been used as knapping hammerstones before shaping as demonstrated by the pitted areas located at their extremity (Fig. 10: 2). Flake blanks are *entame* flakes (n = 5; Fig. 11: 3, 4) and cortical flakes (n = 4; Fig. S7: 3, 4). One cortical flake retained a plain butt. All these flakes are proximal side-struck flakes with an off-set axis.

Depending on the blank, two operational schemes can be distinguished. If the blank is a cobble or a split cobble, the first shaping phase consists of the localization of the tip through one or two longitudinal removals (one on each face), slightly oblique to the morphological axis of the cobble. A single handaxe shows a tip created by the cortex of the cobble blank and by two lateral removals posterior to the first shaping series (Fig. 10: 4). The following shaping phases consist of four to six series of removals (mean = 18.9 removals; Fig. 12A) aiming to modify just the lateral edges making them convergent and give the pointed shape to the tool (Fig. 10: 1, 3, Fig. 11: 1, and Fig. S7: 1). Rarely invasive removals penetrate the blank volume on one face only (Fig. 10: 2, 4, Fig. 11: 2, and Fig. S7: 2). The majority of these handaxes lack all-round shaped edges (Fig. 12B) and their proximal portion is usually unmodified (Fig. 10: 1, 3, Fig. 11: 1, 2, and Fig. S7: 1, 2) or can show areas with concentrated pitting due, in most of the cases, to the previous use of the cobble blank as hammerstone (n = 6; Fig. 10: 2). The edges shaping either does not extend to the tip (Fig. 10: 2, 4), or it reaches the tip only on one face with one or more removals that always start from a lateral edge, never with a longitudinal removal from the distal edge (Fig. 10: 1, 3, Fig. 11: 1, 2, and Fig. S7: 1, 2).

If the blank is a large flake, shaping sequences are generally very short, do not modify the proximal part of the tool and concern only portions of the lateral edges with the intention of creating a pointed final shape. In this case the tip is not modified and results from the flaking of the blank (Fig. 11: 4 and Fig. S7: 3). However, in a few cases, shaping can penetrate portions of the flake blank volume and extend to most of its periphery (Fig. 11: 3, 4 and Fig. S7: 3, 4).

Shaping is mostly 1) reverse (n = 78), when the edge (portion) is configured with separate series of removals, first on one face and then on the other face (Fig. 10: 2-4, Fig. 11: 1, 2, 4; Fig. S7: 1-3), 2) bifacial alternating (n = 10), when the edge is configured with series of removals alternating on the two faces (Fig. 10: 1; Fig. S7: 4), and
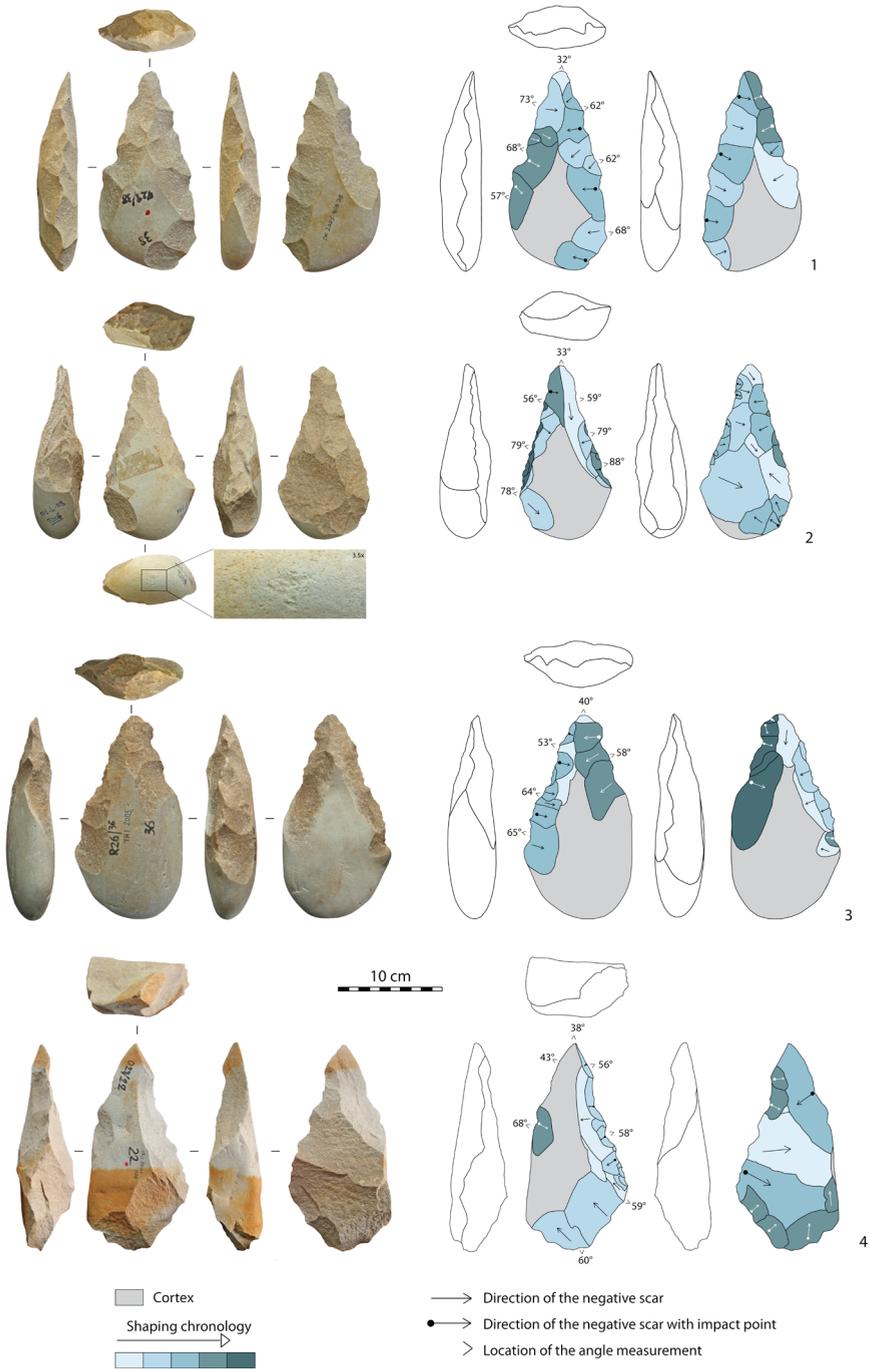
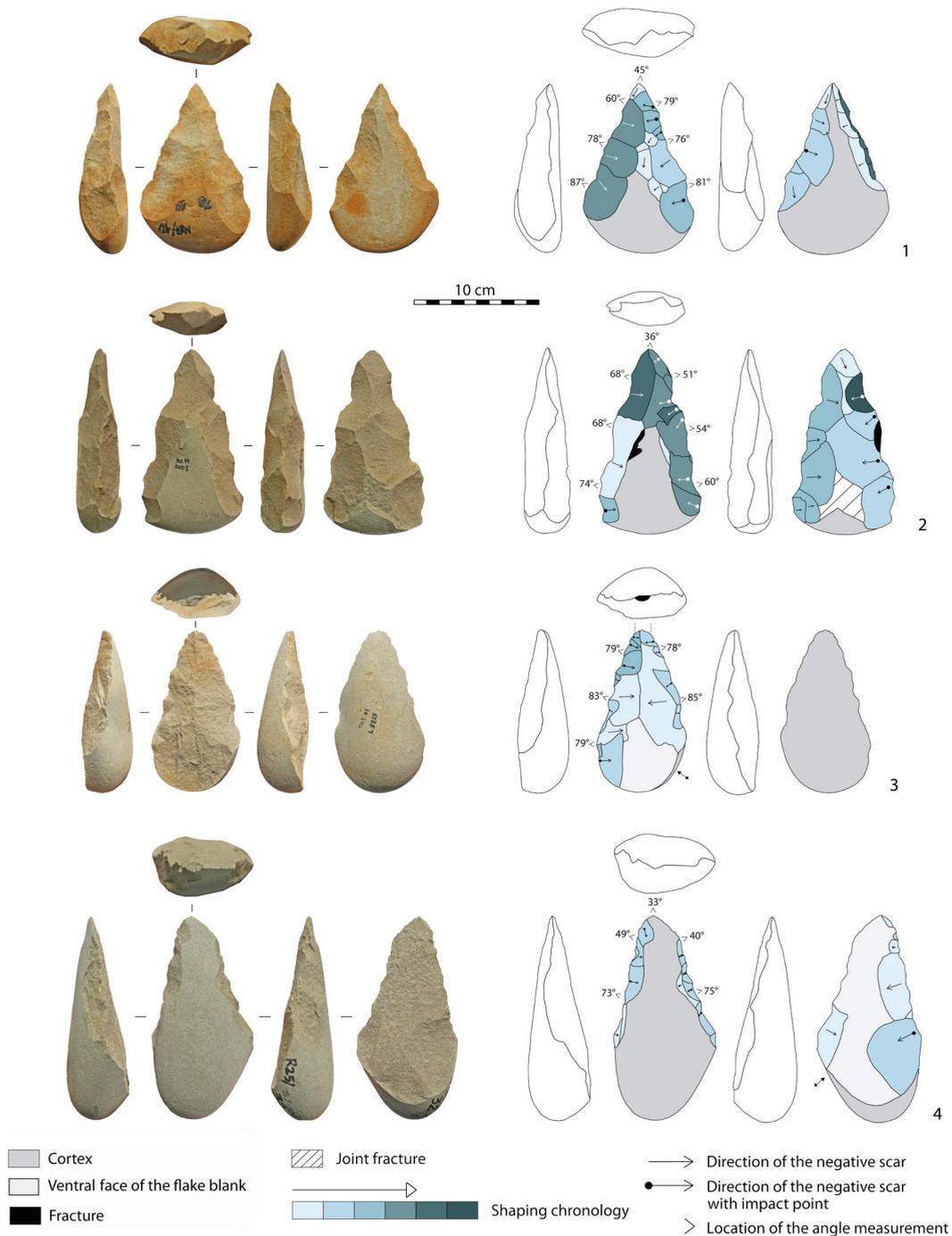Fig. 10 - Pointed handaxes on plano-convex (1), bi-convex (2, 3), and angular cobbles (4).

Fig. 11 - *Pointed handaxes on plano-convex cobble (1), flat cobble (2), and proximal side-struck entame flakes with an off-set axis (3, 4).*
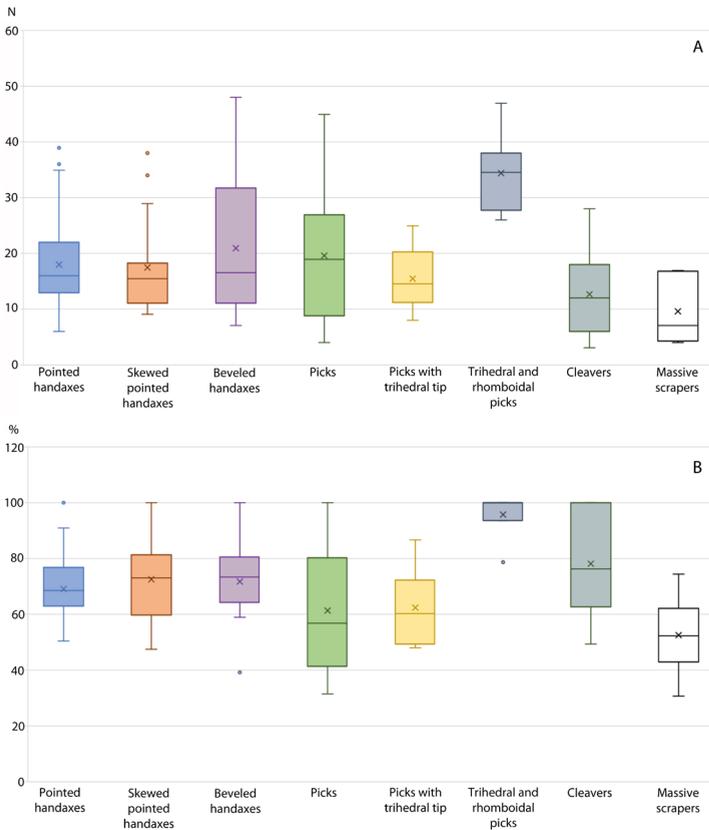
Fig. 12 - Boxplots of the number of the LCT shaping removals (A) and of the cutting edge length with respect to the LCT outline length (B), grouped by tool-types. Boxes extend from the 25th to the 75th percentile of each group's distribution of values. The horizontal line within the box marks the median, the cross within the box marks the mean. Outliers that differ significantly from the rest of the dataset are plotted as individual points beyond the whiskers on the box-plot.

3) unifacial (*n* = 13) when removals involve one face only (Fig. 11: 3). Reverse modality does not seem to be related to a specific blank cross-section, while bifacial alternating shaping is only present on thin and slightly biconvex cobbles (Fig. 10: 1), and unifacial shaping is mostly on *entame* flakes (Fig. 11: 3).

Regardless the shaping modalities, there is a lack of concern for regularized and straight edges, which are mostly denticulated. In a few cases only, the quasi-absence of trimming involves small portions of the edges (Fig. 10: 2, Fig. S7: 1, 4). The angles of the lateral cutting edges therefore show a great intra- and inter-tool variation (Fig. 13) that seems directly proportional to the variation of the thickness of the blank. Usually, these angles vary less when the blanks are thin and their thickness is rather homogeneous when the shaping is bifacial alternating (Fig. 10: 1, 3).

The thickness of the blank affects the angle variation of the lateral edges because 1) removals rarely penetrate the blank volume, 2) shaping is not aimed at the setup of a bifacial and/or bilateral equilibrium plane through the balance of the two opposed surfaces, and 3) the thinning of the blank and the regularization of the edges are mainly absent. The main aim of the edge shaping is exclusively to create their convergence and give the LCT its final pointed shape. Accordingly, these LCTs cannot be considered as bifaces *sensu stricto* (Roche and Texier 1991). This interest in the tip, which can be pointed or slightly convex, is also demonstrated by the fact that its angle is the only one with remarkably similar values (between 29° and 49°; mean = 38°; st. dev = 4.3; Fig. 13) contrary to those of the lateral edges.

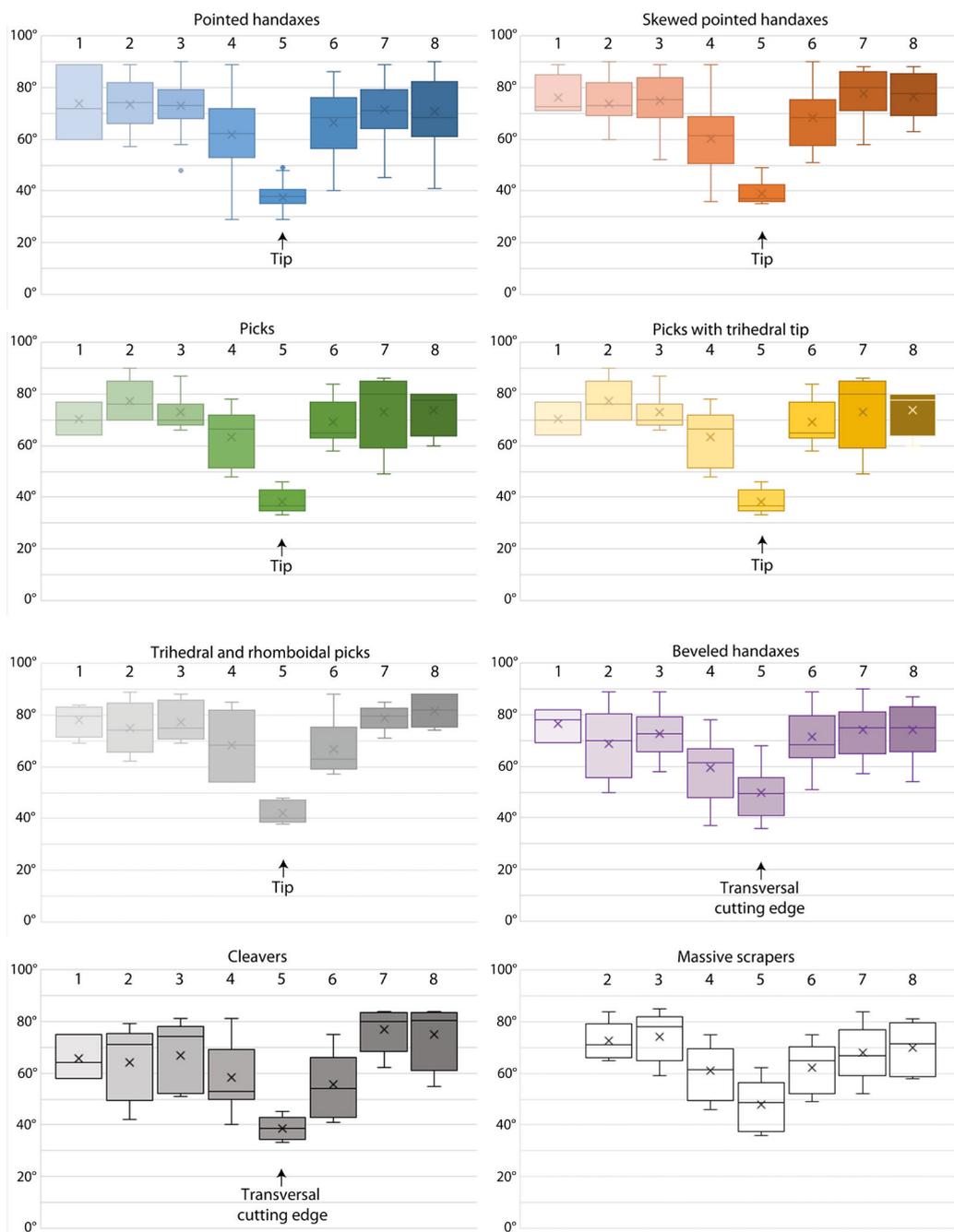Skewed pointed handaxes. This handaxe morphotype (*n* = 23 specimens) is characterized by

Fig. 13 - *Boxplot of the cutting edge angle values grouped by LCT types. Boxes extend from the 25th to the 75th percentile of each group's distribution of values. The horizontal line within the box marks the median, the cross within the box marks the mean. Numbers from 1 to 8 indicate the location of the angle measurement as illustrated in figure S5D.*
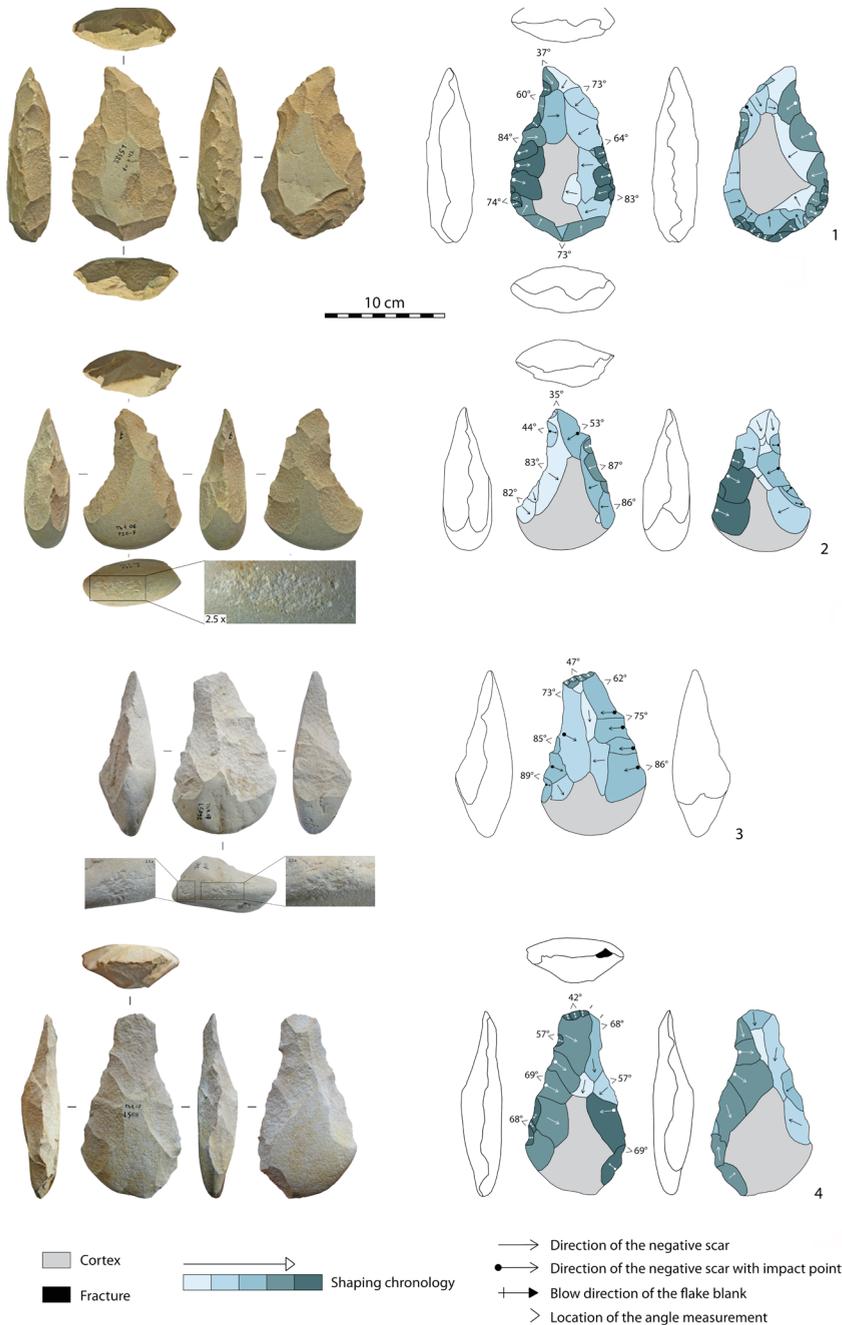
Fig. 14 - *Skewed pointed handaxes on flat cobble (1) and bi-convex cobble (2). Beveled handaxes on bi-convex cobble (3) and plano-convex cobble (4).*

a tip skewed with respect to the morphological axis of the tool. Blanks (Tab. 3) are bi-convex (*n* = 9; Fig. 14: 2) or flat (*n* = 3; Fig. 14: 1) cobbles, split cobbles (*n* = 2), and large side-struck (*n* = 1) or proximal side-strake flakes (*n* = 7). Large flakes are *entame* flakes (*n* = 2), cortical flakes (*n* = 5; Fig. S8: 2), and only in one case the dorsal face of the blank is completely deleted by shaping (Fig. S8: 1). One blank is indeterminable. They are between 108 and 177 mm long (mean 135 mm; Fig. 9A; Tab. S2), with the same elongation index (average L:W ratio = 1.7), and similar thickness values (mean = 43 mm; st. dev. = 7.7; Fig. 9A; Tab. S2) as the pointed ones. In this case also, thickness is the dimension that shows the lowest variation and its mean is very close to that of the unmodified cobbles (49 mm). Their weight varies between 203 and 687 g (mean = 397 g; Fig. 9B; Tab. S2).

The shaping sequences are very similar to those of straight pointed handaxes. The most frequent modifies the lateral edges creating a convergent elongated large tool with a skewed tip and without the intention to balance symmetrical adjacent surfaces. The first operation is the localization of the tip through one or two longitudinal removals (one on each face), slightly oblique to the longest axis of the cobble. Shaping of the lateral edges follows with removals organised in four or five series which are limited to the edges and rarely penetrate the central part of the volume. Shaping sequences are not very long (Fig. 12A) as for pointed handaxes (mean = 18.5 removals) and are in most cases reverse (Fig. 14: 1, 2 and Fig. S8: 1, 2), except for three specimens with unifacial removals. Skewed pointed handaxes with all-round shaped edges are rare (*n* = 2; Fig. 14: 1 and Fig. S8: 2) and their proximal portion remains mostly unmodified (Fig. 14: 3, 4 and Fig. S8: 3). However, it can show areas with concentrated pitting (Fig. 14: 2) due, in most of the cases, to a previous use of the cobble blank as hammerstone (*n* = 3). However, the length of the shaped edges is slightly greater than that of the pointed handaxes (Fig. 12B). In several cases (*n* = 10) one-two very large removals deeply penetrate one edge of the blank creating a long cutting edge and a skewed point (Fig. 14: 2 and Fig. S8: 2).

These removals belong to the first or second series of the shaping sequence and support the idea of planning to obtain a tool with a specific shape of the tip. In the other cases, such a tip is obtained by one or more notches intervening at an advanced shaping stage, which make the lateral edge next to the tip concave and modify the tip axis (Fig. 14: 1 and Fig. S8: 1). In this morphotype also, the tip is not modified after having been created during the first phases of the shaping. Trimming can intervene in the final phase to adjust small portions of the edges. The lateral edges are denticulated and show a great variation of the angles, while the tip angle (mean = 39.5°) does not vary much and is almost equal to that of the pointed handaxes (39°; Fig. 13).

Beveled handaxes. This morphotype accounts for 17 specimens and it is characterized by a transversal cutting edge located on the apical portion (beveled tip) which is straight (Fig. 14: 3 and Fig. S8: 3, 4) or slightly bi-convex (Fig. 14: 4). Only one of these handaxes is shaped on a large flake (Fig. S8: 4), while the others are on bi-convex (*n* = 8; Fig. 14: 3 and Fig. S8: 3), flat (*n* = 4), and plano-convex cobbles (*n* = 4; Fig. 14: 4; Tab. 3). Metrical patterns are very close to those of the previous handaxe morphotypes: the length values are similar to those of skewed pointed handaxes, although the mean is higher (145.4 mm), the elongation index is very close (average L:W ratio = 1.8), and the thickness is rather standard with a constant mean value of 42.5 mm (Fig. 9A; Tab. S2). Their weight varies between 202 and 598 g (mean = 450.2 g; Fig. 9B; Tab. S2).

The chronology and features of the shaping sequences are identical to those of the skewed pointed handaxes: localization of the tip through longitudinal or slightly oblique removals, reverse shaping to create the convergence of the edges and the pointed tool shape, large notches (Fig. 14: 3 and Fig. S8: 3) or continuous removals, which make one distal lateral edge slightly concave, to create a skewed apical part, an unmodified proximal portion which could bear pitted areas mainly due to previous percussion activity (*n* = 4 specimens; Fig. 14: 3). The transversal cutting edge is obtained through a continuous series of marginal retouch (Fig. 14: 3, 4) or through a short notch (Fig. S8: 3)
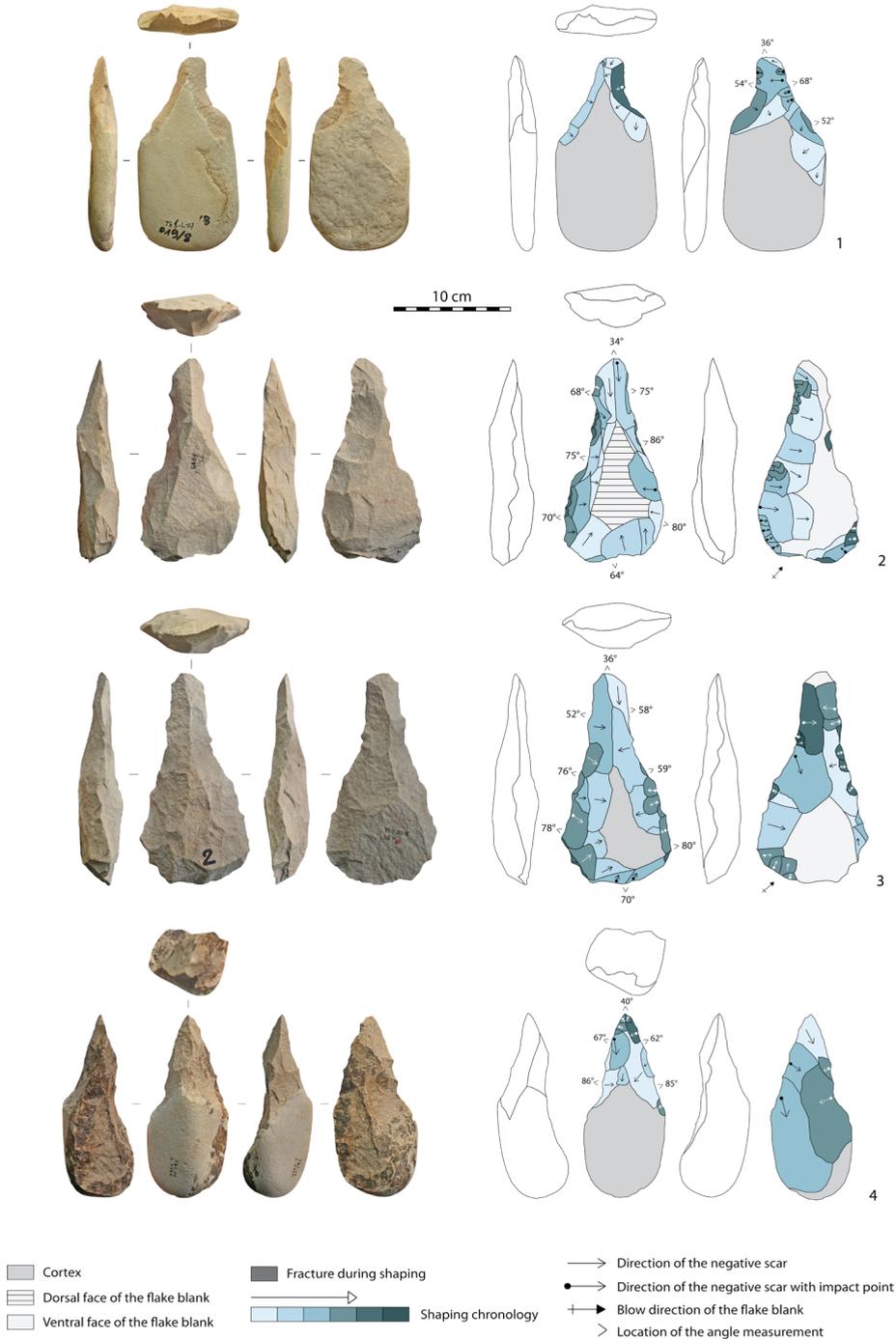
Fig. 15 - Pick with short shaping sequences on flat cobble (1), picks on cortical flakes (2, 3), and pick with a trihedral tip on angular cobble (4).

during the final shaping phase. These latter operations may support the idea of a resharpening of the skewed tip after its breakage. The intention of resharpening of the tip, which excludes a pre-planning of its characteristics, is also documented by the greater variability of the angle of the transversal distal edge compared to that of the tip of the pointed and skewed pointed handaxes (Fig. 13). One question is thus why skewed pointed handaxes only were resharpened. It probably depends on the frequency of the tip breaking which, being skewed, is less resistant to fractures due to use.

Only three items do not present this operational scheme. The beveled tip is obtained through a continuous marginal shaping involving the lateral edges as well as the apical portion (Fig. S8: 4).

Picks. These LCTs have a tip quite distinct with respect both to the lateral edges and to their overall morphology (*n* = 19). Their blanks (Tab. 3) are cobbles (one plano-convex, Fig. S9: 3; eight flat, Fig. 15: 1 and Fig. S10: 1; two angular, Fig. S9: 4), split cobbles (*n* = 1), and flakes (*n* = 7) of which three cortical (Fig. 15: 2, 3) and two *entame* (Fig. S9: 1, 2). Large flake blanks bear a side-struck (Fig. S9: 1, 2) and a proximal side-struck blow direction (Fig. 15: 2, 3).

Picks are between 106 and 186 mm long and in average they are longer (mean 153.8 mm; Fig. 9A; Tab. S2) and more elongated (average L:W ratio = 2) than previous morphotypes, and also thinner (mean = 39 mm; Fig. 9A; Tab. S2). Their weight is extremely variable, between 136 and 678 g (mean = 415 g; Fig. 9B; Tab. S2).

Six of these picks show very short shaping sequences, i.e., few notches on one or both faces which taper the width of the distal half of the blank and create a pointed segment with a straight (Fig. 15: 1 and Fig. S9: 1) or skewed axis (Fig. S9: 2). The tip is pointed or slightly convex and its distal edge is determined by 1) the intersection of the two faces of the flake blank (Fig. S9: 2), 2) by the cobble surface and removals on the other side, detached at the very first phases of the shaping (Fig. 15: 1 and Fig. S9: 3), and 3) by few and very marginal removals (Fig. S9: 1). The distal part of the tip is usually unmodified as well as the basal portion of the tool.
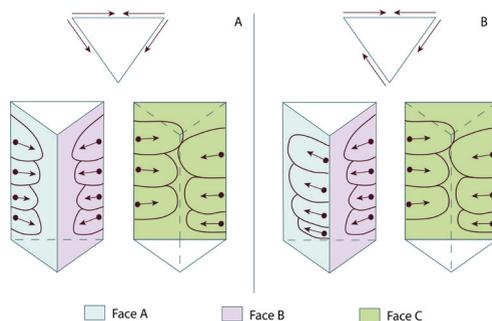

Fig. 16 - *(A) Scheme of the shaping of picks with a trihedral tip. (B) Scheme of shaping from three separate platforms to manufacture a trihedral pick on cobble.*

The shaping sequences of the other ten picks are longer (Fig. 12A), distributed in five-six series of removals. The first phase always corresponds to longitudinal or slightly oblique removals on one or both faces to establish the tip location on the blank. The shaping of the lateral edges follows and for three cases that of the proximal edge. Shaping removals can be reverse (Fig. 15: 2 and Fig. S9: 4) or alternating (Fig. 15: 3 and Fig. S10: 1). The distal half of the tool is thinned by short and wide removals, rarely followed by trimming of edge portion(s), emphasizing the tip segment that is not limited to the very distal end.

Whether unmodified or shaped, the tip is characterized by a little variable distal angle (Fig. 13), with values (mean = 38°; st. dev. = 4.6) close to those of the other pointed LCTs.

One pick bears a pitted area which indicates a hammerstone use of the cobble blank or of the tool itself.

Picks with a trihedral tip. They account for eight specimens and are characterized by a trihedral section at the tip area. Six of them are made on angular large cobbles with a triangular cross-section (Fig. 15: 4 and Fig. S10: 2, 3) and two are on split cobbles (Fig. S10: 4). They are elongated (average L:W ratio = 1.9), shorter (mean = 132.7 mm), slightly thicker (mean = 46.9 mm) and lighter (mean = 379.5 g) than the picks (Fig. 9A, B; Tab. S2).

Shaping follows the triangular profile of the blank without modifying the natural angles among
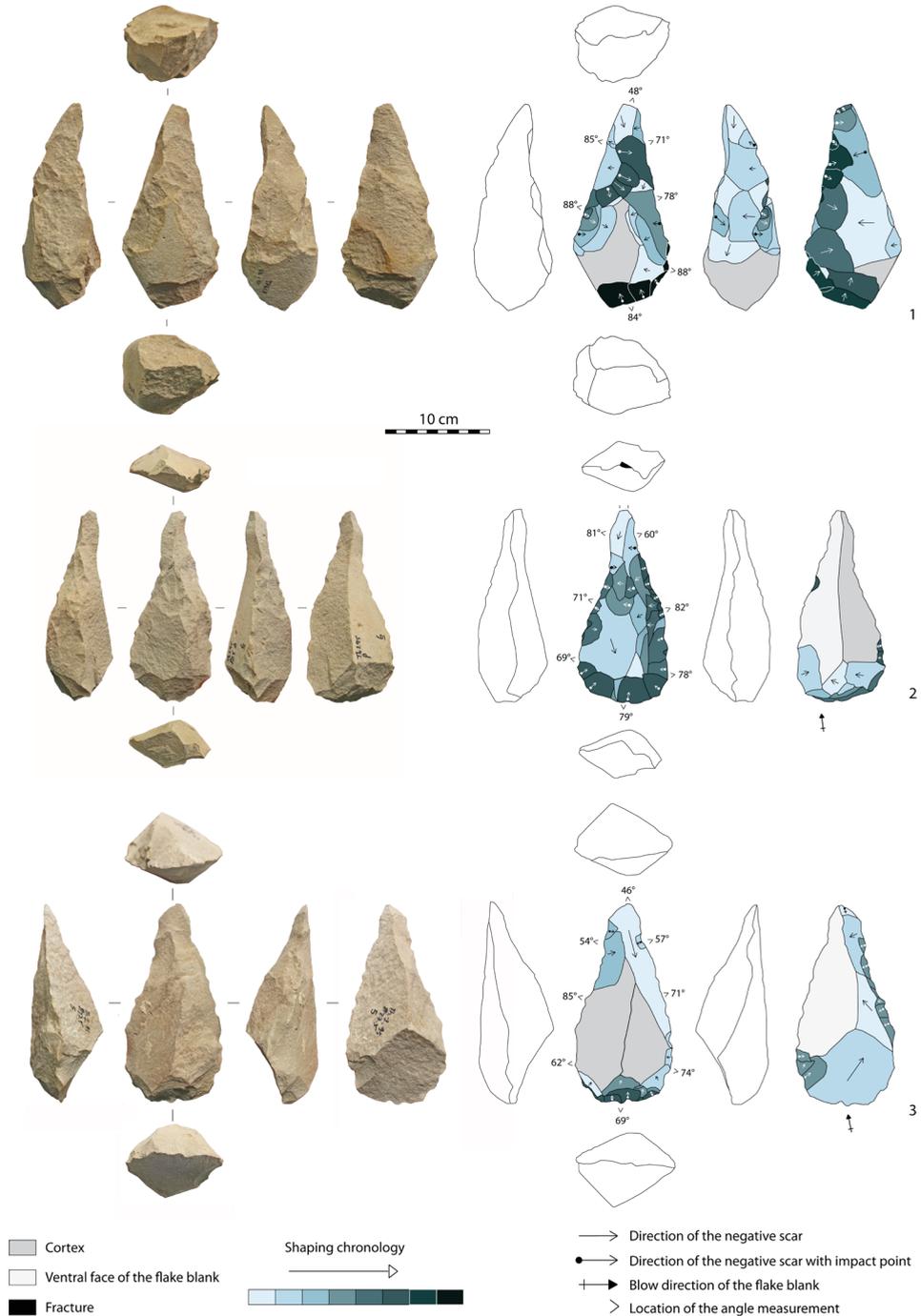
10 cm

Cortex

Ventral face of the flake blank

Fracture

Shaping chronology

Direction of the negative scar

Direction of the negative scar with impact point

Blow direction of the flake blank

Location of the angle measurement

Fig. 17 - (1) Trihedral pick on cobble. (2, 3) Rhomboidal picks on flake.

the three surfaces. However, shaping does not start from three separate platforms because all the removals come from two lateral edges only (Fig. 16A). These picks often show a moderate reduction intensity (Fig. 12A) which involves the distal half of the tool only (Fig. 12B): the main aim was obviously to create a pointed tip independent from the overall morphology of the tool. The location of the tip on the blank is determined by a first series of longitudinal or slightly oblique removals on one or both faces, followed by lateral edge shaping to configure the pointed shape. Some of the removals are short and large notches deeply penetrate the edge giving major emphasis to the tip (Fig. S10: 2, 4). The base of one specimen displays a circumscribed area with battering marks.

Trihedral and rhomboidal picks. Ten LCTs are elongated and robust with a trihedral (*n* = 8) or a rhomboidal (*n* = 2) cross-section involving the (quasi)entire tool volume. These are the largest, most elongated and heaviest morphotypes among the LCTs. Their length varies between 144 and 208 mm long (mean 175 mm), the average L:W ratio is 2.3, and the thickness is greater than in previous types (mean = 60 mm) (Fig. 9A; Tab. S2). Their weight is between 415 and 864 g (mean = 606 g; Fig. 9B; Tab. S2). Blanks (Tab. 3) are large angular cobbles (*n* = 3) and large edge-core flakes (*n* = 4). Three blanks are not identifiable due to the intense shaping. Large unmodified edge-core flakes are absent in the assemblage. However, even if shaping is quite intense, the unmodified residual parts of the different faces allow to assess that these flakes were extracted from large angular blocks by removing their abrupt angles (Fig. 8: 6D, E).

Trihedral picks are shaped from three different striking platforms, i.e. each of the three faces of the blanks is in turn both shaped surface and striking platform (Fig. 16B). However, only two lateral edges are entirely affected by shaping, while the third seems more involved in the tool configuration than aimed to a possible use. The shaping sequences are very long (mean = 36 removals; Fig. 12A), including seven/eight series of removals without final trimming and involve the (quasi)entire contour of the tools (Fig. 12B)

without modifying the original blank geometry (Fig. 17: 1). The first series of removals involves the tip, that is further modified during the last shaping on one face only.

Rhomboidal picks are only two and are made from large flakes. For one specimen (Fig. 17: 2), the four faces correspond to 1) the cortical face of the original block; 2) the ventral face of the flake blank which is interested by shaping only in its proximal portion; 3) two shaped surfaces, one serving both as shaped surface and striking platform, both being intensely shaped through six series of removals and a marginal trimming of small portions of the edges. The tip is the least worked area of the tool. Its rhomboid section is given by a longitudinal removal on one face belonging to the very first phase of the shaping or perhaps corresponding to one of the previous removals on the flake blank, from a subsequent transversal removal on another face, and from the ventral and cortical faces of the flake blank.

The second specimen (Fig. 17: 3) has two cortical surfaces corresponding to the angle of the flaked block, one surface bearing the ventral face of the flake blank, and one flaked surface. Shaping is limited to the tip, to one lateral edge, and to the thinning of the proximal area. The distal part of the tip is created by the ventral face of the flake blank, by a long longitudinal removal that deletes the angle formed by the two cortical surfaces, and by a removal on the other face always detached during the first shaping phase.

The angles of the cutting edges can be very variable, while the tip angle shows less variation, on average slightly wider than those of the other pointed LCTs (mean = 41°; Fig. 13).

Cleavers. Following Tixier's (1956) classification, all the cleavers (*n* = 11) are of 'Type 0', i.e., cleavers with a cortical transverse bit created by the intersection of the ventral surface and the dorsal surface of the flake blank. Blanks are *entame* flakes (*n* = 9; Fig. 18: 1, 3) or cortical flakes (*n* = 2; Fig. 18: 2, 4). The latter could also be *entame* flakes, but since their butt has been removed by the shaping, it is difficult to state with certainty. Eight are side-struck flakes (Fig. 18: 1-3) and three are proximal side-struck flakes with an
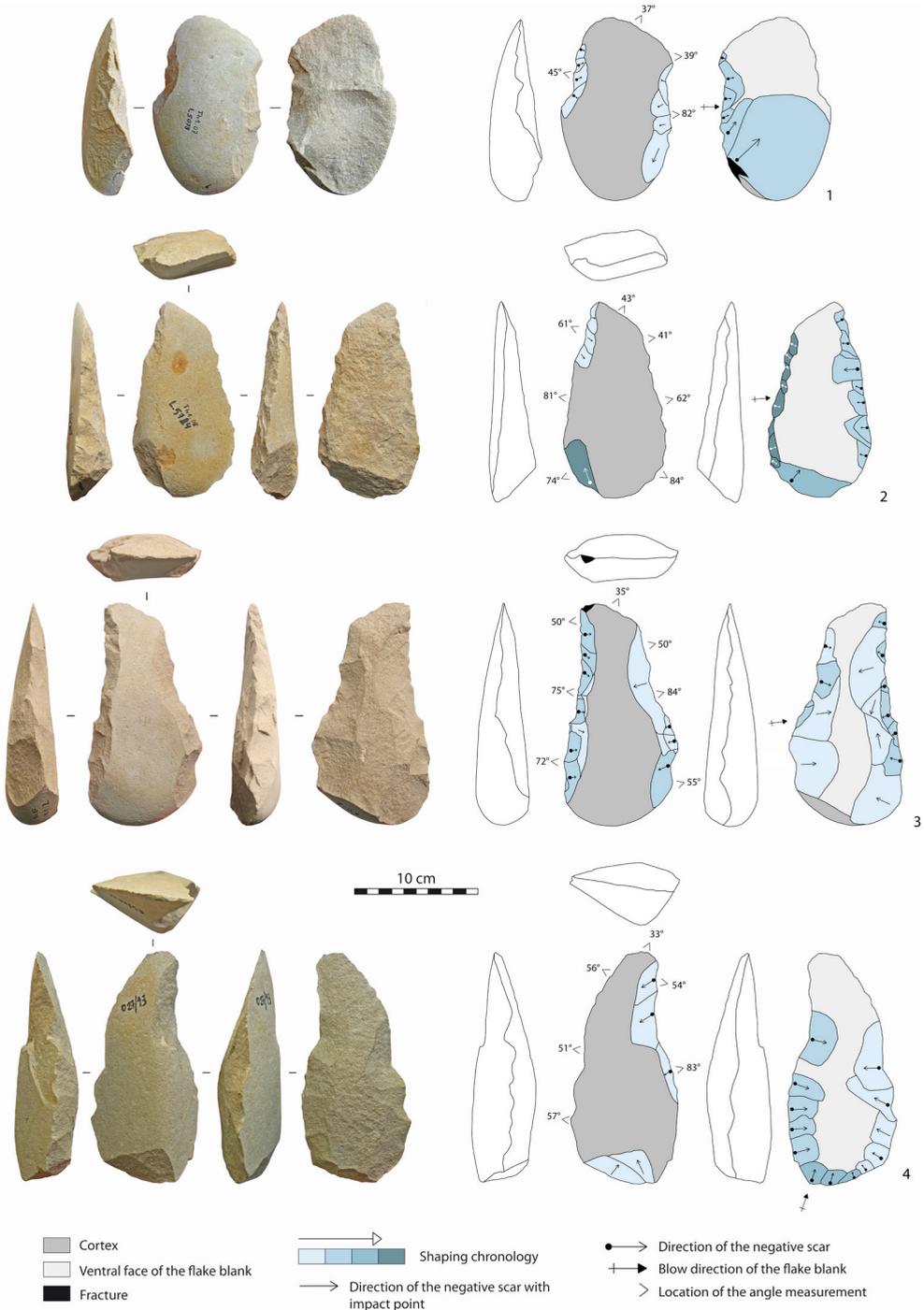
Fig. 18 - *Cleavers on* **entame** *flakes (1, 3) and on cortical flakes with a butt removed by shaping (2, 4).*

offset axis (Fig. 18: 4). The bit is constituted by a rectilinear and oblique cutting edge (Fig. 18: 1-3) and is convex for one specimen (Fig. 18: 4).

Shaping sequences are very short (mean of removals = 12; Fig. 12A): they involve the lateral edges, creating a slightly convergent tool shape, and also the butt portion for two specimens. The lateral edges of the same cleaver exhibit unifacial shaping removals on one edge (or on its portion) and reverse removals on the other edge.

One cleaver shows percussion marks on the proximal extremity of the cobble blank.

They are between 102 and 182 mm long (mean 139.5 mm; Fig. 9A; Tab. S2), with an average L:W ratio = 1.7, and their thickness shows low variation (mean = 41.8 mm; st. dev. = 6.6; Fig. 9A; Tab. S2). Their weight varies between 200 and 657 g (mean = 454.8 g; st. dev. = 133.5; Fig. 9B; Tab. S2).

Quartzite cores

ThI-L1 yielded 442 quartzite cores associated with the small flaking production (90.3 kg). Despite the large dimensions of some cores (Fig. 19C; Tab. S3), all negative scars overlap with the size of small-medium sized flakes. Sixty-one cores (13.8%) are broken. Fracture occurs along the joints after few removals, especially in flat thin cobbles which does not withstand the force of the knapping impacts (Fig. 5E: 2-4).

The remaining 381 cores can be divided into two technologically sets. The first set (*n* = 55) corresponds to the "simple cores" described by Delagnes and Roche (2005), including cores displaying one or two flake scars with a random distribution of distinct faces of the core (Fig. 19A). Their blank shapes, mainly ovoid cobbles/pebbles with flat and biconvex sections, reflect the frequencies observed in the unmodified sample (Fig. S6B, C, Fig. 19B). Two of them display pitted areas located on one protruding part of the cobble blank.

A second set of 326 cores displays an organised flaking (Fig. 19A). Distinctions could be drawn among the following flaking methods:

- Unifacial unidirectional with a cortical striking platform (*n* = 90). These cores have a large dimensional variation (Fig. 19C; Tab.

S3) and are usually on plano-convex cobbles/pebbles (Fig. 19B). Sixteen show pitted areas on one extremity (Fig. 20: 1, 2, 5) and have been previously used as active hammerstones for knapping. The flaked surface corresponds to the convex face of the cobble, whereas the flat natural surface is used as a striking platform without rectification. The corresponding flakes should be wider than long with frequent cortical butts and lateral cortical areas on the dorsal face. The number of flakes extracted from these cores varies between two and 16 with an average of 5.7 flakes per core distributed in one to three series (Fig. 19D). However, this low number does not necessarily correspond to a feeble exploitation, as demonstrated by experimentation (Fig. 20: 6). Negative scars of many cores show a progressive increase in the flaking angle value (from an acute angle to an abrupt angle) from the first to the last series (Fig. 20: 3, 7), documenting a continuous reduction up to the so called *galet tronqué* (*sensu* Roche 1980; Fig. 20: 4, 5, 7). The technique adopted is the direct freehand percussion, but three overexploited *galets tronqués* show small removals with an opposite direction, typical of the bipolar axial percussion on anvil, especially of quartzite (Mourre 2004). One of them was also rotated during bipolar flaking (Fig. 20: 5). Although typologically similar, these cores do not present a final edge retouch which removals completely differ from previous negative scars connected with the flaking process and thus cannot be considered as choppers from a technological point of view. Furthermore, the angle between the flaking surface and the striking platform shows great variation one core from another and does not seem to point towards the intention of shaping an active edge.

- Unifacial unidirectional with a rectified striking platform (*n* = 17). Flakes were extracted from a striking platform rectified by one-two removals, rarely three, to create a suitable flaking angle between 56° and 89° (Fig. 20:
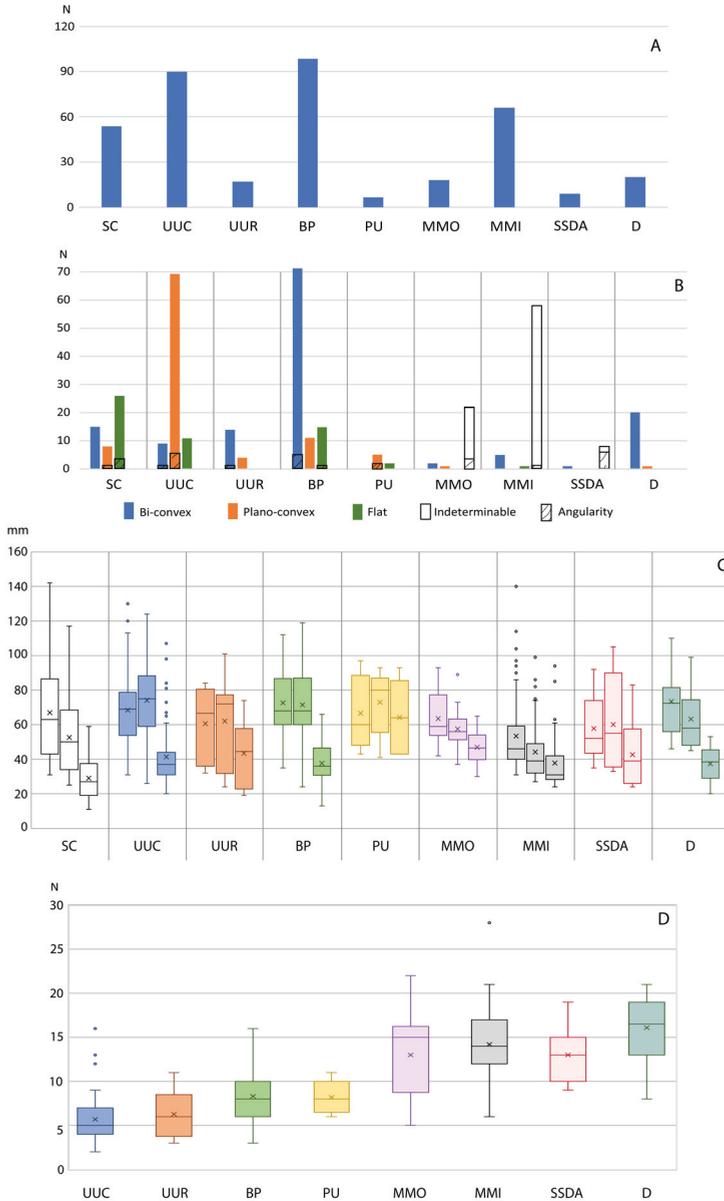
Fig. 19 - (A) Frequencies of small flaking methods (SC: simple cores; UUc: unifacial unidirectional cores with a cortical striking platform; UUr: unifacial unidirectional cores with a rectified striking platform; BP: bifacial partial cores; PU: peripheral unidirectional cores; MMO: multifacial multidirectional orthogonal; MMI: multifacial multidirectional irregular; SSDA: alternate flaking surface system; D: discoid). (B) Frequencies of blank morphology in lateral view and angularity. (C) Boxplot showing length (L), width (W) and thickness (T) distribution (mm) of the cores grouped by flaking method. (D) Boxplot showing the number of negative scars on cores grouped by flaking method. Boxes extend from the 25th to the 75th percentile of each group's distribution of values. The horizontal line within the box marks the median, the cross within the box marks the mean.
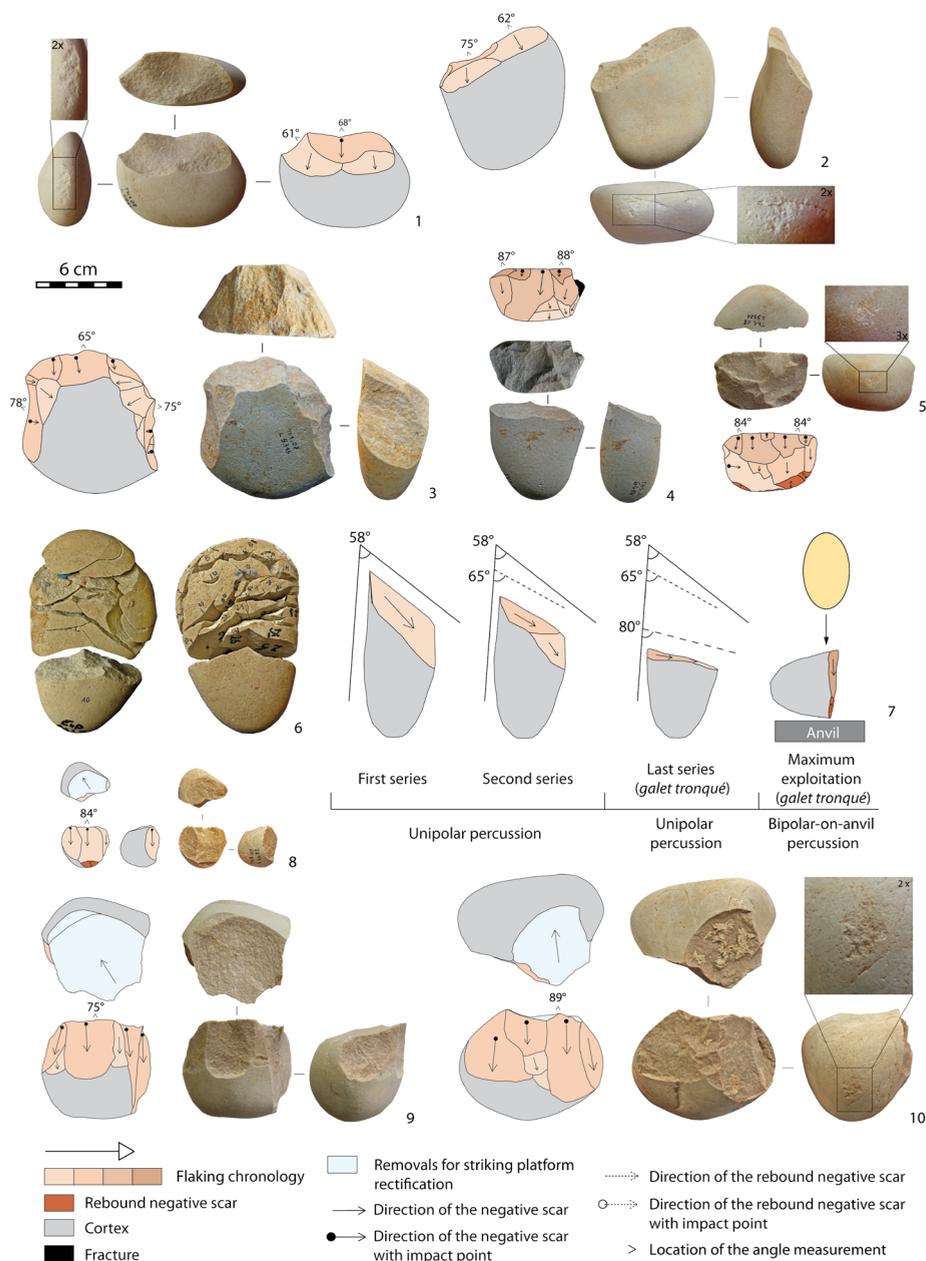
Fig. 20 - *(1, 2) Unifacial unidirectional cores with a cortical striking platform and pitted areas on one extremity. (3) Unifacial unidirectional core with a cortical striking platform. (4, 5) Galets tronqués. (6) Experimental unifacial unidirectional cores with a cortical striking platform. (7) Operational scheme of the reduction sequence from a unifacial unidirectional core with a cortical striking platform to a galet tronqué. (8-10) Unifacial unidirectional cores with a rectified striking platform. Core n. 10 shows pitted areas on one extremity. The technique adopted is the freehand percussion. Only cores n. 5 and 8 show technical aspects of the bipolar axial on anvil technique.*
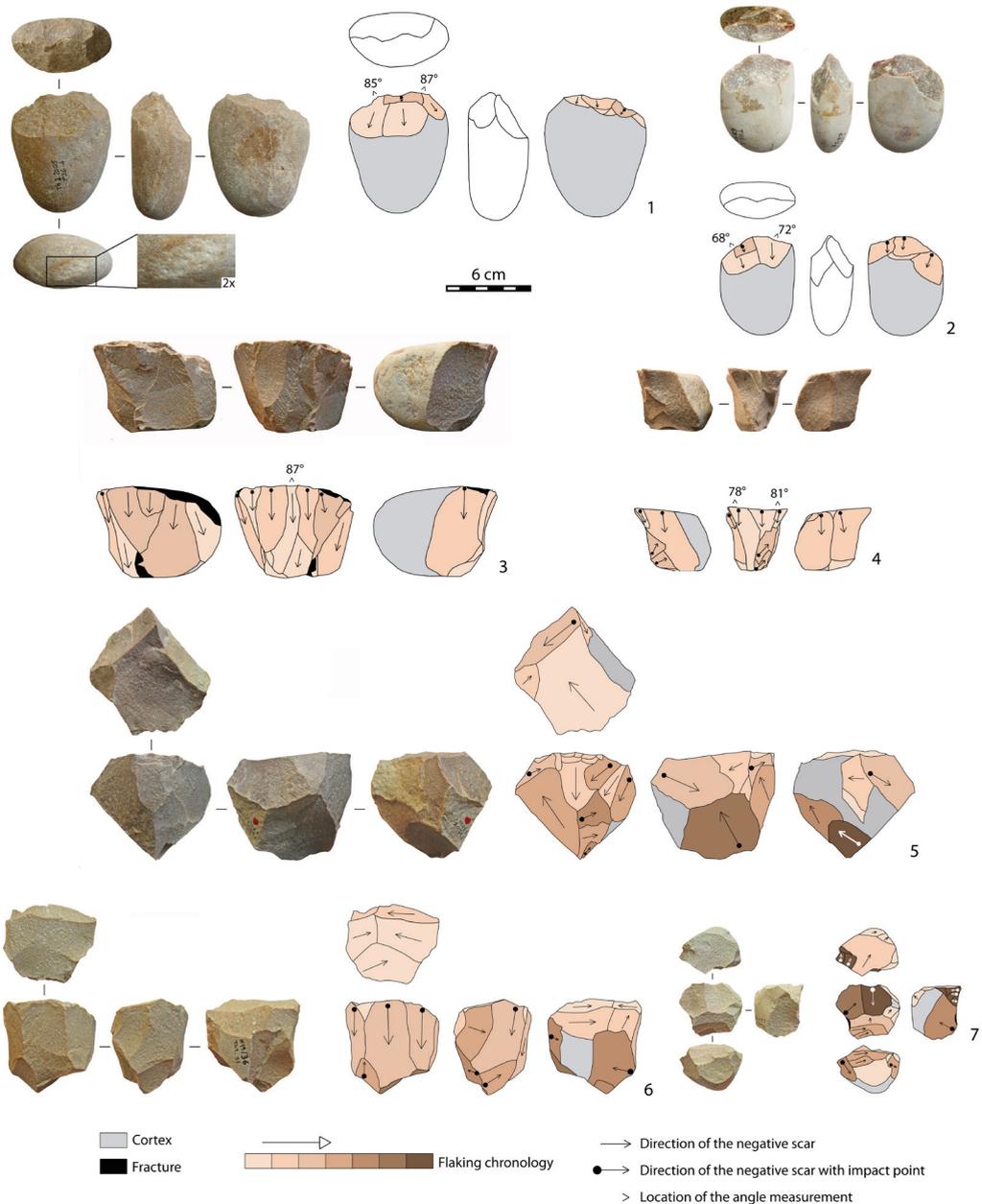
Fig. 21 - *(1, 2) Bifacial partial cores. (3, 4) Peripheral unidirectional cores. (5) Multifacial multidirectional irregular core. (6) Multifacial multidirectional orthogonal core with one preferential flaking surface. (7) Multifacial multidirectional orthogonal core.*

8-10). The blanks are bi-convex and plano-convex cobbles/pebbles (Fig. 19B). Three of these cobbles bear pitted impacts on one extremity (Fig. 20: 10), one on two extremities. Flake negative scars on these cores could be wider than long but many are elongated, with plain or dihedral butts and some of them with lateral and/or distal cortical edges. The low number of extracted flakes (Fig. 19D) seems to correspond to an effective weak exploitation for two main reasons: 1) the angle between the flaking surface and the striking platform does not vary from the first to the second series of removals; 2) the dimensions of these cores vary less than those of the previous ones (Fig. 19C; Tab. S3). A very small core only shows marks of a bipolar axial on anvil technique (Fig. 20: 5).

- Bifacial partial alternating (n = 96). These cores exhibit unidirectional removals on two adjacent surfaces, and each negative scar is used alternatively as a striking platform to flake the adjacent plane (Fig. 21: 1, 2). Knappers preferentially used biconvex cobbles/pebbles (Fig. 19B) exploited on the transversal (39.1%) or longitudinal axis (60.9%), thinner than those used for unifacial unidirectional exploitation (Fig. 19C; Tab. S3). Neither can these cores be considered as choppers because the edge between the two flaking surfaces shows highly variable angles (between 46° and 85°) and it has never been retouched after the completion of flaking activity. For two cores only removals extend along the periphery of the cobble. These cores are feebly exploited but the average of the negative scars is slightly higher than that of the unifacial unidirectional exploitation (Fig. 19D). Corresponding flakes should be wider than long with frequent cortical portions on the dorsal face and cortical backs. Nine of these cores show percussion marks on one cobble protuding zone (Fig. 21: 1).

- Peripheral unidirectional (n = 8). A peripheral flaking surface exploits the quasi-entire thickness of eight thick flat cobbles (Fig. 19B) creating short and wide/thick cores (Fig. 19C; Tab. S3). The striking platform is cortical and corresponds to one of the flat surfaces of the cobble blank (Fig. 21: 3, 4), except in one specimen where it is rectified by a large flat removal. Only one shows percussion marks on one cobble extremity. The angle between the striking and flaking surfaces is abrupt. Cores are overexploited and the number of negatives distributed in two series (Fig. 19D) probably does not correspond to the actual flake productivity. Few additional flakes at a stage when the flaking surface was no longer serviceable were extracted changing the flaking direction (Fig. 29: 4). Flakes belonging to these cores have cortical butts and frequent cortical lateral and distal backs. Their abrupt flaking angle distinguishes them from those produced from unifacial unidirectional exploitation with a cortical striking platform which have an acute angle.

- Multifacial multidirectional irregular (n = 67). Core surfaces were alternatively flaked through multidirectional removals without a clear organisation of the reduction process (Fig. 21: 5). No specific platform preparation was conducted insofar as each negative serves as a striking platform for the following removal on a secant face. The flakes thus produced could have various shapes and are frequently short with thick, asymmetrical cross-sections. These cores have the largest dimensional variation. However, many of them are overexploited and small in size, as evidenced by the average values of the three dimensions (Fig. 19C; Tab. S3). The number of flakes extracted is higher than that obtained with previous flaking methods (Fig. 19D). Usually, all the faces of the core are exploited and, except in a few cases, it is not possible to recognize the original blank (Fig. 19B).

- Multifacial multidirectional orthogonal (n = 18). These cores testify the respect of an orthogonal shape during flaking (Fig. 21: 7). In most cases blank morphology is
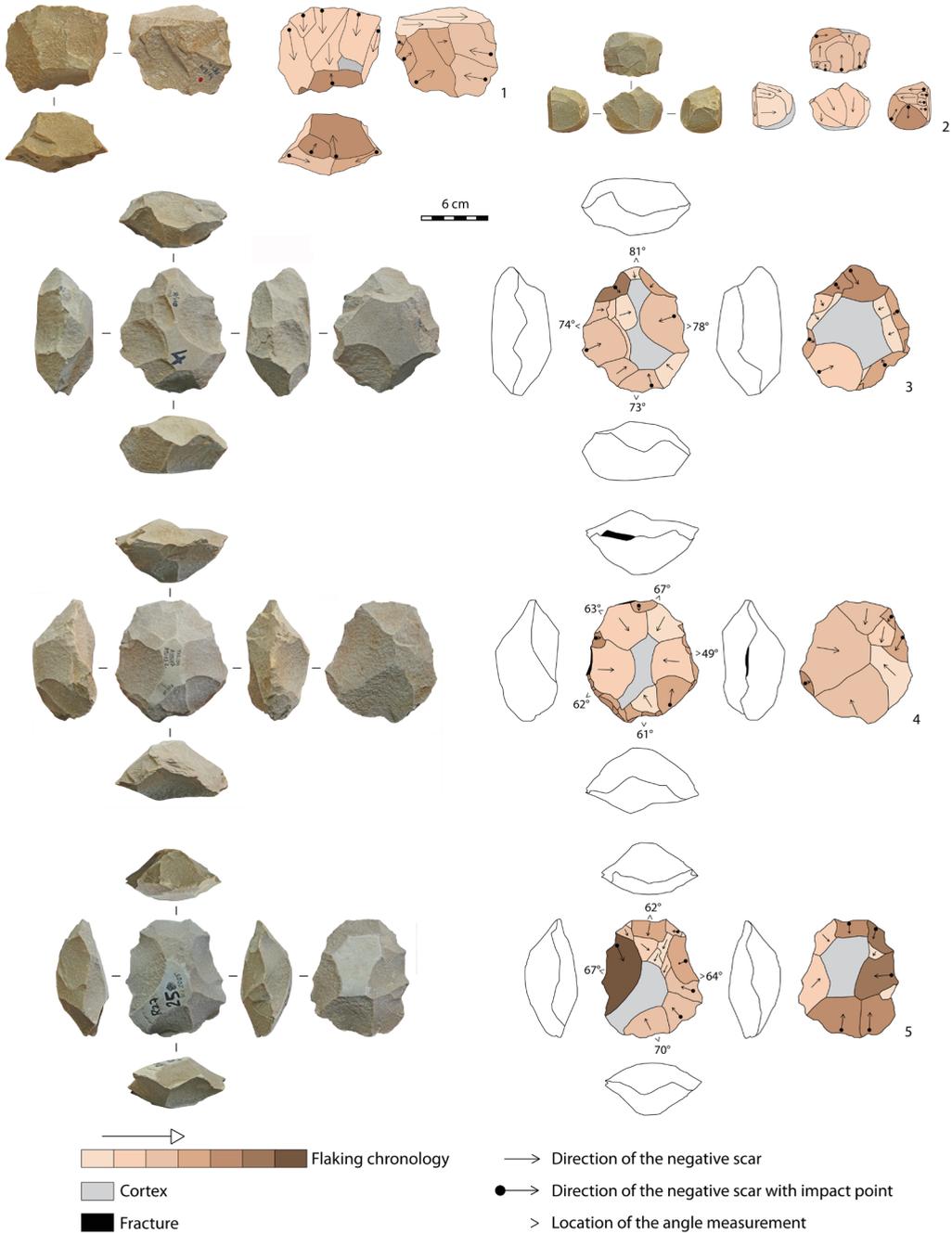
Fig. 22 - (1, 2) SSDA cores. (3-5) Discoid cores.

not recognizable (Fig. 19B) following the intense reduction by several removals (Fig. 19D), and because the same flaking surfaces were repeatedly flaked. Their dimensions are less variable than those of the multifacial multidirectional irregular cores and on average slightly larger (Fig. 19C; Tab. S3). The flakes obtained have characters similar to those obtained with an irregular multifacial multidirectional exploitation but systematically present an orthogonal negative scar system and a flaking angle close to 90°. Four of these cores present a major flaked surface with unidirectional long flake scars exploited at the beginning of the reduction process and multidirectional removals on the other faces that correspond to the final core reduction phase when the main flaking surface was no longer functional (Fig. 21: 6). This major flaking surface produced flakes somewhat elongated, with negatives of unidirectional removals on their dorsal face as well as, at least, one regular and continuous sharp lateral functional edge.

- Alternate flaking surface system [*Système par Surface de Débitage Alternée* (SSDA) *sensu* (Forestier 1992, 1993 and Ashton et al. 1992; *n* = 9)]. Each flaking surface with a unidirectional exploitation become striking platform for an adjacent flaking surface always exploited with unidirectional removals. The flaking is accomplished through a continuous rotation of the core (Fig. 22: 1, 2). Five to six flaking surfaces have been exploited to produce several flakes (Fig. 19D). The corresponding flakes have the following characters: 1) flakes similar to those produced with a unifacial unidirectional exploitation; 2) flakes with a unidirectional series on the dorsal face, orthogonal to the flaking axis of the flake; 3) flakes with more than one unidirectional series on the dorsal face, but orthogonal to each other; 4) flakes with unidirectional series distributed on the dorsal face and on the distal and/or lateral backs. Although the blank morphology is unrecognizable in most of the specimens,

the presence of cobble angular planes can be identified in six cores (Fig. 19B). One of these cores displays percussion marks documenting its probably previous use as hammerstone.

- Discoid (*n* = 21). Discoid cores (Boëda 1993; Jaubert and Mourre 1996; Mourre 2003; Terradas 2003) are bifacial and exhibit two convex, usually asymmetric surfaces which are employed in alternating series of removals as a striking platform and flaking surface (Fig. 22: 3-5). Flakes are detached according to a plane that is secant to the plane of intersection of the two surfaces. The convexity of the two exploited surfaces is natural because knappers used biconvex cobbles as blanks (Fig. 19B). The peripheral convexity is acquired by a mostly centripetal flaking organisation, rarely by tangential removals, and by the ability to maintain a similar angle between the two exploited surfaces along the periphery of the core. The average number of extracted flakes is the highest among all flaking methods (Fig. 19D). The resulting flakes should be mostly short and wide with centripetal or tangential negatives scars on their dorsal face, wide and thick plain, dihedral, or facetted butts with a wide flaking angle, at least one long sharp cutting edge and frequent backed lateral edges.

Quartzite small-medium sized flakes

Small-medium sized flakes account for 1759 items (34.5 kg). Broken flakes (*n* = 881) are very frequent (50.1% of the total; Tab. 1), showing knapping accidents such as *Siret* fractures (19.2 % of the broken flakes), transversal fractures (distal = 30.9%, proximal = 25.9, distal and proximal = 21.2%), or both (2.8%). Only three flakes bear a secondary modification: two show one or two notches (Fig. 23: 13) and one displays an abrupt retouch modifying a lateral edge and two small notches on the distal edge (Fig. 23: 12).

Whole flakes (*n* = 878) belong to all the knapping stages, from the cobble opening to the full production, which is the most represented
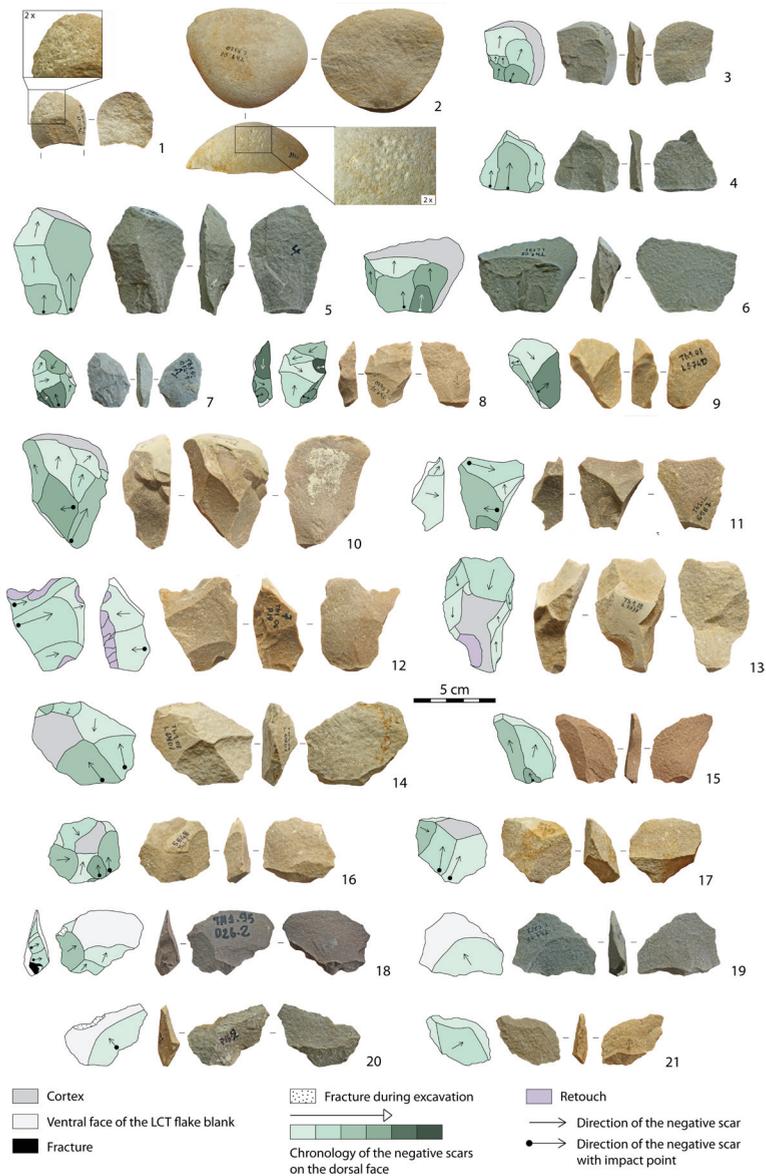
Fig. 23 - *(1) Broken partial cortical flake with battering marks. (2)* Entame *flake with battering marks. (3-6) Flakes with a unidirectional scar system with the same direction of the flake with cortical (4), plain (5, 6), and dihedral butts (3). (7, 8, 10) Flakes with a multidirectional irregular scar system and plain butts. N. 8 has a lateral backed edge and n. 10 is an edge-core flake. (9, 11) Flakes with multidirectional orthogonal scar system, plain butts and backed lateral edges. (12, 13) Retouched flakes with a unidirectional orthogonal scar system, plain butts and backed lateral edges. (14, 15, 17, 21) Flakes with a tangential scar system and a skewed morphological axis. N. 15 is a pseudo-*Levallois *point. N. 14 and n. 17 have partial lateral backs. Butts are facetted (14), plain (15, 21), and dihedral (17). (16) Flake with a centripetal scar system and dihedral butt. (18-20) Kombewa-type flakes with plain (20) and facetted butts (18, 19).*

phase (Fig. 24A). The finest part is also represented (Fig. 24C; Tab. S4) since flakes ≤ 2 cm long account for 11.8% of the whole flakes. Two flakes show pitted areas on the cortical dorsal face documenting the use as hammerstone of the pebble/cobble from which they were extracted (Fig. 23: 1, 2).

Technical features of the whole flakes well represent the operational schemes identified in core analysis. The major difficulty was here to distinguish between products belonging to some flaking methods and flakes resulting from LCT shaping. The main problems are as follows:

1) many LCTs show very short shaping sequences and removals are *entame* flakes, cortical flakes with a plain/dihedral/facetted butts, or partially cortical flakes with cortical/plain/dihedral/facetted butts that can hardly be distinguished from the opening and the first flaking series of a unidirectional unifacial core with a cortical striking platform, of a partial bifacial core, moreover of a discoid core;

2) as demonstrated by the morphology of negative scars on cores and LCTs, the length-to-width ratio of the small-medium flakes is not a distinctive feature of a specific production. Short and wide flakes are not exclusive of the LCT shaping but are also the product of the small flaking. Similarly, longer than wider flakes can be both the product of small flaking and more invasive shaping;

3) likewise, the flaking angle cannot be a distinctive element either due to the type of blanks. Slightly biconvex and plano-convex cobbles are used as blanks both for LCTs shaping and small flaking methods mentioned above. Accordingly, the angles between the two blank adjacent surfaces are very similar and, consequently, the flaking angles of the resulting flakes are also very similar in the first phase of production. Furthermore, the lack of research for bifacial symmetry in LCTs means that the flaking angles of the flakes are very variable because the management of the two adjacent

surfaces follows the morphology of the blank, as for the aforementioned small flaking methods;

4) the thickness of the flakes is a feature claimed to be typical of the LCT shaping (e.g. Bordes 1961; de la Torre and Mora 2018). In the case of LCTs from ThI-L1, this is not a discriminating element because the absence of bifacial symmetry coupled by the lack of a thinning of the tool central volume and of the edge regularization generate flakes with very variable thickness such as those produced during small flaking.

However, we have identified some flakes (*n* = 66) that can be more confidently attributed to the shaping of LCTs on large flake blanks, due to the absence of cores on flake. They are small Kombewa-like flakes belonging to the shaping of the ventral face of a LCT flake blank (Fig. 23: 18-20).

For 47 whole flakes with a length <2 cm it was impossible to recognize the number and direction of the negative scars on the dorsal face. Accordingly, these specimens are not counted in the classification based on the negative scar patterns on the dorsal face. Based on the features of the dorsal face of 831 items, whole flakes can be grouped as follows:

- Flakes with fully cortical dorsal surface (*n* = 112) represent 12.8% of the whole flakes and were flaked exclusively from pebbles/cobbles. Seventy-four of them are *entame* flakes belonging to the very first knapping phase (Fig. 24A). Very few (*n* = 6) are from angular cobbles presenting a thick triangular section that consists of the ventral face and two flat faces of the blank. The others retain plain butts and only one a dihedral butt (Fig. 24D). Their dimensional variability is considerable and the average dimensions are around 40 mm both in length and width (Fig. 24D). The flaking angle is between 104° and 126° (Fig. 24E).

- Unidirectional negative scar pattern (*n* = 200; 22.9% of the whole flakes; Fig. 24B). These flakes have one to five unidirectional negative scars on the dorsal face with the
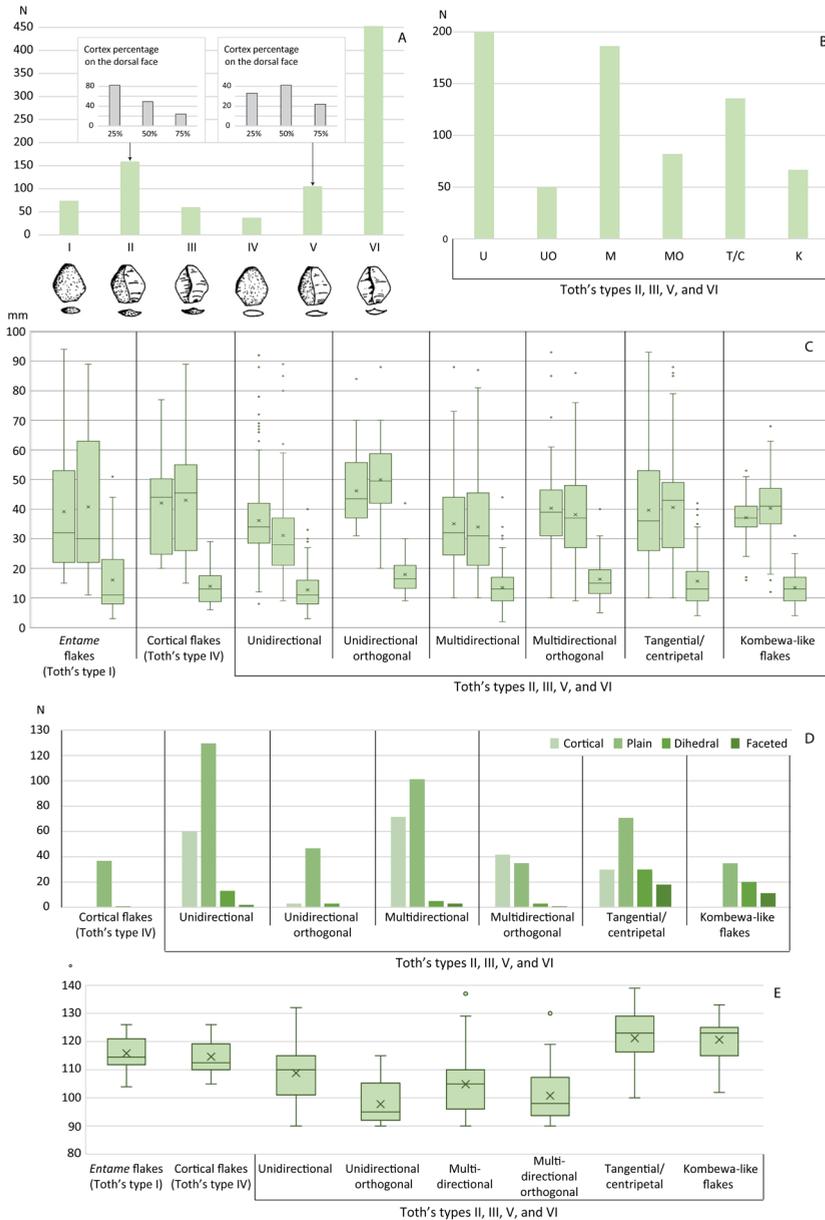
Fig. 24 - *(A) Frequencies of Toth's flake types. (B) Frequencies of the negative scar systems on the dorsal face of the* **Toth's** *(1982) flake types II, III, V, and VI (U: unidirectional; UO: unidirectional orthogonal; M: multidirectional irregular; MO: multidirectional orthogonal; T/C: tangential/centripetal; K: Kombewa-like flakes). (C) Boxplot showing length (L), width (W), and thickness (T) distribution (mm) of the flakes grouped by the aspect of the dorsal face. (D) Frequencies of the butt types of the flakes (except* **entame** *flakes whose butt is always cortical), grouped by the aspect of the dorsal face. (E) Boxplot showing flaking angle values of the flakes grouped by dorsal face aspect. Boxes extend from the 25th to the 75th percentile of each group's distribution of values. The horizontal line within the box marks the median, the cross within the box marks the mean.*

same flaking direction of the flake (Fig. 23: 3-6). 36.5 % of them retain cortical areas mainly in the lateral portions of the dorsal face. Long portions of the edges are sharp and suited for cutting since the flakes with lateral or distal backs are very few (n = 11). Their butts are mainly plain (62.5%) and cortical (20%; Fig. 24D), well in accordance with a unidirectional unifacial core exploitation, and the flaking angle is comprised between 90° and 132° (Fig. 24E). Flakes with plain butts preferentially have a more abrupt flaking angle than those with cortical or faceted butts and could belong to unidirectional unifacial cores with rectified striking platforms or to the unidirectional preferential surfaces of multifacial multidirectional cores. Some of them (27%) are elongated (Fig. 23: 5), while the others have a sub-quadrangular shape (Fig. 23: 3, 6). Some flakes with cortical butts show a decrease of the *chasse* angle[2] between the first and the last negative scars, confirming the hypothesis of a longer reduction sequence for the unifacial unidirectional cores with a cortical striking platform (see section 4.6; Fig. 23: 4). Their size shows a strong variation with a mean length of 36 mm, a mean width of 31 mm, and a mean thickness of 13 mm (Fig. 24C; Tab. S4).

- Unidirectional orthogonal negative scar pattern (n = 50; 5.7% of the whole flakes; Fig. 24B). The technical aspects of these flakes accord with SSDA core exploitation. These flakes exhibit on their dorsal face 1) one series of one to four unidirectional negative scars orthogonal to the flaking axis, 2) two series of three to nine unidirectional removals opposed or orthogonal to each other, or 3) series of unidirectional removals (four to 13) on orthogonal adjacent faces that correspond to the dorsal face and distal or lateral edges (Fig. 23: 12, 13). The latter category is the most frequent and accounts

for 69% of this group. Only five of these flakes retain cortical portions on the dorsal face. Butts are mostly plain (Fig. 24D) and the flaking angle is abrupt (mean = 97°; Fig. 24E) according to an orthogonal management of the core. The flakes of this group have the largest dimensions (mean length = 46 mm; mean width = 50 mm; mean thickness = 18 mm; Fig. 24C; Tab. S4).

- Multidirectional irregular negative scar pattern (n = 183; 20.9%; Fig. 24B). These flakes have various shapes and dimensions (Fig. 24C; Tab. S4) with asymmetrical cross-sections (Fig. 23: 7). Their dorsal faces display two to 13 negative scars with an irregular directional pattern and only 27.2% preserve cortical portion confirming the intense exploitation deduced from the analysis of multifacial multidirectional irregular cores. Some of these flakes (13.1%) present one or two series of unidirectional flake scars together with multidirectional negative removals, which can be related to the multifacial multidirectional cores with one preferential unidirectional flaking surface. The percentage of core edge flakes (62.4%) is very high, which implies a continuous rotation of the flaking surfaces to exploit every available angle (Fig. 23: 8, 10). Butts are mostly cortical and plain (Fig. 24D) and the flaking angle is highly variable (Fig. 24E).

- Multidirectional orthogonal negative scar pattern (n = 82; 9.4% of the whole flakes; Fig. 24B). These flakes show two to eight negative scars with multidirectional orthogonal directions on the dorsal face, most of them (75%) are core edge flakes, and 62.5% retain cortical portions on the dorsal face (Fig. 23: 11, 12). Their morphological and dimensional variation is high (Fig. 24C; Tab. S4), their butts are mainly cortical and plain (Fig. 24D), and the flaking angle is usually abrupt (Fig. 24E).

- Tangential/centripetal negative scar pattern (n = 138; 15.5% of the whole flakes; Fig. 24B). These flakes correspond to the products of discoid core exploitation and LCT

[2] An expression conventionally referring to the angle between the butt and the dorsal face (Inizan et al. 1999).

shaping and show the highest dimensional variation (Fig. 24C; Tab. S4). Products from discoid cores obtained using the centripetal flaking direction are not frequent (*n* = 17). They show sections with a certain degree of symmetry, sub-quadrangular or circular shapes, dihedral or facetted butts (Fig. 23: 16) and are marked by the coincidence of flaking and morphological axes. Commonly, the flakes display a tangential flaking direction with an asymmetric cross-section and with clear opposition between a potential active edge and natural or prepared back. Among them we can distinguish flakes whose flaking axis coincides with their morphological axis (Fig. 23: 17) and flakes with a limited back in continuity with the butt (Fig. 23: 14) or pseudo-Levallois points (Fig. 23: 15, 21), with a deviation of the flaking axis from the morphological axis. The latter can also be associated with the shaping of LCTs. Butts are usually plain or cortical, but the number of dihedral and faceted butts is higher than in the previous groups (Fig. 24D) as well as flaking angles are wider (mean = 122°; Fig. 24E).

- Kombewa-like flakes (*n* = 66; 7.5% of the whole flakes; Fig. 24B). As said above, these flakes can be confidently ascribed to the shaping of LCTs on large flake blanks. They are short and wide with a lower dimensional variation (Fig. 24C; Tab. S4) and their dorsal face preserve portion of the ventral face of the large flake blank coupled by few tangential removals. The morphological and flaking axes can coincide (Fig. 23: 18, 19) or not (Fig. 23: 20). Butts are mainly plain (Fig. 24D) and the flaking angle is wide (Fig. 24E).

Knapping hammerstones

These are the only percussive objects recorded at ThI-L1 (*n* = 30). Despite size differences (Tab. 4), all knapping hammerstones show the same use-wear patterns characterized by concentrated battered areas and impact points located on the most protruding and convex zones of quartzite cobbles (Fig. 25: 1-9), occasionally linked to micro-fractures (cone cracks: Hertz 1882) with a typical circular morphology (Fig. 25: 1, 2). Three hammerstones are broken along the transversal plan and three show fracture (Fig. 25: 9) or removals (Fig. 25: 6) located near the percussion damages or on the opposite side because of the rebound force.

Cobbles used as knapping hammerstones are mainly ovoid bi-convex in shape, but knappers used also subcircular, subquadrangular and subtriangular forms (Tab. 5). Twelve hammerstones have one working zone showing impacts marks, more or less concentrated and superimposed, located at one extremity of the blank (Fig. 25: 6). In one case impact damages extend from the extremity to the edge (Fig. 25: 1, 7). The others have two (Fig. 25: 2-4) or three working zones (Fig. 25: 1, 5, 8, 9), located at the most protruding parts of the cobble blank, suggesting re-orientation of the hammerstone during use in search of new protruding convex areas after exhaustion. In several cases percussive traces are invasive, superimposed and well circumscribed, indicating an intensive use and revealing the ability to strike with precision (Fig. 25: 3-6, 8).

Discussion

Techno-economic systems at ThI-L1

This analysis of the ThI-L1 quartzite industry can be taken as a solid basis to evaluate the techno-economic strategies adopted by hominins at ~1.3 Ma in the Casablanca region. Here we discuss the technical responses to the collected raw materials, the mental templates involved in lithic production, and the relative technological skills. We will consider both these results and those of the analysis of the silicite component recently published (Gallotti et al. 2020; Supplementary Material B and Figs S2 and S3), for a comprehensive interpretation of this early North African Acheulean.

The co-existence of four separate productions in the same assemblage, two of quartzites and two of silicites, is well documented at

Fig. 25 - **(1)** Ovoid plano-convex hammerstone with two working zones. Impacts extend to the edge from the lateral protuding area. **(2, 3)** Subcircular bi-convex hammerstones with two working zones. **(4)** Ovoid bi-convex hammerstone with two working zones. **(5)** Ovoid plano-convex hammerstone with three working zones. **(6)** Subtriangular flat hammerstone with one working zone and one removal. **(7)** Subcircular bi-convex hammerstone with one working zone. Impacts extend to the edge from the protuding area. **(8)** Ovoid plano-convex hammerstone with three working zones. **(9)** Subquadrangular plano-convex hammerstone with three working zones and fracture.

	LENGTH	WIDTH	THICKNESS	WEIGHT
Min.	59	36	22	102
Max.	134	95	63	508
Mean	88.3	66.5	40.3	225
St. dev.	19.7	16.7	10.2	101

ThI-L1. Quartzites were exploited to produce small-medium sized flakes and to manufacture LCTs. Silicites were exploited for the extraction of small flakes and bladelet-like flakes (Gallotti et al. 2020). Raw material patterns show a clear dominance of quartzite (87.7% of the artefacts) when compared to silicite (12.3% of the artefacts), which mimics the lithological composition of the unmodified material (84.7% of quartzite, 15.3% of silicite) recovered at ThI-L1.

Provisioning systems and chaînes opératoire *integrity*

Unmodified quartzite and silicite material is composed of pebbles and cobbles, accumulated by natural agents and/or manuports as a potential source of raw material for knappers. Small quartzite and silicite pebbles are abundant in the water assisted deposits of ThI-L1 and many of them are concentrated at bottom of the layer. The sedimentary architecture implies that low current transported and deposited sediments and slightly re-oriented elongated objects as LCTs (Raynal et al. 2002; Gallotti et al. 2020). Nevertheless, LCTs and the other artefacts both of quartzite and silicite were not water deposited; their very fresh cutting edges indicate that water was not the prime agent of accumulation and do not bring any argument in favour of a residual deposit cumulating different occupational sub-units eroded down to a single layer.

In addition, detailed observation of the silicite artefact and pebble cortex reveals a long history in marine environment, which is not erased by the successive fluvial transportation and sedimentation. This means that either these pebbles derive from marine deposits very close to their final deposition place (ThI-L1 deposit) or that knappers collected them directly in marine beaches or in slightly derived deposits (Gallotti et al. 2020). The same deduction concerns the medium-sized quartzite cobbles, which are present in the deposit in all shapes and sizes that characterize the current cobble beaches, but do not have any specific spatial pattern within the ThI-L1 deposit.

Possibly the presence of large cobbles may not be imputable to natural agents. They are characterized by a rather standard thickness, whereas that of both the medium-sized cobbles and the large cobbles of the current beaches is very variable. Furthermore, their thickness values are very close to that of the large cobbles used for the LCT manufacture and are ideal for the extraction of large *entame* flakes (Sharon 2011). Therefore, they could correspond to manuports imported by knappers from nearby beaches into the site.

Accordingly, the sorting of the ThI-L1 assemblage seems moderate, affecting only the smallest artefacts, as documented by the large deficit of small-medium flakes both of quartzites and silicites. A fragmentation of the *chaînes opératoires* of the silicite small flaking is not conceivable since flaking products belong to all the knapping stages and methods identified, although they are underrepresented compared to the number expected from core flaking. On the contrary, the interpretation of the quartzite *chaîne opératoire* integrity or fragmentation is heavily conditioned by the difficulty to distinguish the products of some flaking methods from the wastes of the LCT shaping. Overall, it seems that, despite the problems related to flakes, all elements of the quartzite small flaking reduction sequences are present in the assemblage, even the knapping hammerstones.

The dynamics of LCT production requires further discussion. The selection and transport into the site of large cobbles suitable directly for LCT shaping support the hypothesis of their *in situ* knapping. Further evidence is provided by the presence of percussion marks on the proximal extremity of many LCTs on cobble, probably used for LCT blank production and for the

Tab. 5 - Shape and working zones of the whole knapping hammerstones.

SHAPE IN FRONTAL VIEW	SHAPE IN LATERAL VIEW			WORKING ZONES				
	BI-CONVEX	PLANO-CONVEX	FLAT	1 EXTREMITY	2 EXTREMITIES	3 EXTREMITIES	1 EXTREMITY AND 1 EDGE	2 EXTREMITIES AND 1 EDGE
Ovoid	12	4	-	6	6	2	-	2
Subcircular	4	1	-	3	2		-	-
Subrectangular	1	2	-	1	-	1	1	-
Subtriangular	2	-	1	2	1	-	-	-
Total	**19**	**7**	**1**	**12**	**9**	**3**	**1**	**2**

extraction of the first large removals for tip location, because they are too large for small flaking. The same cobble forms are also ideal cores to produce large *entame* flake blanks. These cores have never been found at ThI-L1, whereas some unmodified large *entame* flakes are present. This means that many LCT flake blanks were extracted elsewhere and then transported to ThI-L1. However, some of these cores may have been reused as blanks for small flaking since their size does not allow the extraction of more than one large flake. Although this hypothesis cannot be demonstrated without refitting evidence, some unifacial unidirectional cores with cortical striking platform were probably large-sized at the start and their thickness well fit with that of large cobbles and many LCTs. In addition, the hypothesis of an *in situ* shaping of LCTs on flake blanks is supported by the presence of small Kombewa-like flakes in the assemblage.

The trihedral and rhomboidal picks on flakes instead document a fragmentation of the *chaînes opératoires*, at least in the initial phases of block procurement and of flake blank extraction. These are the largest LCTs and their core edge flake blanks possibly required the flaking of giant cores as defined by Sharon (2009). Blocks of such dimensions and morphologies are not frequent among beaches cobbles, whereas they can be found near the primary sources due to their dismantling. They are not even present in

the ThI-L1 deposit as well as large unmodified core edge flakes.

However, in such an extended unit the frequency of the different knapping components belonging to a restricted excavation area may not be representative of the actual *chaîne opératoire* integrity or fragmentation.

Small flaking

Small-medium sized flakes were the intended end product of the quartzite small flaking. They were exceptionally retouched. Before flaking, or between knapping sequences, some cores (8%) were used as knapping hammerstones. One or two protruding zones of the cobble blanks display numerous circumscribed battering marks implying precise and recurrent percussion. Their density is such that the cobble natural surface became pitted. They show the same use-wear patterns and percussion zones observed on the knapping hammerstones, suggesting a highly controlled movement and stable grasp in handling both core and hammerstone during flaking.

Several flaking methods involving constant technical rules are documented, each of them representing the most suitable flaking solution for the original blank shape. Usually, knappers began flaking without any previous technical operation. When cobble blanks have a plano-convex cross-section, the flat surface was used as striking platform to detach unidirectional flakes on the

adjacent convex surface (unifacial unidirectional) or along the peripheral convexity (peripheral unidirectional). Bi-convex cobbles are morphologically ideal cores for bifacial partial and discoid exploitation. Angular cobbles were used for multifacial exploitation which can preserve their original angular planes (SSDA exploitation).

Multifacial cores were intensely exploited thanks to a continuous search for new angles to produce the maximum number of flakes possible. They were usually abandoned at a stage when they were considerably reduced in size or following a knapping accident, or when appeared the impossibility to create new flaking angles. Even the unifacial unidirectional cores with cortical striking platform that would seem feebly exploited, can instead document longer reduction sequences. They required the adoption of the bipolar-on-anvil technique in the final phase of exploitation, when core become too small for handling. The discoid cores produced the highest number of flakes, although they were not overexploited as documented by the residual cortex in the central part of the two opposing surfaces which still retain their convexities.

Preliminary to flaking, a first phase can be present and commonly consists of the rectification of the striking platform to create a suitable flaking angle for the unifacial unidirectional exploitation producing elongated flakes.

This panoply of flaking methods is directly related to the variety of cobble/pebble blank shapes. It is difficult to establish to what extent the adaptation to the original blank shapes was imposed by raw material constraints or was an independent choice. Most likely, the two factors played their role simultaneously, but in different ways depending on the sought outcomes. It is clear that knappers had an in-deep knowledge of the topological structure of the raw materials and of their effects on flaking. Furthermore, flaking method variation does not create a product diversity, but is essentially aimed at maximizing the production. However, when hominins needed to extract products with specific patterns, they were able to add further operational tools to the flaking level-variability. This is the case

for the adoption of the discoid method producing flakes with longer cutting edges and platform rectification to obtain elongated products. The most representative case is the production of bladelet-like flakes of silicite (Gallotti et al. 2020). Small flakes were produced from silicite pebbles using some of the flaking methods documented for quartzite (unfacial unidirectional, bifacial partial, and multifacial multidirectional) and the same technique, i.e., free-hand percussion. Besides, there is evidence of a specific technical process hitherto unknown for these periods which is an intentional production of recurrent bladelet-like flakes exclusively through a bipolar-on-anvil technique. It follows two steps: 1) the splitting of pebbles along the transversal axis to create a split-platform-core, and 2) the removal of bladelet-like products from the pebble's fresh platform. This demanded a strict selection of biconvex pebbles long enough to be split and thick enough to offer an exploitable long peripheral convexity. This bladelet-like flake production is restricted to silicite knapping as it is not observed in the quartzite assemblage, although the knappers had a large quantity of quartzite pebbles available that could have been flaked this way.

All cores do not bear signs of retouch or edge shaping suggesting a potential secondary use as tools and clearly fall into the category of technological waste. Some cores were abandoned after a few removals (simple cores), but there is no obvious technical reason for their discard. They may correspond to the initial flaking stage of structured cores. However, the abundance of raw materials at secondary sources in the Casablanca region may have encouraged such an underexploitation.

LCT production

LCT shaping at ThI-L1 recalls several processes that, repeated on several specimens, produced several tool-types sharing technological, morphological, and dimensional patterns. None of these tools can be defined as "biface" (*sensu* Roche and Texier 1991) because there is no bifacial and bilateral management of biconvex volumes and, even if bifacial shaping exists, it is usually restricted to the edges of the artefacts.

Another common aspect of these LCTs is the conservative proximal mass, usually opposite to the tip on their major axis.

The main aim of the LCT production was to manufacture large pointed tools (handaxes and picks) and LCTs with a transversal edge (cleavers). Beveled handaxes are not a primary focus, as their transversal edge appears mostly due to the resharpening of skewed pointed handaxes after the breakage of the tip. LCTs were usually produced from large cobbles, less often from large flakes detached mainly using the *entame* core method (Sharon 2011).

The production of different LCT types and the intra-type replication of morphologies reflect the existence of genuine mental templates which document a certain level of conceptual complexity. This conceptual level is expressed in the ability to discern the different elements constituting the final tool (overall shape, dimensions, weight, tip, transversal cutting edge, angle of the tip…) and to conceive their relationships both simultaneously (final object) and in sequential order (the cause-effect relations among the different phases of the *chaîne opératoire*), evaluating the consequences of the programmed actions singly and globally at any given moment.

Conceptual schemes are applied through operational schemes based on the blending of LCT blank selection/production and standard shaping procedures. Knappers were able to foresee the final LCT morphometrical patterns by anticipating them through the selection of cobble blanks, directly shaped into handaxes and picks. Beyond the length > 10 cm, the main criteria of cobble choice were a specific thickness or a trihedral cross section that helped to anticipate those of the handaxes and picks. In fact, both the cobble thickness and the cross-section are not modified by shaping which is usually minimally invasive and limited to the edges. When the LCT blank is a large flake, knappers pre-planned its morphology thanks to a specific flaking process consisting of 1) the selection of large thin and bi-convex cobbles as core blanks; 2) the choice of a precise percussion point and blow direction for the extraction of a specific type of *entame* flakes, anticipating the final LCT morphology, i.e. proximal side-struck flake with an off-set axis for pointed handaxes and side-struck large flakes rectangular or oval in shape for cleavers. The precision of the blow struck is confirmed by the absence of impact damage from failed percussions on the butt/bulb area of the large flakes and by the very circumscribed percussion marks visible on the residual cortex of LCTs, previously (or successively) used as hammerstone. This confirms the stable motor habits highlighted for medium-sized hammerstones and the stable grasp in handling also cobbles of larger dimensions.

We prefer to use the term "anticipation" to define the concept regulating this type of preplanning, because the foresight of the final tool-type patterns is not the outcome of a technical process guided by the concept of "predetermination". In technological terms, the predetermination is the pre-planning of the metrical and morphological flake patterns before its detachment through one or more predetermining removals (Mourre 2006). The core preparation affects the striking platform and/or the flaking surface and "aim at controlling several parameters permitting the acquisition of one, several or all morpho-technical characteristic elements of the planned objects" (Texier and Roche 1992, p. 405). In addition, predetermination implies a pre-planned flaking organized in such a way as to repeatedly produce similar products from a single core (Inizan et al. 1999). Methods such as Kombewa (Owen 1938), Victoria West (Jansen 1927; Goodwin 1929, 1934), Tabelbala-Tachenghit (Tixier 1956), and Levallois (Tryon et al. 2005) are good examples of the technical procedures required by predetermined LCT flake blank productions.

On the contrary, *entame* core method does not document a core preparation and only a large flake can be extracted from these large cobbles given their size. Furthermore, if an operation preliminary to the extraction of the *entame* large flakes is documented, it is limited to the rectification of the striking platform to adjust the flaking angle.

From an operative point of view, a more complex flaking process could be linked to the production of trihedral and rhomboidal core

edge flakes, but the small number of these LCTs blanks coupled with the absence of the corresponding cores limit the discussion.

The role played by the anticipation of large flake blank morphometry is particularly evident for the cleavers, which have very short shaping sequences, limited to the edges and never penetrating the volume of the tool. However, even the shaping sequences of the handaxes and picks are not excessively long. They are repetitive and always start with the position of the tip on the cobble blank, followed by the creation of the lateral edge convergence which gives the tool its final morphology. In most LCTs, the tip is not subsequently modified. Shaping procedures very rarely aimed at the thinning of the tool and were only functional to highlight the tip, which in the case of the picks represents a distinct segment in the overall tool mass. When handaxes and picks are made on flake blanks, tip is usually obtained by flaking and its distal edge is rarely modified by shaping. Variations of these schemes produce pointed handaxes with a skewed point shaped by notches that penetrate one or both edges.

The most impressive technical aspect of the LCT production is the standardization of the very acute tip angle, which shows extremely similar values for all tool-types, whether the tip was obtained with flaking or shaping and whatever the thickness of the LCTs. This control of tip working edge angle, in contrast to the large variation in lateral edge angles, is a clear indication of the functional role played by the tip in the use of these LCTs. Most likely, this role is also linked to the morphology of the tip which seems rather unrelated to the overall shape and size of the tool. One exception is the trihedral and rhomboidal picks, where the tip is an integral part of very large, thick, and heavy-duty tools.

The standardization of very acute angles also concerns the cleavers, whose angle of the transversal cutting edge has values very close to those of the handaxe and pick tip. However, in this case it must be considered that this standardization may be due to the use of very similar blanks (*entame* or cortical flakes with plain butt) produced with a single flaking method.

ThI-L1 and the early North African Acheulean

Despite intense research in North Africa, much remains unknown about the earliest settlement phases. In this vast area, the scarceness of archaeological sites in stratigraphic context and with reliable chronometric data prevent the construction of cultural models and large-scale syntheses that link the different bio-geographic African regions at the time of crucial transitions like the emergence of the Acheulean. In this section, we present the available data about Maghrebian sites attributed to early North African Acheulean (Tab. 6) and issues related to their context and technical behaviors.

ThI-L1 in the Moroccan early Acheulean context

Currently, ThI-L is the only early Acheulean site in North Africa with a high-resolution chronostratigraphic framework establishing its age at ~1.3 Ma. Unfortunately, the other sites of the Casablanca region, i.e., SAR-Unit M and S.T.I.C. Quarry, ascribed by Biberson to the first stages of the Acheulean, are indeed stratigraphically more recent (Lefèvre et al. 2021) and moreover, their lithic and faunal assemblages were mostly collected by quarriers in the absence of archaeologists (Biberson 1961a, p. 127, 157, and 161).

At the base of the Sidi Abderrahmane Quarry (Fig. 1), Neuville and Ruhlmann (1941) recorded in layer M of Site B an assemblage of 426 artefacts made of quartzite and feldspathic sandstone from an excavation area of 50 m². This industry was qualified as "Clacto-Abbevillian" (Neuville and Ruhlmann 1941; Balout 1955). It contained Acheulean forms (trihedrons, handaxes, cleavers, spheroids, the "Abbevilian" component), large flakes (the "Clactonian" component) and various forms of cobble tools, associated with a very fragmentary fauna dominated by *Hippopotamus*. At the time, the Clacto-Abbevillian described at SAR-Site B was the oldest recognized lithic industry in North Africa. In the same unit, were collected 48 small-medium flakes attributed to the Tayacian and considered as intrusive due to their typology and the degree of edge abrasion. Biberson (1961a) revised these industries

Tab. 6 - *North African Acheulean sites discussed in this work (HRC: high-resolution chronostratigraphy; LCTs: large cutting tools; SE: systematic excavation; SC: survey collection).*

SITE	HRC	AGE	LITHOSTRATIGRAPHIC CONTEXT	SE	SC	TOTAL ARTEFACTS	LCTs	HUMAN REMAINS	REFERENCES
Ain Hanech, Acheulean level 2 loci	No	1.67±0.04 Ma? (extrapolated)	Calcretes, palaeosoils and colluvia on dissected surfaces.	No	Yes	25	19	Absent	Duval et al. 2021
Thomas Quarry I-L1	Yes	~1.3 Ma	Member 1 Bed 2 of the Oulad Hamida Formation (Fig. S1). Fine to coarse locally trough cross-bedded sands and calcareous mudstone.	Yes	-	3845	219	Absent	Raynal and Texier 1989; Raynal et al. 2001, 2002 2009, 2017; Gallotti et al. 2020; Gallotti et al. 2021; this work
Tighennif	No	Brunhes chron or Jaramillo subchron (?)	No archaeological layers are visible and the deposit with lithic, fauna, and human remains results from the clogging of an old lake basin with a funnel-shaped clay bottom.	Yes	-	2362 from Arambourg and Hoffstetter excavation. Unknown from Jaeger and Hublin excavation	The exact number is unknown. 223 analysed by Balout 1967; 271 analysed by Djemmali 1985; 104 analysed by Sharon 2007;	Present	Arambourg 1955; Arambourg and Hoffstetter 1963; Balout et al. 1967; Djemmali 1985; Geraads et al. 1986; Sharon 2007; Geraads 2016
Sidi Abderrahmane Quarry-Site B-Unit M	No	MIS 13 or MIS 15	Member 1 of the Anfa Formation (Fig. S1). Pudding stone with greyish sandy limestone cement and phosphatic breccia.	Yes	-	426	146	Absent	Neuville and Ruhlmann 1941; Biberson 1961a; Mohib 1991; El Azzouzi 1992; Raynal et al. 2017; Lefèvre et al. 2021
S.T.I.C. Quarry	No	MIS 13 or MIS 15 ?	S.T.I.C. Quarry has been partially filled up. S.T.I.C. Quarry deposits belong to the Anfa Formation (Fig. S1). Raynal et al. 2017 suspected erosion processes of ThI-L1 and a natural mixing of series, sustained by the existence of a karstic systems in both quarries.	Yes	Yes	1081	418	Absent	Biberson 1961a; Bernoussi 1992; Sharon 2007; Raynal et al. 2017; Mohib et al. 2019; Gallotti et al. 2022

and considered 1) that the small-medium flakes attributed to the Tayacian are the wastes of the LCT shaping and 2) that the Clacto-Abevillian industry could be divided into three groups based on the degree of abrasion and thus corresponded to three different industries. One was attributed to the Developed Pebble Culture and the others to the stages I and II of the early Acheulean. Stage II differed from stage I by the higher number of trihedrons, the lack of cleavers, the high number of LCTs on flake, and by the appearance of the use of the soft hammerstone.

Nevertheless, Lefèvre and Raynal (2002) revised the stratigraphy of the site and assessed that this assemblage belongs probably to the bottom part – Member 1- of the Anfa Formation with an age certainly older than MIS 13 (Fig. S1). An age of 492 ± 57 Ka was obtained, indeed, from the bottom of Member 2 of the Anfa Formation on backshore sands (Fig. S1; Rhodes et al. 2006). Moreover, and from a strict stratigraphical point of view, it marks the end of the early Acheulean (Raynal et al. 2017) and not its emergence as assessed by Biberson (1961a).

Mohib (1991) performed an analysis of 142 out of 146 LCTs identified by Neuville and Ruhlmann (1941). The use of large flakes as LCTs blanks is more common than at ThI-L1 and knappers preferred end-struck flakes to proximal side-struck flakes, largely used at ThI-L1. Furthermore, if at ThI-L1 entame flakes are the most used LCT blanks, at SAR-Unit M many flake blanks bear negative scars on their dorsal face belonging to flaking, wide plain or dihedrals butts with very obtuse flaking angles. Shaping consists of large centripetal (semi)peripheral removals and finishing is almost absent. Twenty-six are unifacial LCTs (pointed handaxes and picks with trihedral tip), shaped only on the dorsal face of the flake blank. Seventy-three LCTs show a bifacial shaping to manufacture picks, beveled, and pointed handaxes. Twenty-three are shaped on three surfaces from two striking platforms and eighteen are cleavers. Tixier's cleaver type 1 is added to type 0, the only one present at ThI-L1, and a type 2 specimen is also documented. The

presence of these two types could represent the appearance of new flaking methods to produce cleaver flake blanks involving the predetermination of the transversal cutting-edge.

Stage III of the early Acheulean was identified by Biberson in layer D of the S.T.I.C. Quarry, located beyond the southern extremity of Sidi Abderrahmane-Grande Exploitation Quarry (Fig. 1). P. Biberson discovered the site in 1951, conducted a test-excavation in an area of 6 m² in parallel with quarry works. No additional data are available regarding excavation in the following years during which quarriers collected artefacts and fauna on their own as above stated. Some of the artefacts are typologically similar to those of ThI-L1 which overhangs the S.T.I.C Quarry (Fig. 1a; Fig. S1). We have suspected erosion processes of ThI-L1 and a natural mixing of series, sustained by the existence of a karstic system in both quarries, but it is now impossible to test this hypothesis and to conduct stratigraphic revision or dating attempts since the S.T.I.C. Quarry has been partially filled up (Raynal et al. 2017; Mohib et al. 2019; Gallotti et al. 2022) and the owner prohibits any access to the remaining section.

Biberson analysed 1081 artefacts (97 cobble tools, 418 LCTs, 84 large flakes, 274 flakes, and 145 indeterminable artefacts). All of the artefacts are made of quartzite and felspathic sandstone. Compared to ThI-L1, the production of LCTs is numerically more significant, but given the absence of precise contextualization (see above) it is difficult to draw conclusions. Handaxes represent 72% of the LCTs, followed by trihedrons (24.9%) and few cleavers (3.1%). The main feature of handaxes is their lanceolate and ultrapointed shape, a description that assimilates many of these tools to picks.

While sharing a typological substrate with the previous stages defined by Biberson, the S.T.I.C. industry presents a series of innovations that led Biberson to attribute it to stage III: 1) spheroids perfect their globular shape becoming bolas, 2) handaxes and trihedrons are more refined and elongated, and 3) the use of soft hammerstone improves LCT shaping refinement.

Sharon (2007) studied 107 artefacts out of 1081 analysed by Biberson (83 handaxes, five cleavers, nine cores, and 10 large flakes) stored at *Musée de l'Homme* in Paris. Few data are available for handaxes, which are longer (mean = 165 mm) than those of ThI-L1 and mainly made on proximal side-struck flakes.

Unfortunately, the available data are too poor and fragmented to discuss a possible local evolution of the ThI-L1 early Acheulean. In addition, the lack of reliable pre-Acheulean stratified sites in Morocco prevents us from investigating its origin. The revision of the lithic collections referred to as the Moroccan Pebble Culture (Biberson 1961a) shows that all the materials are geofacts or younger reworked artefacts (El Hajraoui 1985; Raynal et al. 2002). Furthermore, the rich paleontological site of Ahl al Oughlam dated to ~2.5 Ma yielded neither lithic artefacts nor evidence of hominid actions on bones (Geraads et al. 1998).

ThI-L1 in the Algerian early Acheulean context

Pre-Acheulean Algerian lithic series have been mostly collected on surface and in reworked deposits (Hugot 1955; Alimen and Chavaillon 1960; Ramendo 1963; Thomas 1963; Roubet 1967; Heddouche 1980; Sahnouni 2006). The only pre-Acheulean evidence recorded from a stratigraphic context belongs to the Aïn Hanech Formation (Sahnouni et al. 2018) in Algeria, where the last Oldowan occurrence dates to 1.7 Ma. Another possible Early Pleistocene Algerian site with a similar age is Mansourah, located southeast of the city of Constantine. It yielded a quartzite lithic industry (choppers, polyhedrons, cores, and a few flakes) associated with a large mammal fauna which looks contemporaneous with that of Aïn Hanech and might even be slightly older (Chaid-Saoudi et al. 2006).

Concerning the emergence of the Acheulean in Algeria, Duval et al. (2021) announced the discovery of diagnostic early Acheulean artefacts from Oued Boucherit, dating the origin of the Acheulean in North Africa back to 1.67±0.04 Ma. They belong to at least two different sites stratigraphically located immediately above the Oldowan horizon at Aïn Hanech and El Kherba.

The lithic industry consists of 25 artefacts made of limestone such as picks (*n* = 2) and handaxes (*n* = 17), as well as cores (*n* = 3) and flakes (*n* = 3). Based on this evidence, Duval et al. (2021) assessed that the onset of the Acheulean in North Africa is very close to that recorded in East Africa and conceive a multiple African origin.

However, these claims are not supported by consistent evidence and enhancing our current knowledge about the Acheulean emergence demands more reliable data. First of all, the very few artefacts do not belong to a systematic excavation, but they have been collected during surveys in different locations and probably belong to a dismantled calcrete deposit overlying the Oldowan stratum (Duval et al. 2021).

Another weakness concerns the site chronostratigraphy. Two stratigraphic sections from the Oued Boucherit area, comprising essentially continental muds, sands, and disconformable gravels, have been studied for magnetostratigraphy (Sahnouni et al. 2018): the ~30 m-thick section B (Parés et al. 2014), bearing a reverse-normal-reverse polarity sequence, and the ~36 m-thick section A (Sahnouni et al. 2018), located a few hundred meters to the NE of section B and bearing an upper normal polarity interval punctuated by two thin reverse polarity intervals and followed down-section by reverse polarity. An ESR date of 1.92 Ma, with a large uncertainty of ± 0.36 Ma at 2σ, has been obtained in a reverse polarity strata in the lower part of section A.

The two sections do not overlap magnetostratigraphically insofar as they share no common polarity reversals and moreover, do not share potentially correlative lithological marker beds, due to the inherently discontinuous nature of the investigated continental deposits characterized by channelized high energy fluvial gravels and laterally discontinuous sands. The sections have thus been correlated into a virtually continuous stratigraphy by means of altimetric leveling using a Jacob's Staff (Sahnouni et al. 2018). The composite section has been interpreted as a virtually continuous record spanning from 1.65 Ma at the top of section B to 3.93 Ma at the base of section A (Duval et al. 2021).

Of particular interest for our discussion is the age of the Acheulean level in section B. Lithic tools have been found in calcretes, palaeosoils and colluvia on dissected surfaces at the top of section B, close to ground level (Sahnouni and de Heinzelin 1998). This level is currently dated at 1.67 Ma by means of upward extrapolation of the sediment accumulation rate function erected on the Olduvai subchron recovered stratigraphically below (Duval et al. 2021; see also Parés et al. 2014; Sahnouni et al 2018). Parés et al. (2014) pointed out that *per se*, the normal polarity interval in section B could represent a record of either the Jaramillo subchron (0.99–1.07 Ma) or the Olduvai subchron (1.78–1.94 Ma). The attribution of this normal interval to the Olduvai subchron is based on the presence of fossil remains attributed to *Kolpochoerus heseloni* (teeth) and *Anancus* and their comparisons with similar findings from e.g., Olduvai Bed II (Parés et al. 2014; Sahnouni et al. 2018; Duval et al. 2021), albeit *K. heseloni* has been reported also coming from strata attributed to the Jaramillo subchron at the Cornelia-Uitzoek site in South Africa (Brink et al. 2012). Based on these arguments, we believe that further evidence is required to rule out the possibility that the normal polarity interval of section B is in fact a record of the Jaramillo subchron, which would imply an extrapolated age for the uppermost Acheulean level of about 0.9 Ma, and a significant chronostratigraphic gap with the underlying section A of Gauss age.

The other Algerian site that yielded an early Acheulean industry is Tighennif (previously known as Ternifine, and also formerly called Palikao), discovered in 1872, 20 km east of Mascara. The sandy levels of a hillock were worked from 1872 onwards for the building of the village, and soon began to yield fossil bones and artefacts. The great antiquity of the site was definitely established by Pallary in 1928 who discovered a canine of the sabre-tooth cat *Homotherium*. Arambourg led new excavations in 1931, but the largest ones were conducted by Arambourg and Hoffstetter from 1954 to 1956. Thousands of fossils were collected, together with 2362 Acheulean artefacts and several human remains (Arambourg 1955; Arambourg and Hoffstetter 1963; Djemmali 1985). The lithic industry revealed the production of LCTs made of quartzite, sandstone, limestone, and exceptionally of silicites, along with small flaking, mainly of silicites (Djemmali 1985; Geraads et al. 1986).

Two short field campaigns were conducted in 1982-1983 by a team led by Jaeger and Hublin; they resulted in an updated faunal list and a refinement of the stratigraphy and sedimentary context (Geraads et al. 1986). The lower deposits of this site probably belong to a normal magnetic polarity interval, either the Brunhes chron or the Jaramillo subchron (Geraads et al. 1986; Geraads 2016). No data are available on the number of lithic recorded during these new excavations.

Balout et al. (1967) analysed 81 "pebble tools", 107 cleavers, and 126 handaxes. Neither this preliminary typological analysis nor the LCT study by Sharon (2007), provided a comprehensive technological analysis of the Tighennif assemblages.

Although Balout et al. (1967) assessed that Tighennif industry is technologically homogeneous, they encounter some inconsistencies, in particular the coexistence of abundant cobble tools, considered as an archaic component, and the appearance of "more evolved" traits such as the soft hammer knapping, use of the *tranchet* blow technique, and the production of large flakes for LCTs manufacture. They highlighted that these inconsistencies were hard to explain without a precise stratigraphic attribution of the lithic components. As Arambourg and Hofftestetter (1963) pointed out, no archaeological layers are visible and the deposit with lithic, fauna, and human remains results from the clogging of an old lake basin with a funnel-shaped clay bottom. This clogging is due to the rise of underlying Miocene sands under the action of artesian waters. It was therefore accompanied by a subsidence of the bottom of the basin, marked by recesses and micro-faulting. These waterlogged sands appear to have been constantly reworked by artesian griffins. These conditions of deposit made any stratigraphic classification rather illusory. The lack of a precise stratigraphic attribution and the various issues raised over the years about the homogeneity of the Tighennif industry

limit a comprehensive comparative analysis with ThI-L1, allowing only some isolated comparisons.

Djemmali (1985) analysed all the artefacts belonging to 1954-1956 Arambourg's excavations. He again raised the problem of the homogeneity of the industry and divided it into two subsets on the basis of raw material composition and the degree of artefact alteration. The first set was composed of LCTs and small flaking cores and flakes, mainly of quartzite and felspathic sandstone, that show a strong physical alteration. The second set was composed exclusively of small-medium very fresh cores and flakes, mostly of silicites. Another important difference between the two sets is the presence in the second set of core preparation flaking methods for the extraction of predetermined products. One of the most interesting results of this study is that the primary objectives of LCT shaping was the manufacture of a tip with a very acute angle, while the lateral edges were characterized by more open angles with a high variation. This represents a strong technical convergence between the LCT production at Tighennif and ThI-L1. Unfortunately, the problems related to the stratigraphic context were underestimated in the subsequent lithic analyses which concerned only the LCT component.

Sharon (2007) analysed 47 cleavers, 57 handaxes, and 41 large flakes stored at *Institut de Paléontologie Humaine* in Paris. Handaxe and cleaver productions share many technological traits with those of ThI-L1. Handaxes document the use of cobbles and flakes as blanks. Flakes were *entame* flakes or cortical flakes with plain striking platforms, removed after a flake had already been extracted from the cobble core, using its negative as striking platform. These blank types and their obtuse flaking angle look the same that "type 0" of Tixier's (1956) cleaver typology, successively named proto-hachereau or "*hachereau de Ternifine*" by de Heinzelin (1962). Like at ThI-L1, the reconstruction of the *entame* core method is exclusively based on LCTs and large flakes due to the lack of cobble cores. The mean maximal dimension of the *entame* flakes from Tighennif is 147.6 mm, while that of ThI-L1 is 123.3 mm. At Tighennif end-struck flakes were preferred for

cleavers production, while knapper at ThI-L1 produced side-struck flakes. Proximal side-struck flakes dominate as at ThI-L1, producing the final shape for pointed handaxes and another common trait with ThI-L1 is that handaxes from Tighennif present a lack of symmetry. The use of flat cobbles for *entame* flake extraction at Tighennif supports the evidence from ThI-L1: the thickness is a selection criterion for LCT blanks. Nevertheless, an innovation was introduced at Tighennif, i.e., the production of Kombewa flake blanks, which represents a further step of the *entame* core method, after an *entame* flake had initially been removed from a flat cobble. Sharon interpreted the technical behaviors of Tighennif and S.T.I.C. Quarry as representative of the Large Flake Acheulean, while he attributed Thomas Quarry I to an earlier stage because large flakes do not constitute a primary technological praxis and cleavers are very few (not more than 1% among LCTs). Our results strongly question this scenario: not only is the manufacture of LCTs on flake blanks well documented at ThI-L1, although less frequent than that on cobbles, but it is regulated by technical strategies, some of which being also documented at Tighennif (*entame* core method for handaxe and cleaver blank production). The adoption of the Kombewa predetermined flaking method could represent the actual *Rubicon* between the two series, rather than the mere frequency of the LCTs on flake blanks. Unfortunately, given the low-resolution chronostratigraphic context of Tighennif and without a detailed and complete analysis of the series, any synthesis would be meaningless at this stage.

Conclusions

Dated to ~1.3 Ma, ThI-L1 is the earliest Acheulean site of North Africa recorded in an indisputable chrono-stratigraphic context. With over 3800 lithic artefacts, ThI-L1 contains one of the largest stone tool assemblages for this period on the African continent. This study represents the first comprehensive assessment of the techno-economic systems of a North African

Acheulean site, through the analysis of all the components of the assemblage.

At ThI-L1, stone knapping was performed on quartzites and silicites, both available in secondary sources near the site as cobbles and pebbles. Quartzite exploitation documents two productions, one dedicated to LCT manufacture and the other to small-medium sized flakes production. Silicite pebbles, characterized by their small size, were knapped to extract small flakes and bladelet-like flakes.

Quartzite and silicite small flaking was carried out through a variety of methods that represent the best adaptations to the original shapes of the raw materials. The outcome are small and medium sized undifferentiated flakes. However, when need arose, knappers were able to flake products with specific features applying technical solutions and more structured methods as well as conceiving innovative technical processes.

LCTs assemblage is composed by several tool-types with a pointed tip or a transverse cutting edge with remarkably similar morphometric and technical characteristics. Such standardization starts with the strict selection of cobble blanks or with standard flaking procedures to anticipate the final tool patterns and continues during the successive shaping stage with fixed rules that are systematically applied to every tool-type. Selection/flaking and shaping phases were wisely integrated within specific technical projects.

The techno-economic systems highlighted at ThI-L1 document the high diversification of the stone working outcomes in this earliest North African Acheulean, indicating different levels of knowledge and knowhow. Technical projects evidence the complexity of the mental templates involved in stone knapping as well as the flexible structure of the operational schemes.

Currently, the absence of pre-Acheulean sites in Morocco, the wide gap between the pre-Acheulean industries in Algeria and the early Acheulean of Morocco, and the sporadic and low-resolution evidence of the other Moroccan sites classically ascribed to the early Acheulean enable a discussion hinting at a local origin of the ThI-L1 techno-complex.

Author contributions

D.L. and A.M. are co-directors of the French-Moroccan Casablanca program since 2016. J.-P.R., A.M. and R.G. made excavations at ThI-L1. R.G. design research and wrote the paper with contributions of all the authors. R.G., A.M., L.M., and J.-P.R. for lithic analysis; P.F. and J.-P.R. for petroarcheology; M.R. for particle size distribution analysis; D.L., M.E.G., and J.-P.R. for stratigraphy; G.M. for geochronology. All authors discussed and commented on the manuscript.

References

Alimen H (1955) Préhistoire de l'Afrique, Boubée et Cie, Paris.

Alimen MH, Chavaillon J (1960) Presentation de « galets amenagés » des niveaux successifs du Quaternaire ancien de la Saoura. Bull Soc Prehist Fr 57:373–374.

André PJ, Boissin JP, Corsini M, et al (1987) Sur le Cambrien de la région de Casablanca (Maroc): la série de Dar Bou Azza. B Soc Geol Fr 6:1161-1170.

Antoine M (1945) La préhistoire du Maroc atlantique et ses incertitudes, Vol. jubilaire de la Société des Sciences naturelles du Maroc.

Antoine M (1952) Les grandes lignes de la Préhistoire marocaine. IIe congrès panafricain de Préhistoire, Alger-Casablanca.

Arambourg C (1955) Le gisement de Ternifine et l'Atlanthropus. Bull Soc Prehist Fr 52:90-95.

Arambourg C, Hoffstetter R (1963) Le gisement de Ternifine. Archives de l'Institut de Paleontologie Humanine 32:9-36.

Ashton N, Cook JM, Lewis SG, et al (eds) (1992) High Lodge: Excavations by G. de G. Sieveking 1962-8 and J. Cook, 1988, British Museum Press, London.

Balout L (1955) Préhistoire de l'Afrique du Nord, essai de chronologie, Arts et métiers graphiques, Paris.

Balout L, Biberson P, Tixier J (1967) L'acheuléen de Ternifine (Algerie), gisement de l'Atlanthrope. Anthropologie 71:217-238.

Bernoussi R (1992) Étude technologique et statistique de la série lithique de la carrière de la S.T.I.C. à Sidi Abderrahmane (Casablanca). Mémoire de fin d'études du IIe cycle, Institut des Sciences de l'Archéologie et du Patrimoine.

Bertran P, Lenoble A, Todisco D, et al (2012) Particle size distribution of lithic assemblages and taphonomy of Palaeolithic sites. J Archaeol Sci 39:3148-3166. https://doi.org/10.1016/j.jas.2012.04.055

Biberson P (1956) Le gisement de l'«Atlanthrope» de Sidi Abderrahmane (Casablanca), Bulletin d'Archéologie Marocaine 1:39-92.

Biberson P (1961a) Le Paléolithique inférieur du Maroc atlantique. Publications du Service des Antiquités du Maroc 17, Rabat.

Biberson P (1961b) Le cadre palaeogéographique de la Préhistoire du Maroc atlantique. Publications du Service des Antiquités du Maroc, fascicule 16, Rabat.

Biberson P (1967) Some aspects of lower Palaeolithic of Northwest Africa. In: Bishop WW, Clark JD (eds) Background to evolution in Africa, University of Chicago Press, Chicago, p. 447-476.

Bleicher G (1875) Recherches d'Archéologie préhistorique dans la province d'Oran et dans la partie occidentale du Maroc. Matériaux pour l'Histoire primitive et naturelle de l'Homme, p. 193-212.

Boëda E (1993) Le débitage discoïde et le débitage Levallois récurrent centripète. Bull Soc Prehist Fr 90-96:392-404.

Bordes F (1947) Étude comparative des différentes techniques de taille du silex et des roches dures. Anthropologie 51:1-29.

Bordes F (1950) Principes d'une méthode d'étude des techniques de débitage et de la typologie du Paléolithique ancien et moyen. Anthropologie 54:19-34.

Bordes F (1961) Typologie du Paléolithique ancien et moyen, Publications de l'Institut de préhistoire de l'Université de Bordeaux, Mémoire N° 1, Delmas, Bordeaux.

Boudad L, Guislain S (2012) Acquisition de supports prédéterminés destinés à la réalisation de bifaces : l'exemple de sites de surfaces du Sud-Est marocain. Anthropologie 116:364-377. https://doi.org/10.1016/j.anthro.2012.06.003

Boule M (1900) Etude paléontologique et archéologique sur la station paléolithique du lac Karar (Algérie). Anthropologie 11:1-21.

Bourcart J (1943) La géologie du Quaternaire au Maroc. La Revue Scientifique 3224:311-336.

Breuil H (1930) L'Afrique préhistorique. Cahiers d'Art 8-9:449-500.

Brink JS, Herries AIR, Moggi-Cecchi J, et al (2012). First hominine remains from a ~1.0 million year old bone bed at Cornelia-Uitzoek, Free State Province, South Africa. J Hum Evol 63:527-535. https://doi.org/10.1016/j.jhevol.2012.06.004

Cailleux Y (1994) Le Cambrien et l'Ordovicien du Maroc central méridional. Bulletins de l'Institut Scientifique de Rabat 18:10-31.

Cancellieri E (2021) A tentative tale of Stone Age human dynamics in Pleistocene south-western Libya (central Sahara). Libyan Studies 52:36-53. https://doi.org/10.1017/lis.2021.18

Chaid-Saoudi Y, Geraads D, Raynal J-P (2006) The fauna and associated artefacts from the Lower Pleistocene site of Mansourah (Constantine, Algeria). C R Palevol 5:963–971. https://doi.org/10.1016/j.crpv.2006.08.001

Champault B (1966) L'acheuléen évolué au Sahara occidental. Notes sur l'homme au Paléolithique ancien, Museum national d'histoire naturelle, Paris.

Chantre E (1908) L'âge de la pierre dans la Berberie orientale, Tripolitaine et Tunisie. 37e Congrès Association française pour l'Avancement des Sciences, Clermont Ferrand, 2e partie, p. 686-688.

Clark JD (1992) The earlier Stone Age/Lower Palaeolithic in North Africa and the Sahara. In: Klees F, Kuper R (eds) New light on the northern African past, Heinrich Barth Institut, Köln, p. 17-37.

Collignon R (1887) Les âges de la pierre en Tunisie, Matériaux pour l'histoire naturelle et primitive de l'Homme, t. XXI, p. 173-176.

de Heinzelin J (1962) Manuel de typologie des industries lithiques, Institut Royal des Sciences Naturelles, Bruxelles.

Delarue J, Destombes J, Jeannette A (1956) Etude géotechnique de la région de Casablanca. Notes et Mémoires du Service géologique du Maroc 130, Editions du Service géologique du Maroc, Rabat, p. 53-143.

de la Torre I (2016) The origins of the Acheulean:past and present perspectives on a major transition in human evolution. Philos Trans R Soc Lond B Biol Sci 371:20150245. https://doi.org/10.1098/rstb.2015.0245

de la Torre I, Mora R (2018) Technological behaviour in the early Acheulean of EF-HR (Olduvai Gorge, Tanzania). J Hum Evol 120:329-377. https://doi.org/10.1016/j.jhevol.2018.01.003

Destombes J, Jeannette A (1956) Etude géotechnique de la région de Casablanca (géologie, matières premières minérales, sols). Notes et mémoires du Service géologique du Maroc 130, Editions du Service géologique du Maroc, Rabat.

Destombes J, Jeannette A (1966) Mémoire explicatif de la carte géotechnique de la Meseta côtière à l'Est de Casablanca au 1/50 000. Régions de Mohammedia, Bouznika et Ben-Slimane. Notes et mémoires du Service géologique du Maroc 180 bis, Editions du Service géologique du Maroc, Rabat.

Diez-Martín F, Wynn T, Sánchez-Yustos P, et al (2019) A faltering origin for the Acheulean? Technological and cognitive implications from FLK West (Olduvai Gorge, Tanzania). Quat Int 526:49-66. https://doi.org/10.1016/j.quaint.2019.09.023

Djemmali N-E (1985) L'industrie lithique acheuléenne du gisement de Tighennif (Ternifine), Algeria. Thèse 3eme cycle, Museum National d'Histoire Naturelle, Université Pierre et Marie Curie.

Duke H, Feibel C, Harmand S (2021) Before the Acheulean: The emergence of bifacial shaping at Kokiselei 6 (1.8 Ma), West Turkana, Kenya. J Hum Evol 159:103061. https://doi.org/10.1016/j.jhevol.2021.103061

Duval M, Sahnouni M, Parés JM, et al (2021) The Plio-Pleistocene sequence of Oued Boucherit (Algeria): A unique chronologically-constrained archaeological and palaeontological record in North Africa. Quat Sci Rev 271:107116. https://doi.org/10.1016/j.quascirev.2021.107116

El Azzouzi (1992) Étude technologique des éclats et des nucléi du niveau M de Sidi Abderrahmane, Casablanca. Mémoire de fin d'études du IIè cycle, Institut national des Sciences de l'Archéologie et du Patrimoine

El Hajraoui MA (1985) Les industries préhistoriques de la région de la Mamora dans leur contexte géologique et palaeopedologique. Thèse 3eme cycle, Université de Bordeaux 1.

Ennouchi E (1969) Découverte d'un Pithécanthropien au Maroc. C R Acad Sci 269:763-765.

Forestier H (1992) Approche Technologique de Quelques Séries Dites Clactoniennes du Nord-Ouest de la France et du Sud-Est de l'Angleterre. Mémoire de Maîtrise, Université Paris, Nanterre.

Forestier H (1993) Le Clactonien: mise en application d'une nouvelle méthode de débitage s'inscrivant dans la variabilité des systèmes de production lithique du paléolithique ancien. Paléo 5: 53-82.

Gallotti R, Mohib A, Fernandes P, et al (2020) Dedicated core-on-anvil production of bladelet-like flakes in the Acheulean at Thomas Quarry I - L1 (Casablanca, Morocco). Sci Rep 10:9225. https://doi.org/10.1038/s41598-020-65903-3

Gallotti R, Mohib A, Lefèvre D, et al (2022) The African Acheulean: a view from the western Maghreb. Bulletin d'Archéologie marocaine 27:9-28.

Gallotti R, Mussi M (2017) Two Acheuleans, two humankinds: From 1.5 to 0.85 Ma at Melka Kunture (Upper Awash, Ethiopian highlands). J Anthropol Sci 95:1-46. https://doi:10.4436/JASS.95001

Gallotti R, Mussi M (eds) (2018) The Emergence of the Acheulean in East Africa and Beyond. Contributions in Honor of Jean Chavaillon, Springer, Cham.

Gallotti R, Muttoni G, Lefèvre D, et al (2021) First high resolution chronostratigraphy for the early North African Acheulean at Casablanca (Morocco). Sci Rep 11:15340. https://doi.org/10.1038/s41598-021-94695-3

Geneste JM (1989) Economie des ressources lithiques dans le Mousterien du sud-ouest de la France. In: Otte M (ed) L'Homme de Néanderthal, volume 6: La Subsistance, ERAUL, Liege, p. 75-97.

Geneste JM (1991) Systèmes techniques de production lithique: Variations techno-économiques dans les processus de réalisation des outillages paléolithiques. Techniques et Culture 17-18:1-35.

Geraads D (2016) Pleistocene Carnivora (Mammalia) from Tighennif (Ternifine), Algeria. Geobios 49:445-458. https://doi.org/10.1016/j.geobios.2016.09.001

Geraads D, Amani F, Raynal J-P, et al (1998) La faune de Mammiferes du Pliocene terminal d'Ahl al Oughlam, Casablanca, Maroc. The Late Pliocene mammalian fauna of Ahl al Oughlam, Casablanca, Morocco. C R Acad Sci 326:671-676. https://doi.org/10.1016/S1251-8050(98)80259-0

Geraads D, Hublin J-J, Jaeger J-J, et al (1986) The Pleistocene Hominid Site of Ternifine, Algeria: New Results on the Environment, Age, and Human industries. Quat Res 25:380-386. https://doi.org/10.1016/0033-5894(86)90008-6

Gigout M (1951) Etude géologique de la Méséta marocaine occidentale (arrière-pays de Casablanca, Mazagan et Safi). Notes et Mémoires du Service géologique du Maroc 86, t. 1, Editions du Service géologique du Maroc, Rabat.

Gigout M (1958) Réflexions sur les bases du Quaternaire marin. B Soc Geol Fr 7:385-400.

Goldman-Neuman T, Hovers E (2012) Raw material selectivity in Late Pliocene Oldowan sites in the Makaamitalu Basin, Hadar, Ethiopia. J Hum Evol 62:353-66. https://doi:10.1016/j.jhevol.2011.05.006

Goodwin AJH (1929) The Victoria West industry. Annals of the South African Museum 27:53-69.

Goodwin AJH (1934) Some developments in technique during the earlier Sone Age. T Roy Soc S Afr 21:109-123.

Hamoumi N, Izart A (1984) Le Cambro-Ordovicien de la Méséta Côtière et le Dévono-Carbonifère du Bassin de Sidi Bettache. Bull Inst Sci 9:117.

Heddouche AEK (1980) Découverte d'une industrie a galets aménages au Sahara nord-oriental. Libyca 28:105–112.

Hertz H (1882) On hardness, Verhandlugen des vereins zur Befüerung des geweerbe Fleisses, vol. 61, p. 410. Translated and reprinted in English in Hertz's Miscellaneous Papers, Macmillan & Co, London, 1896, Ch. 6

Hovers E, Gossa T, Asrat A, et al (2021) The expansion of the Acheulian to the Southeastern Ethiopian Highlands: Insights from the new early Pleistocene site-complex of Melka Wakena. Quat Sci Rev 253:106763. https://doi.org/10.1016/j.quascirev.2020.106763

Hugot H (1955) Un gisement a pebble tools a Aoulef. Travaux de l'Institut de Recherches Sahariennes 8:131–153.

Inizan ML, Reduron-Ballinger M, Roche H, et al (1999) Technology and terminology of

knapped stone (Préhistoire de la Pierre taillée 5), CREP, Nanterre.

Jansen FJ (1926) A new type of stone implement from Victoria West. South Afr J Sci XXIII:818-825.

Jaubert J, Mourre V (1996) Coudoulous, le Rescundudou, Mauran: diversité des matières premières et variabilité des schémas de production d'éclats. In: Bietti A, Grimaldi S (eds) Quaternaria Nova 6, Reduction Processes (Chaînes Opératoires) in the European Mousterian, Istituto Italiano di Paleontologia Umana, Rome, p. 313-341.

Kuman K, Gibbon RJ (2018) The Rietputs 15 site and Early Acheulean in South Africa. Quat Int 480:4-15. https://doi.org/10.1016/j.quaint.2016.12.031

Leader GM, Kuman K, Gibbon RJ, et al (2018) Early Acheulean organised core knapping strategies ca. 1.3 Ma at Rietputs 15, Northern Cape Province, South Africa. Quat Int 480:16-28. https://doi.org/10.1016/j.quaint.2016.08.046

Lecointre G (1926) Recherches géologiques dans la Meseta Marocaine, Larose, Paris.

Lecointre G (1952) Recherches sur le Néogène et le Quaternaire marins de la côte atlantique du Maroc. Notes et Mémoires du Service géologique du Maroc 99, t. 1, Stratigraphie, Editions du Service géologique du Maroc, Rabat.

Lefèvre D (2000) Du continent à l'océan. Morphostratigraphie et paléogéographie du Quaternaire du Maroc atlantique. Le modèle casablancais, vol. 3, Université de Montpellier III, Mémoire HDR, IIème partie.

Lefèvre D, El Graoui M, Geraads D, et al (2021) Les paléolittoraux plio-pléistocènes de Casablanca, cadre chronostratigraphique et paléogéographique de la Préhistoire ancienne du Maroc atlantique. Bulletin d'Archéologie Marocaine 26:39-70.

Lefèvre D, Raynal J-P (2002) Les formations plio-pléistocènes de Casablanca et la chronostratigraphie du Quaternaire marin du Maroc revisitées. Quaternaire 13:9-21.

Lemonnier P (1976) La description des chaînes opératoires. Contribution à l'analyse des systèmes techniques. Technique et Culture 1:100-151.

Lemonnier P (1986) The study of material culture today: toward an anthropology of technical systems. J Anthropol Archaeol 5:147-186. https://doi.org/10.1016/0278-4165(86)90012-7

Lenoble A (2005) Ruissellement et formations des sites préhistoriques: référentiel actualiste et exemples d'application au fossile, British Archaeological Report International Series 1363, Oxford.

Leroi-Gourhan A (1964) Le geste et la parole. Technique et langage, Albin Michel, Paris.

Leroi-Gourhan A (1971) Evolution et technique. L'homme et la matière, Albin Michel, Paris.

Lotter MG, Kuman K (2018) The Acheulean in South Africa, with announcement of a new site (Penhill Farm) in the lower Sundays River Valley, Eastern Cape Province, South Africa

Quat Int 480:43-65. https://doi.org/10.1016/j.quaint.2017.08.065

Mattingly DJ, Reynolds T, Dore JN (2003) Synthesis of human activities in the Fazzan. In: Mattingly DJ, Dore J, Wilson AI (eds) The Archaeology of Fazzan, Society for Libyan Studies, London, p. 327-375.

Maurin T, Bertran P, Delagnes A, et al (2017) Early hominin landscape use in the Lower Omo Valley, Ethiopia: Insights from the taphonomical analysis of Oldowan occurrences in the Shungura Formation (Member F). J Hum Evol 111:33-53. https://doi.org/10.1016/j.jhevol.2017.06.009

Mohib A (1991) Contribution à l'étude du Paléolithique ancien de Casablanca, l'outillage du niveau M de Sidi Abderrahmane (fouilles Neuville et Ruhlmann 1941). Mémoire de fin d'études du IIè cycle, Institut National des Sciences de l'Archéologie et du Patrimoine.

Mohib A (2001) L'Acheuléen de la grotte des Ours à Sidi Abderrahmane (Casablanca, Maroc) dans son contexte régional (fouilles anciennes et récentes). PhD Dissertation, Institut National des Sciences de l'Archéologie et du Patrimoine.

Mohib A, Raynal J-P, Gallotti R, et al (2019) Forty years of research at Casablanca (Morocco): new insights in the Early/Middle Pleistocene archaeology and geology. Hespéris Tamuda LIV:25-56.

Mourre V (2003) Discoïde ou pas discoïde ? Réflexions sur la pertinence des critères techniques définissant le débitage discoïde. In: Peresani M (ed) Discoid Lithic Technology: Advances and Implications, BAR International Series 1120, Oxford, p. 1-18.

Mourre V (2006) Émergence et évolution de la prédétermination au Paléolithique. In: Astruc L, Bon F, Léa V et al (eds) Normes techniques et pratiques sociale: de la simplicité des outillages pré-et protohistoriques, Éditions APDCA, Antibes, p. 61-74.

Neuville R, Ruhlmann A (1941) La place du Paléolithique ancien dans le Quaternaire marocain. Coll. Hesperis, VIII, Casablanca.

Owen WE (1938) The Kombewa Culture, Kenya Colony. Man 38:203-205.

Pallary P (1888) La station quaternaire de Palikao (département d'Oran), I. Considérations générales. Matériaux pour l'histoire naturelle et primitive de l'Homme, t. 22, p. 221-224.

Parenti F, Mengoli D, Natali L (2015) The Stone Age in Northwestern Libya: Observations Along a Pipeline. Afr Archaeol Rev 32:413-441. https://doi.org/10.1007/s10437-015-9193-8

Parés JM, Sahnouni M, Van der Made J, et al 2014. Early human settlements in Northern Africa: paleomagnetic evidence from the Ain Hanech Formation (northeastern Algeria). Quat Sci Rev 99:203-209. https://doi.org/10.1016/j.quascirev.2014.06.020

Pelegrin J (1985) Réflexions sur le comportement technique. In: Otte M (ed) La signification culturelle des industries lithiques Studia Praehistorica Belgica 4, BAR International Series 239, Liege, p. 72-91.

Perlés C (1991) Économie des matières première set économie du débitage: deux conceptions opposées ?. In: Beyries S, Meignen L, Texier PJ (eds), 25 and d'études technologiques en Préhistoire: bilan et perspectives, Proceedings XI rencontres d'archéologie et d'histoire d'Antibes, October 18-20, 1990, APDCA, Juan-les-Pins, p. 35-45.

Prassack KA, Pante MC, Njau JK, et al (2018) The paleoecology of Pleistocene birds from Middle Bed II, at Olduvai Gorge, Tanzania, and the environmental context of the Oldowan-Acheulean transition. J. Hum Evol 120:32-47. https://doi:10.1016/j.jhevol.2017.11.003

Ramendo L (1963) Les galets aménagés de Reggan. Libyca 11:42–73.

Raynal J-P (2021) Lettre de Casablanca où fut trouvé Homo darelbeidae. Bulletin d'Archéologie marocaine 26:9-38.

Raynal J-P, Mohib A (eds) (2016) Préhistoire de Casablanca. I – La Grotte des Rhinocéros (fouilles 1991 et 1996), Institut National des Sciences de l'Archéologie et du Patrimoine, VESAM VI, Rabat.

Raynal J-P, Gallotti R, Mohib, et al (2017) The Western Quest, First and Second Regional Acheuleans at Thomas-Oulad Hamida Quarries (Casablanca, Morocco). In: Wojtczak D, Al Najjar M, Jagher R et al (eds) Vocation préhistoire. Hommage à Jean-Marie Le Tensorer, Études et Recherches Archéologiques de l'Université de Liège, ERAUL 148, Liege, p. 309-322.

Raynal J-P, Sbihi-Alaoui F-Z, Geraads D, et al (2001) The Earliest Occupation of North-Africa: the Moroccan Perspective. Quat Int 75:65-75. https://doi.org/10.1016/S1040-6182(00)00078-1

Raynal J-P, Sbihi-Alaoui F-Z, Magoga L, et al (2002) Casablanca and the earliest occupation of North Atlantic Morocco. Quaternaire 13:65-77.

Raynal J-P, Sbihi-Alaoui FZ, Mohib A, et al (2009) Préhistoire ancienne au Maroc atlantique. Bilan et perspectives régionales. Bulletin d'Archéologie Marocaine 21:9-54.

Raynal J-P, Sbihi-Alaoui F-Z, Mohib A, et al (2010) Hominid Cave at Thomas Quarry I (Casablanca, Morocco): Recent findings and their context. Quat Int 223-224:369-382. https://doi.org/10.1016/j.quaint.2010.03.011

Raynal J-P, Sbihi-Alaoui F-Z, Mohib A, et al (2011) Contextes et âge des nouveaux restes dentaires humains du Pléistocène moyen de la carrière Thomas I à Casablanca (Maroc). Bull Soc Prehist Fr 108:1-25.

Raynal J-P, Texier J-P (1989) Découverte d'Acheuléen ancien dans la carrière Thomas 1 à Casablanca et problème d'ancienneté de

la présence humaine au Maroc. C R Acad Sci II:1743-1749.

Reygasse M (1930) Les Âges de la pierre dans l'Afrique du Nord (Berbérie). In Histoire et historiens de l'Algérie, 1830-1930 collection du centenaire de l'Algérie, Alcan, Paris, chapitre II, p. 37-70.

Reynolds T (2006) The importance of Saharan lithic assemblages. In: Mattingly D, Mclaren S, Savage E, et al (eds) Environment, Climate and Resources of the Libyan Sahara, Society of Libyan Studies, London, p. 81-90.

Rhodes EJ, Singarayer JS, Raynal J-P, et al (2006) New age estimations for the Palaeolithic assemblages and Pleistocene succession of Casablanca, Morocco. Quat Sci Rev 25:2569-2585. https://doi.org/10.1016/j.quascirev.2005.09.010

Rivière J (1896) L'industrie préhistorique du silex en Tunisie. 25e Congrès Association française pour l'Avancement des Sciences, Carthage-Tunis, 1st part, p. 199-200.

Roubet C (1967) Découverte de nouveaux galets aménagés dans la région sétifienne. Libyca 15:9-14.

Sahnouni M (2006) Les plus vieilles traces d'occupation humaine en Afrique du Nord: Perspective de l'Ain Hanech, Algérie. C R Palevol 5:243–254. https://doi.org/10.1016/j.crpv.2005.09.019

Sahnouni M, de Heinzelin J (1998) The Site of Ain Hanech Revisited: New Investigations at this Lower Pleistocene Site in Northern Algeria. J Archaeol Sci 25:1083-1101. https://doi.org/10.1006/jasc.1998.0278

Sahnouni M, Parés JM, Duval M, et al (2018) 1.9-million- and 2.4-million-year-old artifacts and stone tool-cutmarked bones from Ain Boucherit, Algeria. Science 362:1297-1301. https://doi:10.1126/science.aau0008

Schick KD (1986) Stone Age Sites in the Making: Experiments in the Formation and Transformation of Archaeological Occurrences, British Archaeological Report International Series 319, Oxford 313.

Sharon G (2007) Acheulian Large Flake Industries: Technology, Chronology, and Significance, Archaeopress, Oxford.

Sharon G (2009) Acheulian Giant-Core Technology. A Worldwide Perspective. Curr Anthropol 50:335-367. https://doi.org/10.1086/598849

Sharon G (2010) Large Flake Acheulian. Quat Int 223:226-233. https://doi.org/10.1016/j.quaint.2009.11.023

Sharon G (2011) Flakes Crossing the Straits? Entame Flakes and Northern Africa–Iberia Contact During the Acheulean. Afr Archaeol Rev 28:125–140. https://doi.org/10.1007/s10437-011-9087-3

Sistiaga A, Husain F, Uribelarrea D, et al (2020) Microbial biomarkers reveal a hydrothermally active landscape at Olduvai Gorge at the dawn of the Acheulean, 1.7 Ma. Proc Natl Acad Sci USA 117:24720-24728. https://doi.org/10.1073/pnas.200453211

Stanistreet IG, McHenry LJ, Stollhofen H, et al (2018) Bed II Sequence Stratigraphic context of EF-HR and HWK EE archaeological sites, and the Oldowan/Acheulean succession at Olduvai Gorge, Tanzania. J Hum Evol 120:19-31. https://doi.org/10.1016/j.jhevol.2018.01.005

Stearns CE (1978) Pliocene-Pleistocene emergence of the Moroccan Meseta. Geol Soc Am Bull 89:1630-1644. https://doi.org/10.1130/0016-7606(1978)89<1630:PEOTMM>2.0.CO;2

Tavoso A (1969) Etude des terrasses alluviales du Fresquel (Aude) et des industries préhistoriques associées, Impr. Leconte, Marseille.

Terradas X (2003) Discoid flaking method:conception and technological variability. In: Peresani M (ed) Discoid Lithic Technology: Advances and Implications, BAR International Series 1120, Oxford, p. 19-32.

Texier J-P, Lefèvre D, Raynal J-P (1994) Contribution pour un nouveau cadre stratigraphique des formations littorales Quaternaires de la région de Casablanca (Maroc). C R Acad Sci II 318:1247-1253.

Texier J-P, Lefèvre D, Raynal J-P, et al (2002) Lithostratigraphy of the littoral deposits of the last one million years in the Casablanca region (Maroc). Quaternaire 13:23-41.

Texier P-J, Roche H (1992) The impact of predetermination on the development of some

acheulean "chaînes opératoires". In: Bermudez JM, Carbonell i Roura E, Arsuaga JL (eds) Evolucion humana en Europa y los yacimentos de la Sierra de Atapuerca, Consejeria de Educacion y Cultura, Junta de Castilla y Leon, p. 403-420.

Thomas G (1973) Découverte d'industrie du groupe de la « Pebble Culture » sur le versant nord des monts du Tessala (Algérie). Sa place dans la stratigraphie du Pléistocène inferieur et moyen de l'Oranie. C R Acad Sci D 276:921–924.

Tixier J (1956) Le hachereau dans l'Acheuléen nord-africain. Notes typologiques, Proceedings of the XV session of the Congrès préhistorique de France, July 15-22, Poitiers-Angoulême, p. 914-923.

Toth N (1982) The Stone Technologies of Early Hominids at Koobi Fora, Kenya: An Experimental Approach. Ph.D, Dissertation, University of California.

Tryon CA, McBrearty S, Texier P-J (2005) Levallois lithic technology from the Kapthurin formation, Kenya: Acheulian origin and Middle Stone Age diversity. Afr Archaeol Rev 22:199-229. https://doi.org/10.1007/s10437-006-9002-5

Uno KT, Rivals F, Bibi F, et al (2018) Large mammal diets and paleoecology across the Oldowan–Acheulean transition at Olduvai Gorge, Tanzania from stable isotope and tooth wear analyses. J Hum Evol 120:76-91. https://doi.org/10.1016/j.jhevol.2018.01.002

Uribelarrea D, Martín Perea D, Díez-Martín F, et al (2019) A geoarchaeological reassessment of the co-occurrence of the oldest Acheulean and Oldowan in a fluvial ecotone from lower middle Bed II (1.7 ma) at Olduvai Gorge (Tanzania). Quat Int 526:39-48. https://doi.org/10.1016/j.quaint.2019.09.037

Vaufrey R (1955) Préhistoire de l'Afrique, I, Maghreb, Librairie Masson et Cie, Paris.

Yravedra J, Martín-Perea DM, Díez-Martín F, et al (2019) Level U3.1, a new archaeological level discovered at BK (upper bed II, Olduvai Gorge) with evidence of megafaunal exploitation. J Afr Earth Sci 158:103545. https://doi.org/10.1016/j.jafrearsci.2019.103545

Zahraoui M (1991) La plate-forme carbonatée dévonienne du Maroc occidental et sa dislocation hercynienne. PhD Dissertation, Brest.

Editor, Giovanni Destro Bisol